Materials Today Bio 29 (2024) 101366

Contents lists available at ScienceDirect

Materials Today Bio

journal homepage: www.journals.elsevier.com/materials-today-bio

Leveraging printability and biocompatibility in materials for printing implantable vessel scaffolds

Tianhong Chen [a,1], Haihong Jiang [a,1], Ruoxuan Zhang [a], Fan He [b], Ning Han [c,***], Zhimin Wang [d,**], Jia Jia [a,b,*]

[a] School of Life Sciences, Shanghai University, Shanghai, China
[b] Sino-Swiss Institute of Advanced Technology, School of Micro-electronics, Shanghai University, Shanghai, China
[c] Department of Orthopedic Traumatology, Shanghai East Hospital, Tongji University, China
[d] Shanghai-MOST Key Laboratory of Health and Disease Genomics, Shanghai Institute for Biomedical and Pharmaceutical Technologies, Shanghai, 200237, China

ARTICLE INFO

Keywords:
Bioprinting
Biomaterials
Implantable vessel scaffolds
Printability
Biocompatibility

ABSTRACT

Vessel scaffolds are crucial for treating cardiovascular diseases (CVDs). It is currently feasible to fabricate vessel scaffolds from a variety of materials using traditional fabrication methods, but the risks of thrombus formation, chronic inflammation, and atherosclerosis associated with these scaffolds have led to significant limitations in the clinical usages. Bioprinting, as an emerging technology, has great potential in constructing implantable vessel scaffolds. During the fabrication of the constructs, the biomaterials used for bioprinting have offered significant contributions for the successful fabrications of the vessel scaffolds. Herein, we review recent advances in biomaterials for bioprinting implantable vessel scaffolds. First, we briefly introduce the requirements for implantable vessel scaffolds and its conventional manufacturing methods. Next, a brief overview of the classic methods for bioprinting vessel scaffolds is presented. Subsequently, we provide an in-depth analysis of the properties of the representative natural, synthetic, composite and hybrid biomaterials that can be used for bioprinting implantable vessel scaffolds. Ultimately, we underscore the necessity of leveraging biocompatibility and printability for biomaterials, and explore the unmet needs and potential applications of these biomaterials in the field of bioprinted implantable vessel scaffolds.

1. Introduction

CVDs are among the leading causes of death in humans, claiming 16.5 million lives annually, accounting for 20 % of global deaths [1]. By 2030, the estimated annual mortality from CVD-related diseases will reach 23.3 million [2]. While medications hold potential in reducing CVD-related fatalities, cardiovascular transplantation remains the primary treatment for severe cases in clinical practice [3]. Currently, three types of vascular grafts are available for transplantation: autologous vascular grafts, allogeneic vascular grafts, and synthetic vascular grafts [4–6]. Autologous vascular grafts usually have long-term patency [7], though they are limited by availability [8]. In addition, factors such as the patient's age and the specific location of the graft can influence the long-term patency of the grafts. Allogeneic vascular grafts present challenges, such as complicated operations and immune rejection [9]. Hence, the development of synthetic artificial vascular grafts has emerged as an urgent necessity in the field of CVD treatment [3].

Vessel scaffolds, as one of the potential graft alternatives for CVD treatment, are the constructs employed in the treatment of vascular diseases, including both tubular grafts and constructs for maintaining vascular patency and fostering vascular regeneration [10,11]. They provide a three-dimensional (3D) framework that supports vascular cell adhesion, growth, and the formation of new vascular tissue [12–15]. In order to address the demand for implantable artificial vessel scaffolds, tissue engineering has received increased attention. Tissue engineering involves the combination of biomaterial scaffolds constructed *in vitro* with living cells to create treatment-ready scaffolds [16]. Traditional tissue engineering manufacturing methods include solvent casting, fiber

* Corresponding author. School of Life Sciences, Shanghai University, Shanghai, China.
** Corresponding author.
*** Corresponding author.
E-mail addresses: smztmp@126.com (N. Han), wangzhm@chgc.sh.cn (Z. Wang), jiajia748@126.com (J. Jia).
[1] These authors contributed equally to this work.

https://doi.org/10.1016/j.mtbio.2024.101366
Received 11 July 2024; Received in revised form 10 November 2024; Accepted 23 November 2024
Available online 23 November 2024

adhesion, and electrostatic spinning [17]. Metals/polymers (e.g., expanded polytetrafluoroethylene (ePTFE)) scaffolds, bioresorbable vascular scaffolds (BVS) [18,19] made from degradable materials, and natural vascular scaffolding (NVS) [20] are common types of implantable vessel scaffolds produced by traditional tissue engineering manufacturing methods. The traditional vessel scaffolds, from being non-degradable to bioresorbable and from being bio-inert to bioactive, have greatly developed. However, they are still several challenges along with these scaffolds. For instance, metal scaffolds are susceptible to discontinuities and deformities [21–23]; while there is also a risk of thrombosis associated with BVS [24–26]. The overall manufacturing precision of these scaffolds is still insufficient to meet the clinical needs [27,28]. Moreover, evenly seeding cells throughout the scaffolds and constructing perfusable layered structures become significant challenges with traditional approaches [27,29–31].

Therefore, there is a need for a novel manufacturing approach that can precisely control the types of biomaterials and cells, as well as their distribution within the scaffold. Bioprinting leverages additive manufacturing techniques to print structures with bioinks according to pre-designed structures [32], allowing for the customization of implants tailored to individual patients [5]. Bioprinting holds the potentials to precisely control cell density, to create perfusable tissues, and to fabricate branched vessels to construct complex, multi-layered, and high-precision heterogeneous cellular structures [3,27,33]. It excels at customizing vascular structures to patient specifications and accurately distributing various cell types to form layered biomimetic vascular tissues [29]. Despite demonstrating significant potential in the field of vessel scaffold manufacturing and being anticipated to have a substantial impact in the coming years [30,34], current bioprinting technologies still face several challenges (such as to replicate the natural three-layered architecture of blood vessels). To enhance the fidelity of these vascular constructs, there is a continuous need to refine printing procedures and techniques. Innovative approaches such as co-axial extrusion printing and freeform reversible embedding of suspended hydrogels (FRESH) technology have emerged to address these challenges [35,36]. Furthermore, the integration of existing bioprinting methods with other techniques is being explored to fabricate vessel scaffolds with intricate architectures [37,38]. Thus, future advancements should be directed towards achieving higher resolution in vascular structures and improved biomechanical properties, which may involve the innovation of printing technology, the development of novel bioinks, and a deeper understanding of vascular biology.

Bioinks and biomaterial inks play a key role in bioprinting. Bioinks are defined as "a cellular formulation suitable for processing by automated biomanufacturing techniques, which may also contain bioactive components and materials" [39]. Those (bio)materials that are not prepared directly with cells and are imbedded with cells after printing are called biomaterial inks. Biomaterial inks can be used to produce scaffolds for cell seeding, bioreactors, implants, or they can be used in conjunction with bioink manufacturing, such as thermoplastic polymers [39]. The bioinks or biomaterial inks with good printability and biocompatibility are indispensable for the manufacture of implantable vessel scaffold [40]. Biomaterial used in the bioink can also significantly impact the rest ink components, including cells and soluble factors. The biomaterials applied in bioprinting need possess the physical and chemical properties similar to various types of natural extracellular substrates, allowing them to mimic the cellular environment [28].

The properties of biomaterials influencing the vascularization after implantation are physical, chemical and biological properties [41] (e.g. the accuracy and cell survival affected by viscosity [42,43]). Therefore, it is necessary to fine-tuning the comprehensive properties of the biomaterials to provide the optimal microenvironment for the cells inside or around the scaffolds. Additionally, it is optimal for biomaterials to provide a microenvironment conducive to endothelialization of vessel scaffolds. Endothelialization is an essential process in the vascular system, crucial not only for forming the protective barrier between blood and the vessel wall but also for its anticoagulant properties that prevent inflammation and thrombosis in vessel scaffolds [44,45]. Consequently, biomaterials for vessel scaffolds need to possess bioactivity that promotes cell adhesion and endothelialization [44].

Despite the inherent challenges in replicating the biocompatibility and biological activity, and mechanical properties of natural blood vessels in artificial ones, the characteristics of biomaterials play a pivotal role in the successful fabrication of vessel scaffolds. While a wealth of literature exists on the application of biomaterials in vascularized tissue engineering [27,41,46–48] and the burgeoning field of 3D printed vessel scaffold technologies [8,29,49,50], a comprehensive review that thoroughly examines the selections and designs of these biomaterials (or biomaterial combinations) for printing vessel scaffolds is notably absent. This study aims to bridge this gap by providing an extensive review of biomaterials (or biomaterial combinations) suitable for 3D printing of vessel scaffolds. It encompasses an analysis of material types, their properties, current applications, and potential avenues for future enhancements. The objective of this analysis is to pinpoint the essential attributes (such as printability and biocompatibility) of biomaterials and to provide guidance on the materials design for implantable vessel scaffolds.

Thus, this article initially outlines the standards that must be satisfied by implantable vessel scaffolds and provides a detailed discussion on the manufacturing technologies of conventional vessel scaffolds, as well as the performance features of the resulting vessel scaffolds. Subsequently, the focus shifts to the various biomaterials frequently utilized in bioprinting implantable vessel scaffolds, examining their properties, including printability, biocompatibility and processability, as well as the bioprinting techniques employed. The discussion will also touch upon their potential applications in the realm of implantable vessel scaffolds. Finally, the article culminates with our perspective and foresight regarding the current unmet needs in the domain of biomaterials for bioprinting implantable vessel scaffolds (Fig. 1).

2. The requirements for the production of implantable vessel scaffolds and the conventional methods of manufacturing vessel scaffolds

2.1. The classification and the requirements of implantable vessel scaffolds

Several types of blood vessels exist in the human body, each with distinct sizes, cellular compositions, extracellular matrix (ECM) and functions [8]. The human vasculature comprises arteries, veins, and capillaries, which together facilitate the circulation of blood, oxygen delivery, nutrient exchange, and waste removal throughout the body [8]. From the perspective of size, blood vessels can be classified into large vessels (inner diameter (ID) $>$ 6 mm), small vessels (ID 1$\sim$6 mm) and microvessels (ID $<$ 1 mm) [8]. From the structural perspective of the vasculature, arteries and veins have three layers: an inner endothelial cells (ECs) lining (tunica intima), a middle smooth muscle cells (SMCs) layer (tunica media), and an outer fibroblast/ECM layer (tunica adventitia); Arterioles and venules have an inner EC layer (tunica intima) and a thin surrounding SMC layer (tunica media); while capillaries consist of a single EC layer forming the inner lining (tunica intima) [8]. For more detailed information on the structure and function of these vessels, please refer to the literature [8,51–54].

Vessel scaffolds, made from biomaterials, can be categorized and assessed based on dimensions, structure, and functionality, following the classification system of natural blood vessels. One of the straightforward way to classify the vessel scaffolds is based on size and structure. However, methods of assessing the fulfilled functions of vessel scaffolds have not been standardized. In this review, we attempt to summarize the existing evaluation criteria from three aspects: biocompatibility and biological activity, mechanical properties and physical properties [29,46,55]. The detailed requirements and descriptions are

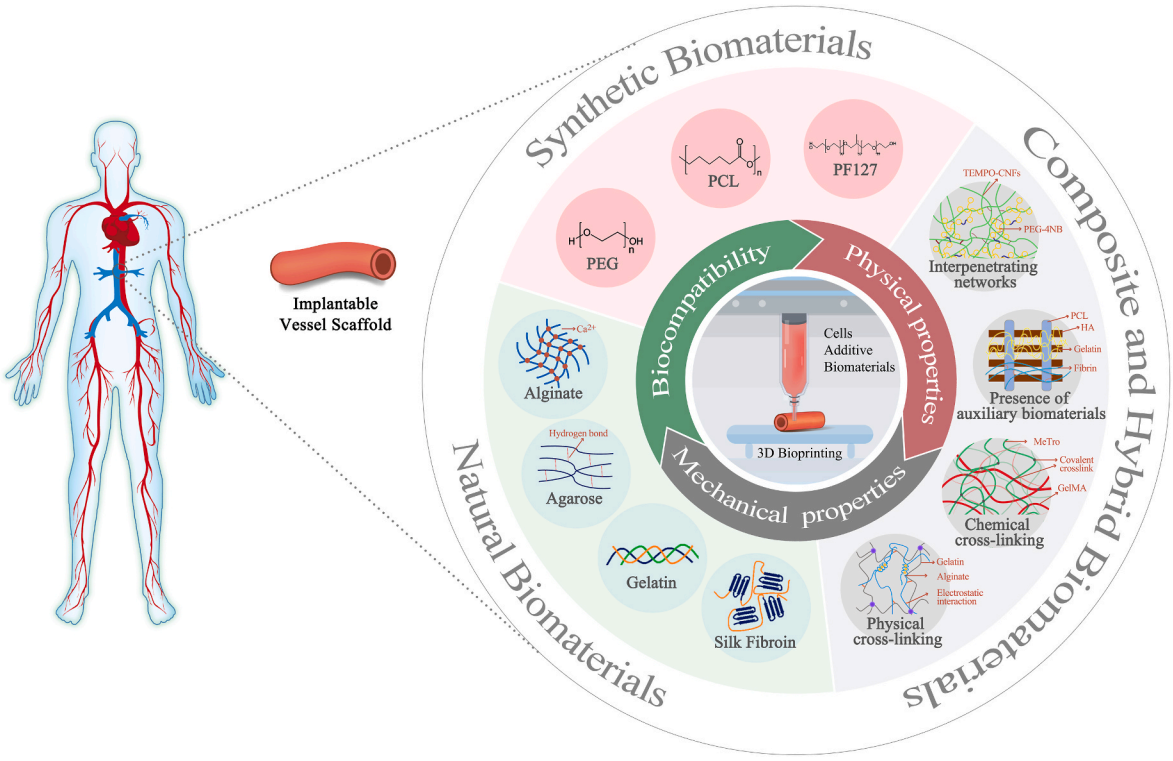

Fig. 1. Schematic illustration of biomaterials for bioprinting implantable vessel scaffolds. Utilizing bioprinting to fabricate implantable vessel scaffolds, the biomaterials required are of paramount importance. There are natural biomaterials (e.g., Alginate, Agarose, Gelatin, Silk Fibroin), synthetic biomaterials (e.g., polyethylene glycol (PEG), PCL, PF127) and composites (e.g., GelMA-MeTro, TEMPO-CNFs and PEG-4NB). Fig. 1 also illustrates the formation of composite and hybrid biomaterials through the incorporation of crosslinking principles, such as non-covalent and covalent crosslinking. The fundamental properties of the implantable vessel scaffolds, including biocompatibility and biological activity, mechanical properties and physical properties should also be considered.

presented in Table 1.

2.2. The conventional manufacturing approaches of vessel scaffolds

Traditional methods of fabricating tissue engineered vascular grafts (TEVGs) include electrospinning, freeze-drying, mold casting, and cell sheet technology. Electrospinning enables the development of small artificial threads from a variety of polymers using an electrical gradient, capable of generating nano-to micro-scale fiber structures that allow the presence of porous structures in the prepared vessel scaffolds that support cell adhesion and migration [17,64]. Liu et al. [64] have successfully fabricated small diameter vessel scaffolds (ID = 6 mm) with mechanical strength akin to the human saphenous vein and continuous endothelial lining through the application of electrospinning technology. Freeze-drying techniques also produce scaffolds with a porous structure, and the manufactured vessel scaffolds are easy to store [65]. Utilizing this technology, silk fibroin (SF) has been processed into vessel scaffolds with mechanical properties akin to those of arteries, reducing the risk of thrombosis [11]. Mold casting, in which material is placed around a tubular mold for vascular fabrication, is simple to prepare and can be combined with other methods (e.g. freeze-drying) [65,66]. By adjusting the mold size, mold casting technique can manufacture a variety of vessel scaffolds. It is capable of producing microvessels (outer diameter (OD) = 0.6 mm), which possess the ability to be perfused and have a continuous endothelial monolayer [67]. Additionally, this technology can also create small-diameter vessels (OD = 5 mm). These vessels not only have good endothelialization but also exhibit excellent mechanical properties, such as a burst pressure exceeding 4000 mmHg [66]. In addition, to reduce the use of synthetic or exogenous materials, the cell sheet technique has been developed. It is a technique that uses the ability of cells to produce ECM *in vitro* to create tissue sheets, which are then rolled around a cylindrical mandrel to form a tubular structure [68,69]. Currently, the blood vessels manufactured using this method have been validated in animal transplantation experiments, particularly within the bodies of nude mice, successfully achieving *in vivo* tissue anastomosis of small-diameter vessel scaffolds with a diameter of 4.2 mm, reaching a patency rate of 86 %, and promoting the regeneration of the vascular matrix [69]. The features of these methods, the biomaterials used, and the characteristics of the fabricated vessel scaffolds are summarized in Table 2.

Table 2 indicates that traditional methods have now been able to produce TEVGs with micrometer diameters, good mechanical properties, and implantabilities. However, these methods commonly exhibit certain drawbacks, such as limited ability to accurately customize the vascular structure, difficulties in fabricating small blood vessels (ID: 1 ~ 6 mm) and microvessels (ID: < 1 mm) with intricate structures and branching networks, and reliance on a single, simplistic vascular shape. For instance, cell sheet technology is time-consuming, costly, and prone to contamination, making it difficult to use for emergency surgeries and may cause an immune response if using allogeneic cells [59,69]. Electrospinning technology and freeze-drying technology can affect the protein structure by contacting with organic solvents during manufacturing [17,65]. But all these shortcomings can be well compensated by bioprinting, which can precisely manufacture according to the designs of the constructed vascular models, so as to prepare complex blood vessels with multiple sizes and structures. In the future development, it is suggested to apply the above-mentioned techniques with bioprinting to overcome their innate drawbacks to fabricate complex implantable vessel scaffolds.

3. Bioprinting methods

Depending on the printing principle, bioprinting methods are mainly classified into nozzle-based extrusion and inkjet printing, and laser/

Table 1
Requirement of implantable vessel scaffolds [29,46,55].

Requirement		Description	Ref.
Biocompatibility and biological activity	High cell viability	High cellular survival, metabolic activity, and proliferation rates.	[55]
	Specific markers	Particular proteins or ECM proteins secreted by cells that can reveal the status and function of vascular cells and identify blood vessels.	[55]
	Cell morphogenesis	Cellular morphogenesis similar to that *in vivo*.	NA
	Cellular function	Capabilities of cells to perform their intended roles.	[56]
	Cellular migration	Capabilities of cells to move to specific locations.	[56]
	Cellular differentiation	Capabilities of cells to develop into various cell types.	[56]
	Cellular engraftment	Capabilities of cells to successfully integrate into host tissues.	[56]
	Nontoxicity	No toxic effects on the body.	NA
	Nonimmunogenicity	No inflammatory response in the body.	NA
	Nonthrombogenicity	The ability to maintain smooth blood flow after implantation.	[29]
	Nonsusceptibility to infection	Resistant to bacterial adhesion.	NA
	Ability to grow for pediatric patients	The ability to self-growth and remodeling after surgery.	[29]
	Maintenance of a functional endothelium	The ability to form a functional layer of ECs with a smooth, semi-permeable and anti-thrombotic surface.	[29]
Mechanical properties	Compliance similar to native vessel	The ability to resume its original size or shape.	[57–59]
	Burst pressure similar to native vessel	Maximum pressure that can be withstood before acute leakage occurs.	[29,59]
	Kink and compression resistance	The ability to resist bending and remain open when subjected to external pressures.	[59,60]
	Good suture retention	Maximum tensile force of the suture that maintains the suture between the vessel scaffold and the human blood vessel.	[29,59]
	Tensile strength	Maximum tensile force to keep vessel scaffold material from fracturing.	[46]
Physical properties	Biodegradability	The dissolution rate of biomaterial molecules should be tailored to meet the specific needs of particular cells or tissues.	[61]
	Swelling	The extent of volume expansion in a liquid environment due to liquid absorption by scaffold materials.	[62]
	Structural fidelity	The degree to which the designed structure of a scaffold is maintained.	[63]

*Most of the literature does not provide detailed numbers when discussing parameters, therefore the parameter section has not been included in the table.
**Parameters related to key properties such as compliance, burst pressure, suture retention, and tensile strength are introduced in some literature. Please refer to the corresponding literature [46,59,64] for detailed information.
***Processability is an essential requirement for implantable vessel scaffolds, encompassing attributes such as low manufacturing costs, wide availability in various lengths and diameters, sterilizability, and ease of storage. However, since there are no detailed references in all the literature, this aspect is not discussed in the table.

light-based laser-induced forward transfer (LIFT) and vat-photopolymerization (Fig. 2A) [72]. It is understandable that the compatible printing methods may vary due to the different physico-chemical properties of the biomaterials [50,73–75], which can directly affect the mechanical strength of the fabricated implantable vessel scaffolds. For instance, GelMA is widely used in vat photo-polymerization due to its photocrosslinking properties of the GelMA; whereas collagen has been widely used in extrusion and inkjet printing. The nature of the biomaterial also influences the parameters of bio-printing. For example, nozzle diameter is an important parameter for nozzle-based bioprinting. A nozzle diameter that is too large can reduce the resolution of bioprinting; while one that is too small may cause clogging with high-viscosity bioinks. Therefore, it is crucial to choose an appropriate nozzle diameter that aligns with the viscosity characteristics of the biomaterials being used [15,72]. In addition, different printing method may also greatly influence the cellular activities in the bioink [76,77], which indirectly affects the qualities of the fabricated vessel scaffold. Bioprinting time is an important consideration, influenced by multiple factors including bioink viscosity, nozzle size, and structural complexity [15,78,79]. Generally, the ranking of printing speeds is as follows: inkjet, vat-photopolymerization > LIFT > extrusion (Fig. 2B) [72]. A systematic framework for evaluating specific techniques like coaxial printing remains to be developed, indicating a significant area for future study. Therefore, the choice of bioprinting method and the correlated bioinks (materials and cells) are critical to the success of the fabrications.

Extrusion printing is one of the most widely used methods, in which bioink is extruded from a nozzle by pressure control [72]. As shown in Table 3, extrusion printing offers versatility in the types of biomaterials that can be used, accommodating a wide range of viscosities required for successful printing. In order to manufacture implantable vessel scaffolds of different sizes and structures in a faster and easier way, extrusion methods have been continuously advanced, developing from simple extrusion to: (1) Coaxial printing using extrusion with multiple coaxially placed nozzles (Fig. 3A(i)) [35], which allows for faster and easier preparation of continuous hollow tubular structures with controlled diameter and length compared to normal extrusion [15,80–82]. It is evident from Table 3 that, influenced by the size of the coaxial nozzle, coaxial printing is particularly suitable for the fabrication of small and micro unbranched vessels.; (2) FRESH printing [36], by utilizing a support bath, can effectively facilitate the crosslinking process of low-viscosity biomaterials (Fig. 3A(ii)). This allows for an expansion of the concentration range of biomaterials suitable for extrusion printing. However, this method requires materials with superior rheological characteristics for both the suspension bath and the bioink. The bioink should exhibit shear-thinning properties, maintaining stability across varying temperatures. Additionally, the support bath should have

Table 2
Vessel scaffolds manufactured by conventional methods.

Manufacturing method	Methodological features (advantages and disadvantages)	Examples of fabrication of vessel scaffolds			Ref.
		Biomaterials or materials	Dimensions of scaffolds	Characteristics of vessel scaffolds	
Electrospinning	**Advantages:** Capable of forming nano- to micro-scale fibrous structures resembling protein fibers with interconnected pores; Compatible with 3D bioprinting; **Disadvantages:** Potential denaturation of proteins due to the use of organic solvents in the manufacturing process; Inability to co-produce with cells; Risk of structural loss of control during the manufacturing.	SF	ID: 5 mm OD: 6 mm	Tensile strength: 3.57 MPa; Elongation: 12 %; Porosity: above 80 %.	[70]
		Poly(dl-lactide)–poly (ethylene glycol) (PELA)	ID: 6 mm OD: 6.9 mm	With a continuous endothelium covering the entire luminal surface and a highly aligned SMCs layer with ECM; Higher tensile strength, rupture strain, and suture retention strength than human femoral artery; Rupture pressure and radial compliance are the same as human saphenous vein.	[64]
Freeze-drying	**Advantages:** Capable of forming porous structure conducive to cell growth; **Disadvantages:** Inability to co-produce with cells; Potential denaturation of proteins due to the use of organic solvents in the manufacturing process.	Decellularized aortic matrix (DAM), poly-L-lactide acid (PLLA), PEG	ID: 4 mm OD: 6 mm	Robustness against cell contraction and elasticity for cell communication; Supporting adhesion and growth of endothelial and SMCs.	[65]
		Silk proteins	ID: NA Thickness: 750 μm	Low thrombogenicity; Mechanical properties compatible with the mammary artery (including rupture pressure, suture retention strength and compliance).	[71]
Mold casting	**Advantages:** Fast and easy preparation; Available in combination with freeze-drying. **Disadvantages:** Challenging to produce intricate vessel scaffolds.	Collagen-Elastin analogs	Scaffold 1: ID: 1.29 ± 0.07 mm OD: 1.73 ± 0.08 mm; Scaffold 2: ID: 4.01 ± 0.02 mm OD: 4.49 ± 0.06 mm	Compliance close to natural veins; Adequate suturability; Rupture pressure not as high as natural arteries, but approximately three to four times the maximum physiological pressure.	[59]
		Methacrylated gelatin (GelMA)	OD: 0.6 and 1.2 mm Thickness: 120–400 μm	Capable of continuous media perfusion; Mechanical properties of the vascular structure change significantly with GelMA concentration; With a continuous EC monolayer showing a strong barrier function.	[67]
		Fibrin	ID: 4 mm OD: 5 mm	Rupture pressures >4000 mmHg; Compliance = sheep femoral arteries; Anisotropy: natural artery-like; Vascular channels: smooth, no dilatation/ mineralization; Lumen diameters: stable; Recellularisation: extensive, majority α-Smooth muscle actin (α-SMA); Endothelialisation: complete at 24 weeks, high elastin deposition.	[66]
Cell sheet technology	**Advantages:** Not dependent on synthetic or exogenous materials; **Disadvantages:** Long preparation time, not available for urgent clinical use.	Human fibroblast-derived ECM	ID: 4.5 mm OD: NA	Vascular constructs with SMC: enhanced vasoactivity and mechanical properties; Increased resistance, contractility; Storage: long-term viability; Patency: sustained over time; Considerations: extended generation, high costs.	[68]
		Collagen, elastin-like protein polymers	ID: 4.2 mm OD: 5 mm	Better mechanical properties than saphenous veins; Ease handling, good suturability; Implantation (225 days): increased diameter, 86 % patency; Anastomosis: successful with *in vivo* tissues, no failure; Presenting anti-thrombotic properties; Endothelial cell fusion; Vascular regeneration; Substantial immune response.	[69]

self-healing capabilities and be capable of photo-crosslinking [83]; (3) Rotary bioprinting involves printing hollow channels on a rotating rod through vertically oriented extrusion of the print nozzle (Fig. 3A(iii)). This method effectively interacts with axial rotation of the stepper motor module, thereby saving the deposition time of the support or sacrificial material. As a result, it can significantly reduce the printing time of the vascular structures, enabling low-cost and more rapid preparation of these structures [33,38,84]; and (4) Multi-nozzle printing, facilitated by multiple nozzles technology, enhances efficiency through faster material transitions and the simultaneous operation of multiple nozzles (Fig. 3A (iv)) [15]. This approach streamlines the bioprinting of multi-layered vessel scaffolds, expediting the fabrication of intricate structures [85, 86]. In conclusion, extrusion printing has seen significant advancements, evolving from basic extrusion techniques to more sophisticated methods that enhance the efficiency and versatility of vessel scaffold fabrication.

Inkjet printing is another nozzle-based printing technology, common methods include drop-on-demand printing (Fig. 3B) [90]. Inkjet printing

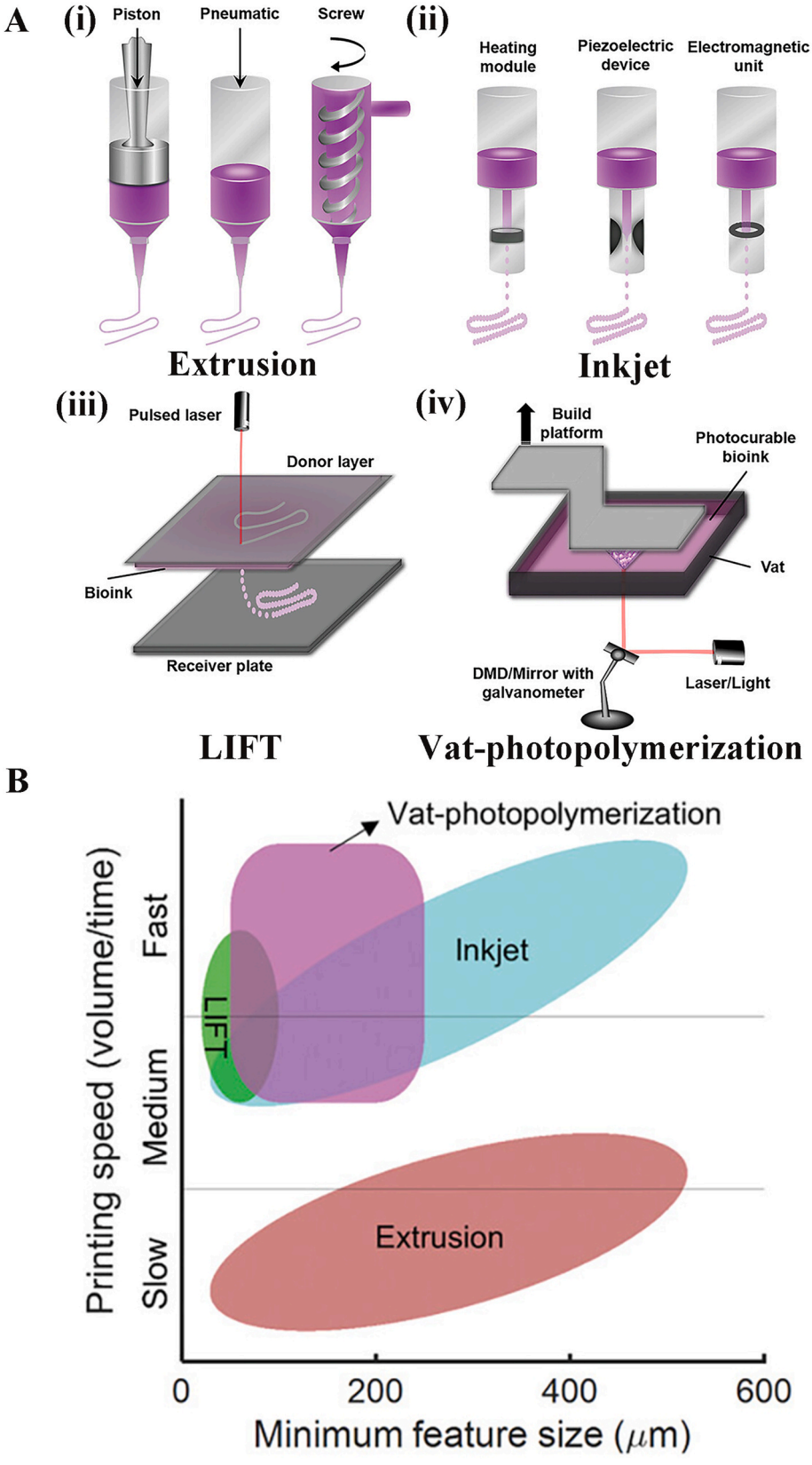

Fig. 2. Bioprinting methods for vessel scaffold fabrication and speed comparison of them. A) Schematic showing the different bioprinting methods. i) Extrusion; ii) Inkjet; iii) LIFT; iv) Vat-photopolymerization. Reproduced and adapted with permission [72]. Copyright 2021, John Wiley and Sons. B) Speed comparison of different printing methods. Reproduced and adapted with permission [72]. Copyright 2021, John Wiley and Sons.

Table 3
Bioprinting methods for implantable vessel scaffold printing.

Categorization of bioprinting methods	Bioprinting methods	Features of the methods (advantages and disadvantages)	Examples of bioprinted vessel scaffolds				
			Biomaterials	Printing parameters	Scaffold dimensions, layer numbers, thickness	Biological data	Ref.
Extrusion bioprinting ($30–10^7$ mPa s)	Normal Extrusion	**Advantages:** Suitable for biomaterials with a wide range of viscosities; **Disadvantages:** Low print speed.	Alginate, Collagen	Nozzle pressure: 100 kPa; Nozzle size: 25 G¼ inch lock-tip nozzle.	Dimensions: 100–200 μm diameter; Layer numbers: 3 layers (inner, middle and outer); Thickness: NA.	Detectable cell markers CD31, NG2, α-SMA, CD34; able to engraft into the chicken chorioallantoic membrane (CAM) and connect with CAM vessels and perfuse *in vivo*.	[87]
			Polycaprolactone (PCL), Gelatin	Nozzle ID: 300 μm; Printing temperature: 18 °C; Pneumatic pressure: 90–100 kPa.	Dimensions: approx. 280 μm in diameter; Layer numbers: NA; Thickness: NA.	Cell survival at day 7 exceeded 90 %; Secreted markers: CD31; Forming actin network with collagen deposition; Forming vascular lumen.	[85]
	Coaxial Printing	**Advantages**: Adjustable channel dimensions for a variety of tube diameters; Feasible high throughput manufacturing of long continuous tubes; Suitable for the manufacturing of small and microvessel scaffolds; **Disadvantages:** Difficult to print multi-layered and branched vascular structures.	Gelatin-PEG-tyramine (GPT), Gelatin	Bioink flow rate: 2 mm/s; Nozzle stroke feed rate: 10 mm/s stroke feed rate; Inner tip model: 30 G; Outer tip model: 22 G.	Scaffold without cells: Dimensions: ID 485.5 ± 31.1 μm, OD 670 ± 39.1 μm; Layer numbers: NA; Thickness: NA. Cell-containing scaffold: Dimensions: elliptical cross-section, with a long axis dimension of 880 μm and a short axis dimension of 240 μm; with an OD of 983.09 ± 37.6 μm; Layer numbers: 2 (core layer containing HUVEC and outer layer containing HDF); Thickness: NA.	Human dermal fibroblasts (HDFs) maintaining more than 80 % cell viability within 2 h; Human umbilical vein endothelial cells (HUVECs) maintaining more than 80 % cell viability after 2 days.	[88]
			Alginate, Collagen, Fibrin	Bioink flow rate: 1–6 ml/min; Print speed: 1–16 m/min; Needle types: 26 G flat head, 20 G, 18 G.	Dimensions: hollow channel sizes from 0.69 ± 0.01 mm to 1.18 ± 0.04 mm, inner gel layer sizes from 1.05 ± 0.02 mm to 1.47 ± 0.05 mm, outer gel layer sizes from 1.85 ± 0.06 mm to 2.31 ± 0.05 mm; Layer numbers: 2; Thickness: NA.	Long-term viability of cells; Adhesion of cells.	[15]
	FRESH	**Advantages:** Applicability to low-concentration biomaterial; Possibility of manufacturing complex and hollow structures; **Disadvantages:** Requirements for the rheological properties of the suspension bath and bioink.	GelMA, Methacryloyl-substituted recombinant human tropoelastin (MeTro)	Extrusion pressure: 15 kPa; Extrusion speed: 30 mm/s speed; Printing temperature: 8–10 °C.	NA.	85 % or more cell viability at 7 days; Secretion of the cell marker CD31.	[36]
	Rotary Printing	**Advantages:** Ability to deposit layers for forming multilayer structures; **Disadvantages:** Restriction of ID by the	Gelatin, Fibrin	Needle type: 4 G; Linear extrusion rate: 100 mm/min; Rotating shaft: 4.9 mm OD polystyrene rod;	Dimensions: length 20 mm, ID 4.9 mm, OD 10.9 mm; Layer numbers: NA; Thickness: NA.	Circumferential arrangement of fibroblasts near the vascular surface; Spindle-shaped cells in the inner layer of	[84]

(*continued on next page*)

Table 3 (*continued*)

Categorization of bioprinting methods	Bioprinting methods	Features of the methods (advantages and disadvantages)	Examples of bioprinted vessel scaffolds				
			Biomaterials	Printing parameters	Scaffold dimensions, layer numbers, thickness	Biological data	Ref.
		rotating axis; Difficulty in printing branched and complex structures.		Extrusion flow rate: 1–7 ml/min.		the vessel (lumen side); Increased collagen deposition.	
	Multi-nozzle printing	**Advantages:** Reduction in material transition time; Simultaneous printing with multiple nozzles; **Disadvantages:** NA.	Decellularized extracellular matrix (dECM), Pluronic F127 (PF127)	Printing temperature: 4 °C; Nozzle size: 150 μm conical plastic needle.	Dimensions: 6 mm in diameter; Layer numbers: 3; Thickness: NA.	Pre-vascularization of ECs occurring in the cell layer	[86]
			Oxidized alginate (OA), Gelatin	Needle size: 23 G; Nozzle pressure: up to 2 bars.	Dimensions: 400 μm; Layer numbers: NA; Thickness: NA.	Increased cell viability and doubling of cell number after 14 days of long-term cell culture.	[89]
Inkjet bioprinting (3–30 mPa s)	Drop-on-demand printing	**Advantages:** Controlled droplet volume; Suitable for low-viscosity bioinks; Fast printing speed; High resolution; **Disadvantages:** Difficulty in fabricating thick structures and multi-material structures; Limited in the construction of large-diameter multi-layer blood vessels.	Agarose, Collagen	Nozzle diameter: 150, 300 and 600 μm.	NA.	High cell viability; Extension and migration of ECs.	[90]
			Collagen, Fibrin	Solenoid micro-valve diameter: 0.15 mm; Nozzle diameter: 0.3 mm; Print pressure: 0.5 bars; Valve opening time: 450 μs.	Dimensions: about 1 mm in diameter; Layer numbers: 3 (endothelial layer, SMC layer, fibroblast layer); Thickness: 425 μm.	High cell viability (>83 %); Secretion of markers (VE-Cadherin, SMA, collagen IV); Continuous ECs forming on the inner surface of the lumen after 4 days; ECs maturing after 3 weeks of dynamic culture; SMCs distributing around the membrane endothelium with elongated, healthy cells that mimic the membrane medium.	[91]
LIFT (1–300 mPa s)	MAPLE DW	**Advantages:** Negligible thermal and UV damage; Available to initiate and direct self-organization of tissue components; **Disadvantages:** Mechanical stress/strain damage during jet/droplet formation and descent.	Matrigel	Laser energy: 0.5–1.5 μJ/pulse; Laser spot: elliptical ~8 × 11 μm^2; droplet diameter ~50 μm; Spacing from each other along the branching/stemming structure: 50–150 μm.	NA.	Cell survival was close to 100 %; ECs self-organised to form a lumen.	[92]
			Alginate	Laser fluence: 1445 mJ/cm^2; Substrate speed: 80 mm/min; Repetition rate: 10 Hz; Direct write height setting: 2 mm.	Straight tube: Dimensions: 5.0 mm in diameter and 6.5 mm in height; Layer numbers: NA; Thickness: 2.3 ± 0.3 mm. Y-shaped tubular constructs: Dimensions: inclination angle of 45°, diameter of 5 mm, total height of about 9.5 mm; Layer numbers: NA; Thickness: 1.4 ± 0.3 mm. Y-shaped constructs: Dimensions: 5 mm diameter, total height 9.5 mm; Layer numbers: NA; Thickness: 2.5 ± 0.3 mm.	Cell viability >60 %.	[93]

(*continued on next page*)

Table 3 (*continued*)

Categorization of bioprinting methods	Bioprinting methods	Features of the methods (advantages and disadvantages)	Examples of bioprinted vessel scaffolds				
			Biomaterials	Printing parameters	Scaffold dimensions, layer numbers, thickness	Biological data	Ref.
VAT photopolymerization (250–5000 mPa s)	SLA	**Advantages:** Capable of producing large arbitrary shapes and hollow structures; **Disadvantages:** NA.	Poly (ethylene glycol) methacrylate (PEGMA)	Light layer thickness: 200 μm; Layer exposure time: 100 s, 120 s, 160 s.	Dimensions: bifurcated tubular structure (OD 6.2 mm); Layer numbers: NA; Thickness: NA.	Increased metabolic activity of the cells from day 4 to day 14; Evenly distribution of the cells.	[94]
			Polytrimethylene carbonate (PTMC)-based resins	Light wavelength: 365 nm; Light intensity: 17 mW/cm^2.	Dimensions: internal width of about 224 μm; Layer numbers: NA; Thickness: 152 μm.	HUVECs attachment after 4 h and formation of a near-fusion layer after 3 days of static incubation.	[95]
			GelMA	Light type: UV; Irradiation intensity: 50 mW/cm^2; Exposure time: 20 s.	NA.	Spreading and proliferation of cells occurred over a long period of time; Forming a confluent layer of HUVEC on the surface of the scaffold; Secretion of cell markers (CD31, vWF, Ki67).	[13]
	DLP	**Advantages:** Ability to generate an entire layer of the desired pattern in one pass; Enabling the fabrication of 3D structures with complex geometries; Micron-level print resolution; High printing speeds; Good pattern flexibility and scalability; **Disadvantages:** Not suitable for biomaterials that are difficult to rapidly photocure or have excessively high viscosity.	GelMA	UV intensity: 10 mW/cm^2; Exposure time: 30 s; Layer thickness: 150–200 μm.	Dimensions: OD 3.2 mm, ID 2 mm; Layer numbers: NA; Thickness: 0.6 mm.	Cell survival >70 %.	[96]
			GelMA	Light wavelength: 365 nm; UV intensity: 7.9 mW/cm^2; Exposure time: 20 s.	Dimensions: branch height of 10 mm; Layer numbers: NA; Thickness: 200 μm.	Cell viability 80 % after 48 h.	[97]
Combinatorial methods	Extrusion Printing + Photocrosslinking	**Advantages:** Capable of enhancing the stability of the structure by photocrosslinking after extrusion; **Disadvantages:** NA	Gelatin-Norbornene (Gel-NOR)	Light wavelength: 405 nm; Light exposure time: 1 min; Light intensity: 60 mW/cm^2; Needle size: 19 G.	Microvessels formed by cellular self-assembly; Dimensions, layer numbers, thickness: NA.	Secretion of cellular markers (CD31, α-SMA).	[98]
			Catecholin-functionalized methacrylate gelatin (GelMA/C); PF127	Laser beam: 190 μm; Laser wavelength: 355 nm; UV output intensity: ~20 μJ; Extrusion speed: 0–100 mm/s; Extrusion flow rate: 0–1.0 ml/s; Outer needle model: 18 G; Inner needle model: 22 G.	Dimensions: diameter of 900 μm; Layer numbers: 2 layers (smooth muscle layer and endothelial layer); Thickness: NA.	Total cell viability >100 % at day 7; Cell secretion markers: α-SMA, CD31, Vinculin, F-actin and VE-Cadherin, vWF, Myo; Angiogenesis and smooth muscle differentiation; Connections between printed blood vessels and host mouse blood vessels occurring.	[37]
			GelMA, Poly (-ethylene glycol) -tetra-acrylate (PEGTA)	External needle model: 20G; Internal needle model: 30G Internal needle; UV wavelength: 360–480 nm; Optical Power: 6.9 mW/cm^2; Light	Dimensions: OD 500–1500 μm, ID 400–1000 μm; Layer numbers: 3; Thickness: 60–280 μm.	Gradual increasing of cellular metabolic activity; Proliferation of cells, filling the walls of the tubes after 21 days to form complete vessel-like structures; Cell survival rate >80 %;	[81]

(*continued on next page*)

Table 3 (*continued*)

Categorization of bioprinting methods	Bioprinting methods	Features of the methods (advantages and disadvantages)	Examples of bioprinted vessel scaffolds				
			Biomaterials	Printing parameters	Scaffold dimensions, layer numbers, thickness	Biological data	Ref.
				Source Distance: 8 cm.		Secretion of markers (CD31 and α-SMA).	
	Bioprinting + Microfluidics	**Advantages:** Facilitating the switching and mixing of different bioinks in multi-material printing; **Disadvantages:** NA	NA	NA	NA	NA	[15, 82]
	Bioprinting + Electrostatic Spinning	**Advantages:** Electrostatic spinning to fabricate high-strength, highly elastic nanoscale structures with ductility and ECs adhesion; **Disadvantages:** NA.	GelMA, PCL	Nozzle Diameter: 300 μm; Printing Pressure: 100 kPa; Printing Speed: 5 mm/min; Rotation Speed: 40 rpm; Temperature: 20 °C; Needle Model: 18 G Needle; Flow Rate Jet: 1 ml/h. Voltage: 25 kv; Rotation Speed: 1000 rpm.	Dimensions: 1.78 mm ID; Layer numbers: 2 layers (GelMA holder as outer layer and electrostatically spun PCL as inner layer); Thickness: 0.78 mm for the outer layer and 0.31 mm for the inner layer.	Good proliferation of HUVECs, with 97.38 ± 0.35 % cell viability at day 7, forming a flattened cell layer; Good proliferation of SMCs with cell viability consistently exceeding 90 %; Fully spreading of cells into a linear shape at day 7, with orderly arrangement along the direction of the print; Secretion of collagen by the cells.	[38]
			Alginate, Polyethylene oxide (PEO)	DC voltage: 10.5 kv; Cylindrical electrode diameter: 360 μm; Parallel deposition time: 3 min; Electric field: 0.075 kV/mm.	Microvascular	Cell viability: 90 %.	[14]
	Bioprinting + Mold Casting	**Advantages:** Simple and easy fabrication of tubular structures achieved by three steps; **Disadvantages:** NA	NA	NA	Dimensions: 600–800 μm; Layer numbers: NA; Thickness: NA.	NA	[80]

*The parentheses in the "Categorization of Bioprinting Methods" section specify the ideal viscosity for biomaterials corresponding to each method.

technology is suitable for fabricating low-viscosity bioinks, with faster droplet ejection than extrusion printing and precise droplet control, enabling the creation of higher-resolution structures [99]. Nonetheless, it has its limitations, such as the capacity to produce thick structures and multi-material constructs being restricted, which may reduce its application in the preparation of large-diameter multi-layer vessel scaffolds [72].

LIFT technology uses a pulsed laser to irradiate the bioink in the donor layer, causing it to produce droplets and transfer them to the receiver plate in a voxelated manner [72,92]. LIFT can also be adapted to other forms, such as Matrix-assisted pulsed-laser evaporation direct-write (MAPLE DW) (Fig. 3C) [93]. The LIFT technique may subject cells to mechanical stress and strain during the jetting/droplet formation and deposition process, which could potentially lead to cell necrosis and death. However, with its high resolution and rapid printing speed, LIFT technology offers the potential for high-precision and quick printing of vessel scaffolds.

Vat photopolymerization utilizes precise light pattern generated by digital micromirror device (DMD) to selectively expose photocurable bioink to light, achieving the crosslinking of the entire layer (Fig. 3D–E) [72,94,97]. With the use of some high-resolution digital light processing (DLP) light engines, the bioink can solidify within a few hundred milliseconds, thus providing a rapid printing speed [72,97]. Additionally, this technology offers high flexibility in pattern design and good scalability, giving it a significant advantage in the field of bioprinting [72,96]. Photo-initiators are crucial substances in light-based printing methods, capable of promoting the crosslinking of groups within biomaterials, thereby initiating the polymerization process. The degree of crosslinking in the biomaterials can be regulated by controlling the type and concentration of the photo-initiator, as well as by adjusting the wavelength and duration of the light exposure [100]. However, cellular responses within printed structures are influenced by the biocompatibility of the photoinitiator, the byproducts it generates (like free radicals), and light exposure parameters (light intensity, wavelength and duration) [100,101]. These features are listed in Table 3.

Different bioprinting methods can be effectively combined to meet the diverse fabrication requirements of vessel scaffolds. For instance, the integration of coaxial extrusion with stereolithography (SLA) has successfully produced hollow bilayer blood vessels. These vessels not only mimic the biological and functional characteristics of natural blood vessels but also demonstrate biocompatibility and biological activity *in vivo*, as evidenced by their ability to anastomose with the innate blood vasculatures of mice without triggering severe inflammatory responses [37]. Furthermore, the synergy of bioprinting with traditional techniques such as electrospinning [14,38] and microfluidics [82] addresses specific fabrication challenges. As illustrated in Table 3, these combinatorial strategies are essential for the realization of complex vessel scaffolds. Ultimately, selecting the appropriate printing method in

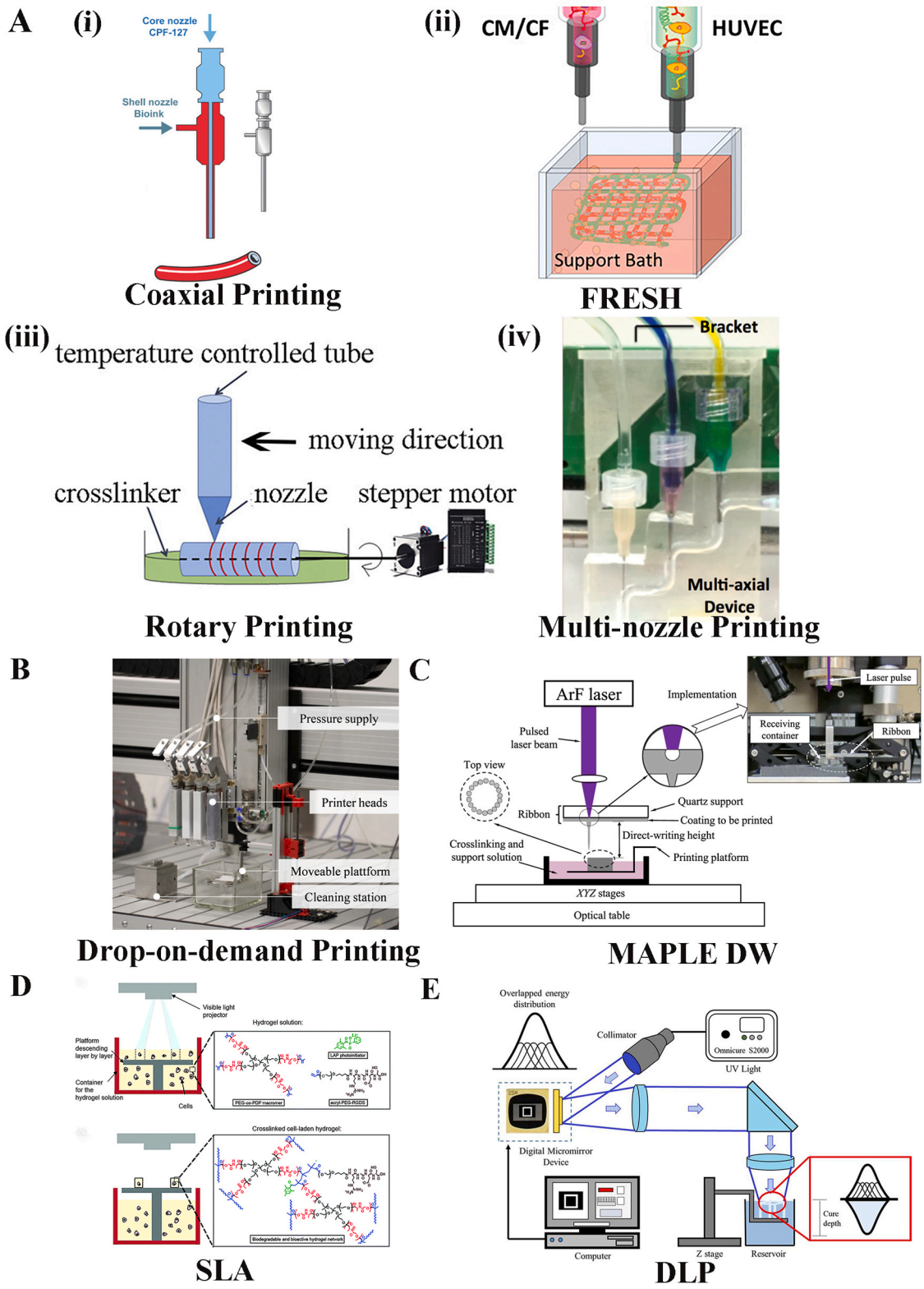

Fig. 3. Specific printing methods for implantable vessel scaffolds. A) Advanced extrusion printing methods. i) Coaxial Printing. Reproduced and adapted with permission [35]. Copyright 2017, John Wiley and Sons. ii) FRESH. Reproduced and adapted with permission [36]. Copyright 2020, John Wiley and Sons. iii) Rotary Printing. Reproduced and adapted with permission [33]. Copyright 2020, Elsevier. iv) Multi-nozzle printing. Reproduced and adapted with permission [15]. Copyright 2018, IOP Publishing. B) Drop-on-demand printing. Reproduced and adapted with permission [90]. Copyright 2016, IOP Publishing. C) MAPLE DW, a common form of modified LIFT. Reproduced and adapted with permission [93]. Copyright 2015, IOP Publishing. D) SLA, a method of vat-photopolymerization. Reproduced and adapted with permission [94]. Copyright 2015, Royal Society of Chemistry. E) DLP, a method of vat-photopolymerization. Reproduced and adapted with permission [97]. Copyright 2020, Elsevier.

conjunction with suitable biomaterials is crucial for the successful fabrication of vessel scaffolds tailored to transplantation needs.

4. Biomaterials used in 3D bioprinting implantable vessel scaffolds

Biomaterials used for bioprinting implantable vessel scaffolds can be classified as natural and synthetic biomaterials in terms of their origin. Natural biomaterials are isolated from living organisms [30]. Synthetic biomaterials are prepared by chemical synthesis [30,102]. The composite and hybrid biomaterials with manageable physicochemical properties and good biocompatibility can also be obtained by combining several different types of biomaterials.

4.1. Natural biomaterials

Natural biomaterials can simulate the ECM environments with great biocompatibilities. Natural biomaterials can be roughly classified into carbohydrate based and protein based according to their structural properties. The applications of these biomaterials in bioprinting vessel scaffolds have been shown in Table 4.

4.1.1. Carbohydrate biomaterials

Carbohydrate (based) biomaterials, which are composed of repeated monosaccharide units covalently linked by glycosidic bonds, offer significant benefits for bioprinting, including biocompatibility, suitability for natural degradation, and a range of sourcing options [42]. In addition, carbohydrates contain easily modifiable functional groups whose physicochemical properties can be customized; while polysaccharide units also play an important role in cell signal transduction [108]. However, there are limited bioactivities for carbohydrates to directly induce vasculature generation or vascular morphogenesis. Therefore, carbohydrate biomaterials are one of the widely used base (blank) materials for bioprinting vessel scaffolds including alginate (and its modifiers), agarose, nanocellulose, etc [109].

4.1.1.1. Alginate and its modifiers. Alginate is a long chain biomaterial with anionic properties extracted from brown algae [110]. Alginate has controllable mechanical properties that are influenced by the monosaccharide [16,111] units in them and ions [18]. It features a gentle gelation process, making it suitable for cell encapsulation [18]. Nevertheless, the ionic cross-linking within the alginate is reversible, which makes it susceptible to degradation and compromises its long-term stability [42]. Therefore, multiple strategies have been developed (e.g., three-stage cross-linking method [110] and using of dual-core coaxial nozzles [112,113]) to promote its cross-linking. Sun et al. [113] employed coaxial printing technology to fabricate a hollow single-layer vessel scaffold from sodium alginate. This scaffold exhibits high mechanical strength (ultimate stress reaching up to 1.88 MPa, elastic modulus reaching up to 2 MPa), and a suitable degradation rate. Moreover, it demonstrated excellent biocompatibility and biological activity for the proliferation of HUVECs. Alginate can also be prepared into alginate microspheres with porous structure and high flexibility using electroassisted ink-jet printing technology to promote the adhesion and proliferation of ECs and the formation of prevascular tissue [114]. Alginate is capable of bioprinting heterogeneous multilayered blood vessels of different diameters (9 μm-5 mm) with a branch structure [15,33,35,81,82,87,103].

Alginate hydrogels exhibit low degradability *in vivo*, primarily due to two reasons. Firstly, the molecular weight of the chains produced by the dissociation of sodium alginate is unpredictable, and only chains with a molecular weight below 50 kDa can be excreted by the kidneys [18]. Secondly, mammals lack enzymes capable of degrading sodium alginate, making it difficult to break down high molecular weight alginate chains [18]. In addition, the molecular interaction between alginate and mammalian cells is weak, leading to poor cell adhesion [18].

To address these issues, the chemical modification of alginate is an effective approach. For instance, oxidizing alginate with an oxidizing agent (e.g. sodium periodate) can convert carbonyl groups into aldehyde groups, which then react with adjacent hydroxyl groups to form hemiacetals, thereby enhancing its degradability. Oxidized alginate (OA) contains more reactive chemical groups (e.g. aldehyde groups), and thus shows better degradation performance [115]. The free radicals generated during the oxidation process cause the polymer to slowly break down, reducing the molecular weight, hardness, and stiffness of OA, allowing a variety of cells to attach, to grow and to proliferate. New tissues can be formed on the scaffold of OA, and it has good potential to induce the vascular tissue formation [18]. Sakai et al. [105] developed OA crosslinked Alg/gelatin hydrogels using OA as a crosslinking agent. This biomaterial had cell-adhesive surfaces and enzymatic degradability, and could form a channel with a layered cellular structure in collagen for the potential in vascular engineering (Fig. 4A–B).

Further development of OA is promising for bioprinting vascularized tissues and vessel scaffolds. Both the oxidation degree and the concentration of OA solution together affect its viscosity, which in turn further affects the fidelity of the structure and the cells in it. Jia et al. [79] tested 30 formulations of OA with different oxidation degrees and concentrations, and obtained the optimal viscosity range according to three printing suitability criteria (i.e. cell suspension in the printing structure, printing resolution and cell viability, which provided a good reference for the preparation of OA-based bioinks (Fig. 4C). They further modified OA by incorporating 1 % RGD peptides to promote cell attachment and diffusion. Similarly, Barrs et al. [104] modified RGD and a vascular endothelial growth factor (VEGF) mimetic peptide with a matrix metalloproteinase-cleavable linker (MMPQK) in OA. RGD and MMPQK peptides can promote vaso-specific matrix assembly. Compared with unmodified alginate, the structure printed by the modified biomaterial enhanced vascular morphogenesis at day 7 and formed a tubular capillary network with a lumen diameter of approximately 9 μm at day 14 (Fig. 4D).

In summary, although OA shows great potential in bioprinting and tissue engineering, a series of technical and biological challenges need to be overcome to realize its wide application in clinical therapy. Future research may need to focus on the combinatorial modifications of materials, the optimization of cytocompatibility, the precise construction of vascularized structures, and the long-term evaluation of functionality and clinical efficacy of applications.

4.1.1.2. Agarose. Agarose, a natural polysaccharide extracted from red algae, is renowned for its exceptional temperature sensitivity and adjustable mechanical strength, making it a valuable biomaterial in the realm of bioprinting and tissue engineering [42,116]. At low temperatures, agarose chains spontaneously form stable double helices, a structure that is crucial for its gelling properties [42]. The internal cavities within these helices engage in hydrogen bonding with water molecules, which contributes to the gel's thermoreversible nature and its ability to form a vessel scaffold for cell encapsulation.

Due to its natural reticulated structure and porosity, agarose can support cell encapsulation in bioprinting and is conducive to the permeation of oxygen and nutrients [42,117]. Agarose, being biologically inert, exhibits minimal cytotoxicity and is non-immunogenic. However, it lacks adhesive motifs and the cell-matrix interactions necessary for mechanical transduction, possessing anti-adhesive nature, limiting cell adhesion and proliferation [42,117]. Interestingly, this characteristic can be utilized to fabricate a microwell system that promotes cell aggregation, enabling the spontaneous formation of a capillary-like network and lumen [106]. The anti-adhesive nature of agarose also allows it to serve as a support material for scaffold-free vascular bioprinting. Cylindrical agarose molds support the fusion of the contained cellular cylinders to form vascular shapes, which can then

Table 4
Natural and synthetic biomaterials for bioprinting vessel scaffolds.

Biomaterial, common concentrations, and suitable printing methods	Advantages	Disadvantages	Improvements	Types of vessel scaffolds achieved	Ref.
Alginate 0.5–5 % (w/v) Extrusion; LIFT; Cellular electrospinning + 3D printing process	**Printability**: easy to process and produce; fast cross-linking; adjustable chemical and physical properties; shear-thinning. **Biocompatibility**: non-toxic; biodegradable; non-immunogenic.	**Printability**: poor stability; easily degraded. **Biocompatibility**: restricting cell adhesion and proliferation; hindering oxygen and nutrient transportation at high concentrations.	(1) Composite biomaterial inks with collagen, sodium alginate oxide, gelatin, nanocellulose, fibronectin, agarose, SF, PEO, and carbon nanotubes; (2) Physical cross-linking mechanism (Ca^{2+}, Ba^{2+}); (3) Cell adhesion capability and degradability by modificaitions.	**Size**: wide range of diameters, from microvessels (9 μm in diameter) to small vessels (5 mm in diameter). **Shape**: straight; branched large-diameter vessels. **Layers**: heterogeneous multilayered vessels.	[14,15, 33,42, 81,82, 93,87, 89,103, 104]
OA 7.5–8 % (w/v) Extrusion	**Printability**: high degradation rate. **Biocompatibility**: high cell adhesion; promoting cell-substrate interactions.	**Printability**: low viscosity; reduced integrity; low printing accuracy.	(1) Composite biomaterial inks with sodium alginate and gelatin; (2) Cell adhesion capability by peptide modification.	**Size**: microvessels (500 μm–1 mm). **Shape**: straight tube.	[89, 105]
Agarose 0.5–3 % (w/v) Inkjet; Extrusion	**Printability**: temperature-dependent gelation mechanism; regulated mechanical and rheological properties; porous; malleable; simple gelation. **Biocompatibility**: cellular encapsulation; no cytotoxicity.	**Printability**: low compressibility; low degradability. **Biocompatibility**: detrimental to cell adhesion.	(1) Composite biomaterials inks with collagen, nanocellulose, and sodium alginate; (2) Prepared as agarose microwells that can form capillaries.	**Size**: microvessels (<10 μm). **Shape**: branching capillary network.	[42,90, 106]
Nanocellulose 0.5 % (w/v) Extrusion; SLA	**Printability**: rheological properties; high elastic modulus; low density; high specific surface area; easy surface modification. **Biocompatibility**: degradability; low cytotoxicity; structural similarity to ECM.	**Printability**: poor mechanical properties; easy to dissociate.	(1) Composite biomaterial inks with alginate and agarose; (2) Prepared as modified biomaterials.	NA.	[42,62]
Collagen 0.015–0.25 % (w/v) Extrusion; Inkjet	**Printability**: NA. **Biocompatibility**: promoting synthesis of angiogenic ECM biopolymers and supporting angiogenesis; promoting cell attachment, cell migration, cell-cell and cell-gel interactions.	**Printability**: slow cross-linking; low modulus of elasticity; low fidelity; poor mechanical properties.	(1) Composite biomaterial inks with alginate, fibrin, and gelatin.	**Size**: from microvessels to small-diameter vessels (2.31 mm in diameters). **Shape**: straight tubes, branching capillary network. **Layers**: heterogeneous multilayered vessels.	[15,32, 90,87, 91]
Gelatin 3.5–15 % (w/v) Extrusion; SLA	**Printability**: thermally reversible properties; shear-thinning; tunable printability; low cost; multiple sources; degradable. **Biocompatibility**: containing RGD sequences that promote cell adhesion; facilitating cell survival and growth.	**Printability**: poor mechanical properties.	(1) Composite biomaterial inks with sodium alginate, sodium alginate oxide, fibronectin, carbon nanotubes, GelMA, collagen, and hyaluronic acid (HA); (2) Elastase microbial transglutaminase (mTG) to promote cross-linking; (3) Using PCL scaffold as a support structure; (4) Modification with tyramine and methacryl group; (5) As a sacrificial material to form vascular channels.	**Size**: from microvessels to small diameter vessels (5 mm in diameters). **Shape**: straight tubes, branching capillary network. **Layers**: heterogeneous multilayered vessels.	[32,33, 82,84, 85,88, 89,91, 107]
GelMA 5–7 % (w/v) Extrusion; SLA	**Printability**: photopolymerizable; inexpensive and easy for synthesis; tunable physical and mechanical properties; hydrophilic. **Biocompatibility**: low immunogenicity; promoting cell adhesion and proliferation.	**Printability**: poor mechanical properties.	(1) Composite biomaterial inks with recombinant human elastin, alginate, PEGTA, and gelatin; (2) Stabilization can be improved by photocrosslinking after printing; (3) Using PCL scaffold as a support structure; (4) Prepared as modified biomaterials.	**Size**: from microvessels to small diameter vessels (5 mm in diameters). **Shape**: straight tubes; branching capillary network; branched large diameter vessels. **Layers**: heterogeneous multilayered vessels.	[13,36, 38,81, 97,96, 107]
Gel-NOR 5 wt% Extrusion + SLA	**Printability**: customizable mechanical properties; high cross-linking efficiency; high resolution; less sensitive to the detrimental effects of oxygen inhibition. **Biocompatibility**: promoting self-assembly of human stromal and ECs into microvessels.	NA.	(1) Can be processed in both two printing methods.	**Size**: microvessels. **Shape**: branching capillary network.	[98]
GelMA/C 15–20 wt% Extrusion + SLA	**Printability**: controlled mechanical strength; rapid oxidative cross-linking. **Biocompatibility**: high cell adhesion.	**Printability**: slow degradation. **Biocompatibility**: foreign body reaction *in vivo*.	(1) Used with PF127 as a sacrificial material; (2) Can be processed in both two printing methods.	**Size**: microvessels (900 μm in diameters). **Shape**: straight, branched large diameter vessels. **Layers**: heterogeneous bilayer vessels.	[37]

(*continued on next page*)

Table 4 (*continued*)

Biomaterial, common concentrations, and suitable printing methods	Advantages	Disadvantages	Improvements	Types of vessel scaffolds achieved	Ref.
GPT 2 % (w/v) Extrusion	**Printability**: high cross-linking rate; high storage modulus; degradable; tunable physicochemical properties. **Biocompatibility**: high cell viability.	**Printability**: low degradation rate.	(1) Used with gelatin as a sacrificial material.	**Size**: microvessels (600 μm–1000 μm in diameters).	[88]
Fibrin 0.5–2.5 % (w/v) Inkjet; Extrusion	**Printability**: high adhesion. **Biocompatibility**: promoting collagen synthesis; inducing angiogenesis; promoting cell adhesion.	**Printability**: low printing accuracy; poor mechanical properties.	(1) Composite biomaterial ink with collagen, gelatin, alginate, HA, etc; (2) Using cross-linking agents (e.g., thrombin) to promote cross-linking.	**Size**: small vessels (1 mm–2.31 mm in diameters). **Shape**: straight vessels. **Layers**: heterogeneously layered vessels.	[15,32,84,85,91]
SF 2–5 % Extrusion	**Printability**: good air and moisture permeability; high modulus; high tensile strength. **Biocompatibility**: biodegradability; cell-compatible cross-linking pattern.	**Printability**: low viscosity of non-crosslinked SF, not suitable for printing.	(1) Biomaterial ink with sodium alginate; (2) Addition of molecules that can interact with it (e.g. poloxomer, interaction with SF in terms of hydrogen and hydrophobic bonding).	**Size**: microvessels (500 μm–700 μm in diameters). **Shape**: straight tubes.	[71,103]
dECM 3 % (w/v) Extrusion	**Printability**: phase change temperature sensitive properties; shear thinning. **Biocompatibility**: promoting cellular activity; enhancing tissue function; accelerating therapeutic effects; little risk of host immunity.	**Biocompatibility**: tissue specific.	(1) Biomaterial ink with alginate; (2) Used with F127 as a sacrificial material.	**Size**: small vessels (1 mm–6 mm in diameters). **Layers**: multilayer.	[35,86]
PEG Extrusion	**Printability**: good hydrophilicity and water solubility. **Biocompatibility**: non-immunogenic.	**Biocompatibility**: lack of cell adhesion groups.	(1) Composite biomaterial ink with nanocellulose; (2) Photocrosslinking; (3) Methacrylate RGD coupled to PEGDA/PEGTA.	**Size**: microvessels (600 μm–1000 μm in diameters).	[62,88]
PEG-co-PDP/RGDS 10 % (w/v) DLP based SLA	**Printability**: adjustable swelling capacity, degradation rate and mechanical stiffness; photocrosslinkable. **Biocompatibility**: cell proliferative; cell active; biodegradable.	NA.	(1) Adjustment of light exposure time to adjust the swelling capacity, degradation rate and mechanical stiffness of hydrogels.	**Size**: small and large vessels (2.75 mm–6.2 mm in diameter). **Shape**: straight tubes, branched large diameter vessels.	[94]
PEGTA 2 % (w/v) Extrusion	**Printability**: high crosslink density; porous structure; high mechanical strength. **Biocompatibility**: inducing better cell growth and spreading.	**Biocompatibility**: detrimental to cell adhesion.	(1) Composite biomaterial ink with GelMA and alginate.	**Size**: microvessels and small vessels (500 μm–1500 μm in diameter). **Shape**: straight tubes. **Layers**: multilayered vessels.	[81]
PCL Extrusion; Nanofiber Electrospinning	**Printability**: excellent rheological property and viscoelasticity. **Biocompatibility**: good biodegradability and biocompatibility.	**Biocompatibility**: detrimental to cellular encapsulation.	(1) As a support structure for vascular structures, covering PCL scaffolds with biomaterials that can form blood vessels.	**Size**: from microvessels to millimeter-sized large vessels. **Shape**: straight tubes. **Layers**: multilayer vessels.	[14,38,85]
PF127 13 % (w/v), 40 wt% Extrusion	**Printability**: wide viscosity range; shear thinning properties; temperature sensitive. **Biocompatibility**: low toxicity.	**Printability**: tends to swell and spread, leading to low resolution of printed structures.	(1) Often used as a sacrificial material.	**Size**: microvessels and small vessels (600 μm–6 mm in diameter). **Shape**: straight tubes, branching vessels. **Layers**: multilayer vessels.	[80,86,103]

*"Advantages" and "Disadvantages" include Printability and Biocompatibility for each material. NA if not mentioned.
**"Improvements" include Composites, Printing methods, etc.
***"Types of vessel scaffolds achieved" include the Size, Shape, and Layers of vessel scaffolds. NA if not mentioned.

be removed after the vessels are formed [118].

Notably, the absence of specific enzymes to degrade agarose in the human body leads to its low *in vivo* degradability, requiring consideration of its degradability and possibly the addition of exogenous enzymes to enhance it [117].

4.1.1.3. Nanocellulose. Nanocellulose, a sustainable nanomaterial, is extracted from wood or plants through mechanical, enzymatic, or chemical processes; it is also synthesized by specific bacteria [119]. There are three different types of nanocellulose: cellulose nanofibrils (CNF), cellulose nanocrystals (CNC), and bacterial nanocellulose (BNC). Nanocellulose boasts unique physicochemical properties, including high elasticity, low density, high specific surface area, and ease of surface modification. It is structurally similar to the ECM, exhibiting low cytotoxicity and good biocompatibility. Nanocellulose can be chemically modified with functional groups or by grafting biomolecules onto its hydroxyl, aldehyde, carboxyl, and sulfate groups [119,120].

Nanocellulose can be surface-modified easily, and its printability can be enhanced through chemical modification, such as the preparation of 2,2,6,6-tetramethyl-1-piperidinyloxy (TEMPO)-oxidized CNFs, which can interact with Ca^{2+} through electrostatic interactions [62]. Although nanocellulose itself does not possess cell adhesion capabilities, its high aspect ratio, large surface area, and nanoscale crystalline structure are conducive to promoting cell adhesion and proliferation [119,121]. To compensate for its lack of cell adhesion, nanocellulose can be biofunctionalized with additives like proteins, peptides, polysaccharides, or

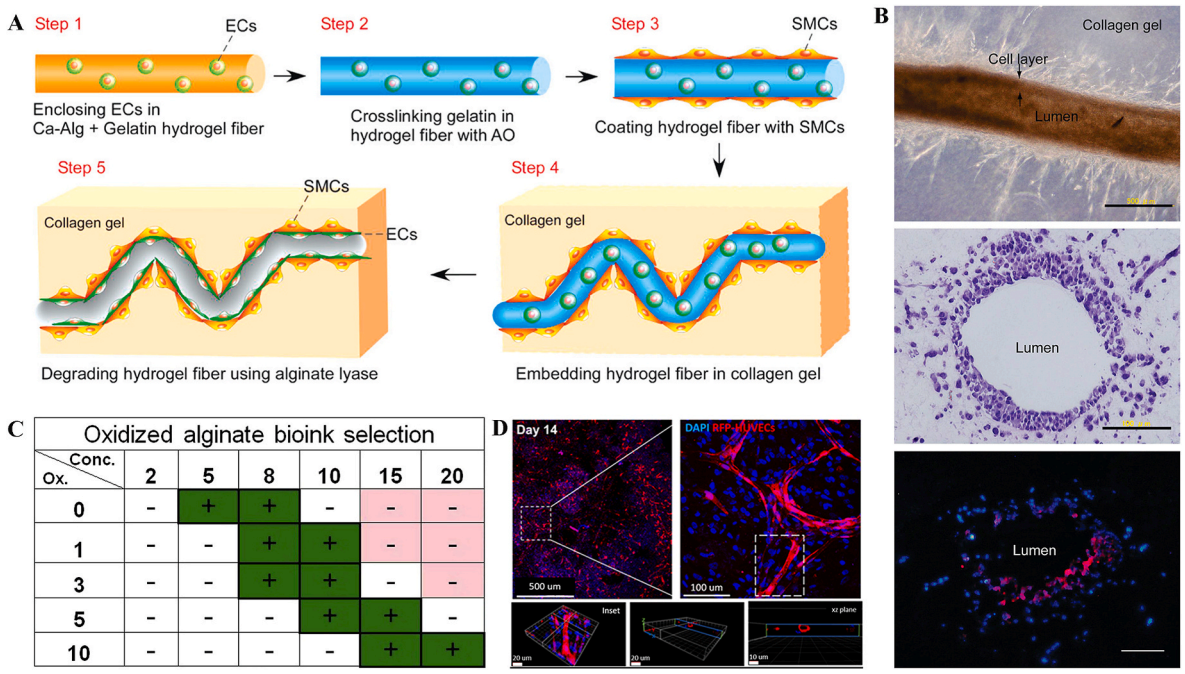

Fig. 4. Modified alginate in vessel scaffold printing. A) Schematic Illustration of the Fabrication of a Tubular Construct with Layered ECs and SMCs in a Collagen Gel. Reproduced and adapted with permission [105]. Copyright 2008, American Chemical Society. B) Photographs and H&E stained cross-sections of bioprinted tubular structure and fluorescence microscopic image of a cross-section of the cell layer at 6 days after fiber degradation using alginate lyase. Reproduced and adapted with permission [105]. Copyright 2008, American Chemical Society. C) Summary table of the preferable range of alginate samples with high printability (green) based on the three established printability criteria. Reproduced and adapted with permission [79]. Copyright 2014, Elsevier. D) 3D reconstruction and ortho-slices showing a lumenized endothelial tube. Reproduced and adapted with permission [104]. Copyright 2021, American Chemical Society.

bioactive drugs to enhance its inherent lack of cell adhesion [120]. Mixtures of nanocellulose with alginate and agar have been studied for the construction of vascularized human tissue with perfusable channels [42]. However, novel refining modification techniques, advanced gelation methods, and extended applications in tissue engineering and bioprinting, particularly for vascular fabrication are still the challenges in the future.

In summary of section 4.1.1, although these biomaterials with the potential for printing vessel scaffolds are primarily derived from plants, algae, and microorganisms [110,116,119][], this may lead to a deficiency of corresponding enzymes in the human body to degrade these materials. However, the controlled biodegradation of these materials can be achieved by the addition of specific degradation enzymes, such as alginate lyase [105] and agarase [117]. Additionally, these carbohydrate materials are not conducive to cell adhesion due to the lack of cell adhesion motifs [18,120,122], but their rich hydroxyl groups and other functional groups can be chemically modified to obtain tunable physicochemical properties [123]. Therefore, it is necessary to chemically modify these biomaterials, or to add with exogenous enzymes for biodegradation, or to mix with other substances (such as collagen) to form composite biomolecules.

4.1.2. *Protein biomaterials*

Protein (based) biomaterials, known for their favorable biocompatibility, are commonly sourced from mammals and arthropods, such as silkworms. These biomaterials facilitate the attachment and proliferation of vascular cells and can be used for bioprinting of vessel scaffolds [71,124]. The most commonly used protein biomaterials in the manufacture of implantable vessel scaffolds are collagen, gelatin (and its modifiers), fibrin and SF.

4.1.2.1. Collagen. Collagen is the basic structural element of connective tissues and can be obtained from a wide range of sources, including animals and bacteria [125]. Collagen has the ability to form fibers with adjustable self-assembly under different conditions (e.g. temperature, pH and ionic strength) [110], and can form collagen networks mainly through tangles *in vitro* [126]. In addition, collagen, a highly cellular-active biomaterial [90], enhances cell viability and supports cell proliferation, adhesion, and spreading, while also significantly facilitating vascular network formation and stability [127].

Collagen contains the RGD sequence (a recognition site for cells), enabling cell adhesion [128]. Particularly, GFPGER sequence from collagen I promotes stress fiber formation and enhances cardiovascular cells' contractility, guiding endothelial organization into multicellular capillary sprouts. It also interacts with β1 integrins to induce actin stress fibers, which is crucial for angiogenesis [129,130].

Considering the fibrillar structure, collagen chains can form a triple helix in a neutral pH environment, which is essential for the stability of the resulting vascular networks [124]. Collagen fiber dimensions—size, thickness, and length—substantially affect cell activities. For example, long and thick collagen fibers can promote cell elongation, while variations in fiber size may enhance ECs contractility, leading to vascular branching [131]. The migration of ECs is guided by the alignment of collagen fibers, allowing for the direct regulation of vascular network formation through the arrangement of these fibers [131]. At the early stage of vascular network formation, ECs dynamically interact with collagen, leading to the remodeling of the matrix network through both new ECM deposition and proteolytic degradation. This process also releases growth factors and cytokines that can direct angiogenesis [132].

Despite its excellent biocompatibility, collagen's slow gelation rate can result in a non-uniform distribution of cells [133]. To overcome this, collagen is often combined with other materials, such as alginate, to create heterogeneous multilayered blood vessels in a wide range of diameters. These composite vessels exhibit potential for use as implantable vascular structures.

4.1.2.2. Gelatin and its modifiers. Gelatin is the product of denatured collagen, and its chemical structure also contains the Gly-X-Y amino acid

repeat sequence and adhesive peptide ligands, such as RGD. Therefore, gelatin possesses good cytocompatibility, which can improve cell integration and tissue repair [133–135]. Gelatin contains high molecular weight components that can be crosslinked at a lower temperature (e.g. below 35 °C). Heat treatment can further reduce the molecular weight of gelatin [84]. In addition, gelatin is heat sensitive and changes its state by altering the degree of cross-linking of hydrogen bonds at different temperatures [33,47]. Gelatin can be used as a sacrificial material to form a network of hollow channels capable of transporting oxygen and nutrients [136], with the potential to fabricate implantable vascular structures. Gelatin can also form a variety of modified biomaterials that can be used for transplantable vascular printing (e.g. GelMA, Gel-NOR, GelMA/C and GPT). All of them have shown the potential to be printed into vessel scaffolds.

GelMA is capable of photocrosslinking under the action of a photoinitiator and has adjustable mechanical properties that enable the printing of cell-containing, highly complex microscale tissues and structures for vascular engineering. Soft GelMA promotes angiogenesis of human ECs. GelMA can be photopolymerized by UV light, albeit with potential cell damage due to the light and toxic photoinitiators [47,137,138]. Alternatively, it can crosslink under visible light in a more intricate but safer process for cells [139,140]. Ramón-Azcón et al. [138] combined dielectrophoresis (DEP) and bioprinting techniques to co-culture myoblasts and ECs in GelMA, enabling the cells to maintain their functionality over an extended period and forming a stable 3D structure. It also has the potential to be printed into some complex vascular structures. Abudupataer et al. [137] also used GelMA as a biomaterial to construct a model of a blood vessel simulating the interactions between the vessel wall and the blood flow on a microfluidic chip using the co-culture model of ECs and SMCs, which could have simulated different types of blood vessels *in vivo* by changing cell types and flow parameters.

To further print vessel scaffolds with capillary networks, Soliman et al. [98] chemically modified gelatin with norbornene group to form Gel-NOR, which promoted the self-assembly of vascular cells into microcapillaries. Gel-NOR had customizable mechanical properties and high crosslinking efficiency, which could be used to prepare channels with a resolution of 200 μm. Moreover, the fabrication process, which combines extrusion and photolithography, allows for the creation of vascularized structures with customizable fiber diameters, spacings, and orientations (Fig. 5).

In spite of capillary formation, the printing of vascular branch structure is also worth studying. Cui et al. [37] synthesized GelMA/C with good printability, controllable mechanical strength, rapid oxidative crosslinking and high cell adhesion, and printed vascular structures with straight and bifurcated tube structures. Vessel scaffolds printed with GelMA/C showed good perfusion and permeability, as well as good vascular activity. The scaffolds could be transplanted into mice, and the anastomosis between the scaffolds and the host cell layer was completed in 2 weeks, and the vascular remodeling was completed in 6 weeks, gradually forming a hollow and mature vascular structure.

Modified gelatins also play an important role in the arrangement of vascular cells in implantable scaffolds. Hong et al. [88] synthesized a modified gelatin, GPT, by designing tyramine-gelatin containing tyramine functional groups, and adding PEG as the spacer between tyramine and gelatin. Tyramine increased the crosslinking rate and storage modulus, and decreased the degradation rate of GPT. PEG increased the gelation rate. They successfully printed perfusable vascular structures using a coaxial printing method with gelatin cores containing HUVECs and GPT sheaths containing HDFs. More importantly, the modified biomaterial could realize radial distribution of multiple vascular cells in the vascular structure.

4.1.2.3. Fibrin. Fibrin is the main matrix component of blood clots with high surface tension and acceptable swelling/degradation properties [124,130]. The gelling rate, hardness and ultrastructure of fibrin gel can be regulated by the concentration of thrombin and fibrinogen [141]. The hardness of crosslinked hydrogel can be improved with the increase of fibrin content [91]. Fibrin contains the RGD sequence, which can interact with integrin receptors on the surface of ECs, thereby facilitating the interaction between cells and the fibrin matrix to support cell adhesion [47]. For vasculature development, ECs can form a network of blood vessels [142] with interconnected capillaries [143] in fibrin. To utilize fibrin gels in vascular engineering, it is necessary to optimize the properties of fibrin gels by adjusting thrombin and fibrinogen concentrations. Clinical use of fibrin gels in vascular engineering faces challenges: (1) ensuring long-term gel stability and vascular functionality; (2) constructing vascular networks with appropriate structure, flow dynamics, and tissue interaction; addressing biocompatibility, immunogenicity, and medical practice compatibility; (3) precisely controlling gelation for optimized degradation and maturation. These efforts are crucial for advancing fibrin gel applications in vascular manufacturing and regenerative medicine.

4.1.2.4. SF. SF is a natural material extracted from silkworm silk and is a tough bio-protein fiber. SF has high modulus and high tensile strength,

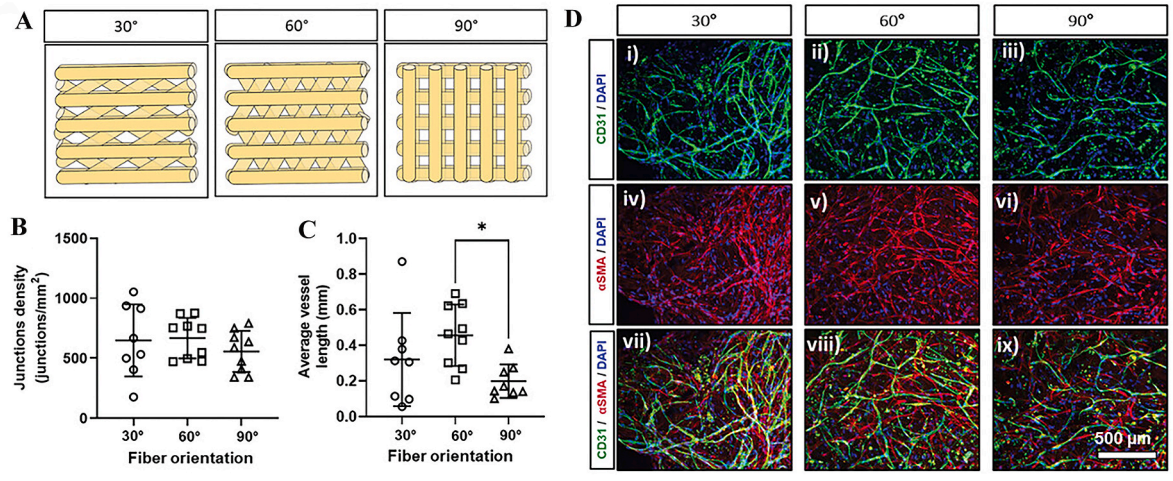

Fig. 5. Bioprinted vascular structures with different fiber diameters, spacing and orientation fabricated from Gel-NOR. A) Structural diagrams of layered vessels printed at different angles (30°, 60°, 90°) using modified gelatin polymers. B) Quantification of average vessel junctions density after 7 days of culture. C) Quantification of average vessel length after 7 days of culture. D) Cross-sectional views of the constructs. Reproduced and adapted with permission [98]. Copyright 2021, John Wiley and Sons.

and also supports vascular cell attachment, proliferation, and differentiation [71,103]. The sol-gel transition of aqueous SF can be induced by adjusting temperature and pH [103]. SF lacks the bioactive domains necessary for cell adhesion, proliferation, and differentiation [144,145]. Hence, it is less effective compared to materials such as collagen. However, SF contains amino acid side chain residues that can be chemically modified to "decorate" growth factors and adhesion factors through surface modification techniques [146,147]. There have been studies using the techniques of electrospinning [70] and mold casting [71] to fabricate SF into vessel scaffolds, as well as studies that have used SF as a part of a composite material to bioprint perfusable, layered microchannels [103]. To ensure the safety and efficacy of SF in the fabrication of blood vessels and in clinical therapies, future research needs to synthesize expertise in materials science, biology, and clinical medicine.

Overall, compared to carbohydrate-based materials, protein-based materials exhibit superior biocompatibility. They are mainly sourced from animal tissues [125], possibly innately containing or being capable to incorporate motifs that promote cell adhesion [47,128] and enhance cell attachment. The human body can also produce the relevant degradation enzymes, rendering these materials biodegradable [148]. Yet challenges remain with the printability of some of these materials. Collagen, for instance, presents issues such as a relatively low modulus of elasticity [91]. Collagen necessitates a prolonged period for complete cross-linking—approximately half an hour at 37 °C [133]. Moreover, the low viscosity of fibrinogen can affect the stability of the print and the strength of the final product [15,91]. There are two common ways to overcome these limitations (1) improving the bioprinting technique (e.g., FRESH): [37]; (2) making modified biomaterials or composite biomaterials into bioinks (e.g., coupling methacrylate groups for collagen [149]).

4.1.3. dECM

dECM can also be prepared as bioink. dECM is made by removing cells and extracting the ECM using chemical, physical or enzymatic methods from tissues [150]. dECM is available from a wide range of tissue sources and can recapitulate the inherent microenvironments of original tissue including composition, structure, and biomechanical properties, preserving the majority of ECM components such as collagen, glycosaminoglycans, and elastin in the original tissue [35]. dECM not only has phase change temperature sensitive properties and shear thinning [86], but also has excellent biocompatibility and little risk of host immunity for bioprinting. However, dECM also has the disadvantage of being time-consuming and uneconomic to prepare. The dECMs from different sources have distinct compositions, resulting in a dECM bioink that is tissue specific and cannot be characterized by a single or several representative biomolecules [151]. dECM can be used to fabricate multilayered blood vessels with good mechanical strength [86], and can also be composited with alginate to fabricate perfusable vessel scaffolds [35].

Summarizing, dECM has shown great potential in vascular engineering. However, for dECM to achieve broad clinical use, challenges across multiple fronts must be addressed: material preparation, ensuring tissue specificity, assessing immunogenicity, developing composite materials, facilitating clinical translation, and refining manufacturing techniques. Future research should focus on these key issues to realize the vascular fabrication using dECM.

4.2. Synthetic biomaterials

Synthetic biomaterials are chemically prepared to mimic the natural components of ECMs [102], such as PEG, PF127, PCL, polyvinyl alcohol, polylactic acid, etc. In this section, PEG and its modifiers, PCL, PF127, which are widely used in vessel scaffold printing, are selected to be reviewed here.

4.2.1. PEG and its modifiers

PEG is a linear polyether compound with good hydrophilic and water-soluble properties. Its physical properties can be changed by adjusting the water content [102]. PEG can be modified by coupling with other groups, such as acrylic acid with PEG to form photo-crosslinkable poly(ethylene glycol) diacrylate (PEGDA) or PEGTA [152]. In addition, PEG has the advantages of biocompatibility and non-immunogenicity [153,154], but PEG lacks the groups that can make cells adhere.

PEGDA and PEGTA are two commonly used modified PEGs that can be used for vascular printing. A diacrylate group is added to both ends of the PEG chain to form PEGDA. PEGDA has branched tetrad structures with multiple active cross-linking sites, which can be cross-linked under light conditions to form a porous, strong mechanical structure. PEGDA has a controllable crosslinking rate influenced by multiple factors (e.g. the molecular weight of PEGDA, the concentration of solutes, the types and the concentrations of photoinitiator). In addition, performing the modifications of PEGDA make the biomaterials to allow cells growing and spreading [47,81,155]. For instance, RGD ligand can be added to PEGDA to make up for the inability of PEGDA to support vascular cell adhesion for further vasculature development [90].

4-arm PEGTA is also a modified biomaterial of PEG. It can be stably cross-linked under illumination and possesses good printability. These attributes can improve both the mechanical properties and cross-linking stability of the scaffolds. Compared to PEGDA, PEGTA has better shear storage modulus and biocompatibility, which can form porous scaffolds more conducive for cell growth and migrations [156]. The vascular cell adhesion and biodegradability of PEGTA can also be improved by coupling RGD peptides and matrix metalloproteinases (MMP) sensitive sequences in the network to simulate the extracellular environment. Schukur et al. [157] modified PEGTA with RGD peptides so that the ECs contained therein preferentially differentiated. PEGTA can also be mixed with other biomaterials to produce composite biomaterials, an example of which will be described in the next section.

4.2.2. PCL

PCL is a semi-crystalline biomaterial known for its excellent formability at low temperatures, along with superior rheological properties and viscoelasticity [158]. It also boasts good biodegradability and biocompatibility [158]. PCL undergoes non-enzymatic hydrolysis under physiological conditions, breaking down into 6-hydroxyl caproic acid and acetyl coenzyme A, which are metabolized through the citric acid cycle and excreted, facilitating *in vivo* degradation [159]. Despite its slow degradation rate, with the homopolymer PCL requiring 2–4 years to fully break down [160], the inherent stability of PCL makes it an excellent candidate for long-term implantable vessel scaffolds. PCL has been utilized in the fabrication of acellular, bioabsorbable scaffolds with little elastic retraction and shortening [161], such as small-diameter blood vessels [38] with good biological and mechanical properties comparable to those of natural blood vessels. The PCL support frame, with its high elastic modulus, precisely regulates cell traction forces by controlling the collagen and actin networks in the ECM, influencing cell growth, migration, and differentiation. It also withstands cell contractile forces to provide essential mechanical signals that significantly affect vascular network formation, angiogenesis, branching patterns, and tissue organization [85,162–164]. PCL is widely used in 3D printing, but is not suitable for cell encapsulation and is often used as a support structure in blood vessel printing [165].

4.2.3. PF127

PF127 is a material with thermo-reversible properties, playing the role of a sacrificial material in 3D printing technology [166], especially in the manufacture of vessel scaffolds with complex internal cavity structures. Using extrusion printing technology, PF127 can form a temporary support structure to maintain the shape stability of the vessel scaffold during the manufacturing process [167]. Although PF127 is

traditionally not used for cell encapsulation and is rarely considered a biomaterial, its reduced toxicity and bio-inertness make it a potential carrier for cells or drugs [168,169]. In the field of bioprinting, the gel form of PF127 can be used to carry cells or drugs, therefore, this article will explore the application of PF127 as a biomaterial. PF127 has a wide range of viscosities, and shear thinning properties that reduces the stress on cells during extrusion [48,168]. For example, Xu et al. [86] printed multi-layer, multi-branch and pre-vascularization hollow channels (Fig. 6A) and a small-diameter vessel with high cellular viability and three-layer structure with elastic modulus similar to that of natural aorta (Fig. 6B). Peng et al. [80] also printed a tubular channel wall that enabled high viability of HUVECs (Fig. 6C–D). The thermal reversibility of PF127 gives it a good potential to form blood vessels, but also makes it expands and diffuse easily in hydrogels, leading to a low resolution of printing structure [47,169].

Compared to natural materials, synthetic materials are favored for their superior mechanical properties and customizable processability, which aids in the printing of vessel scaffolds with high mechanical performance and high resolution [170]. Synthetic polymers contain hydrolysable covalent bonds that can undergo hydrolysis. Particularly when the molecular weight is low (less than 3000 Da), these polymers can be degraded by cells [171]. However, the hydrolysis products may trigger inflammation and immune responses [172], and the hydrolysis process typically takes longer time compared to enzymatic degradation [171]. Furthermore, synthetic materials often miss motifs that promote cell adhesion, which is detrimental to cell attachment and proliferation. Therefore, to compensate for these deficiencies, it is common to blend synthetic materials with natural materials or to modify adhesive sequences on the surface of synthetic materials (such as RGD-PEGTA [157]).

4.3. Composite and hybrid biomaterials

It is difficult for a single type of biomaterial to meet all the needs for printing implantable vessel scaffolds [41]. Therefore, biomaterials with different advantages are combined to offset their innate defects and to make a composite or hybrid biomaterial that can leverage between printability and biocompatibility. Composite and hybrid biomaterials are blends that retain the original properties of their constituents while potentially introducing new characteristics. Composite biomaterials typically consist of a blend of components across various sizes, while hybrid biomaterials involve mixing at the nano- or molecular scale [148,149]. In this paper, we categorize biomaterials with an interpenetrating network structure and auxiliary components as composites biomaterials. In contrast, those connected at the molecular level by covalent or non-covalent bonds are termed hybrid biomaterials.

Since collagen, gelatin and alginates are three widely used components for composite or hybrid biomaterials during bioprinting, this section will classify the composites in terms of these three materials. Because of the limited cytocompatibility, synthetic biomaterials are seldom used as a single component during printing transplantable blood vessels. Therefore, several examples of used synthetic polymers in composite or hybrid biomaterials are also briefly reviewed here. These composite and hybrid biomaterials for bioprinting vessel scaffolds are shown in Table 5.

4.3.1. Collagen-containing biomaterials

Since most of the bioinks with collagen only have low viscosities, it is difficult to print vessel scaffolds with good mechanical properties. Other components need to be added to improve the mechanical properties.

Agarose has certain rigidity, and Köpf et al. [90] combined collagen with agarose, developing a composite biomaterial capable of producing wrapped human umbilical artery smooth muscle cells (HUASMCs) rigid vessel scaffolds by drop-on-demand printing methods. Collagen and agarose can form a spongy agarose hydrogel with small pore sizes and a coarser fibrous collagen network interpenetrating the hydrogel, which improved the mechanical properties, the water retention capacity and the stability of the composite biomaterials.

Alginates can also improve the viscosity of the collagen-contained bioinks. Dogan et al. [87] used alginate/collagen type I to prepare a composite biomaterial, successfully printed a network of blood vessels with multiple layers (with intima, media, and outer membranes similar

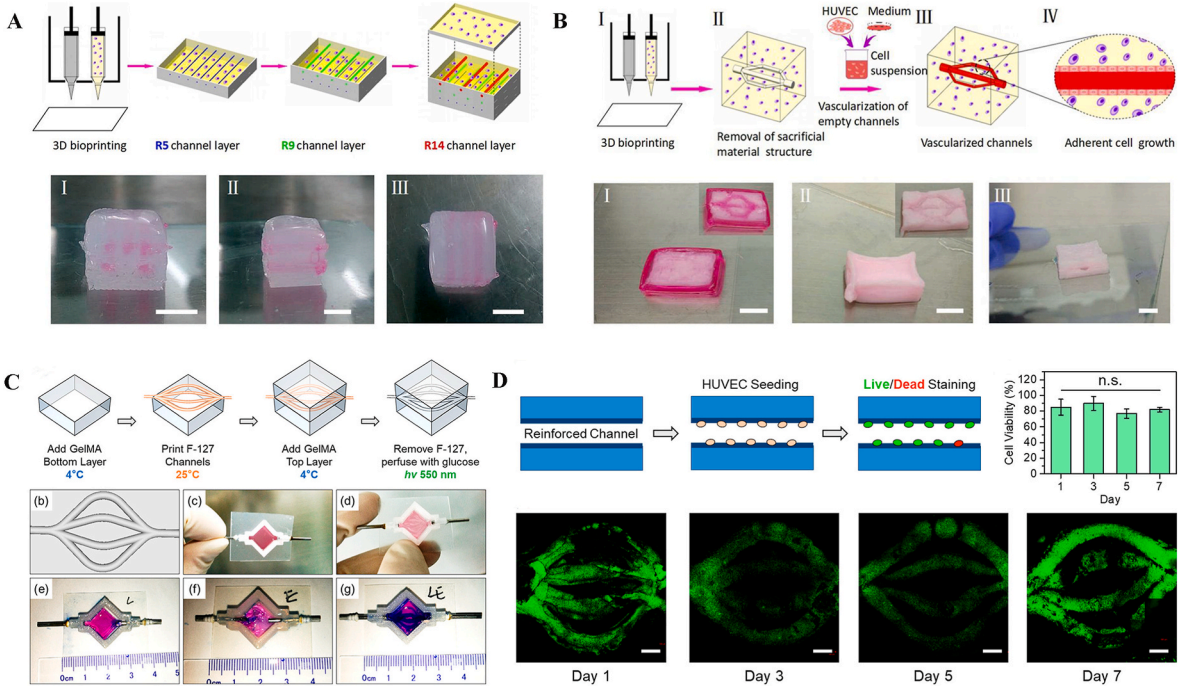

Fig. 6. Vascular channels printed with PF127 as the sacrificial material. A)-B) Multilevel channel structure and a multibranch channel structure printed in dECM with PF127 as the sacrificial material. Reproduced and adapted with permission [86]. Copyright 2018, MDPI. C)-D) Vascular channels printed in GelMA and other substances with PF127 as the sacrificial material. Reproduced and adapted with permission [80]. Copyright 2021, American Chemical Society.

Table 5
Composite and hybrid biomaterials for bioprinting vessel scaffold.

Composite biomaterials and printing methods	Cells	Properties of composite biomaterials	Role of each biomaterials	Printed structures and their evaluation	Ref.
2 % (w/v) alginate + 0.015 % (w/v) type I collagen Extrusion	Human induced mesodermal progenitor cells (hiMPCs)	**Biocompatibility**: supporting cell attachment, cell migration, cell-cell and cell-gel interactions.	Alginate: fast crosslinking. Collagen I: supporting cell migration, proliferation, and morphogenetic events in composite biomaterials.	**Size**: microvessels (100 μm–200 μm in diameter). **Shape**: branches, layers. **Layers**: three layers of blood vessels showing endothelial, mesothelial, and epithelial membranes. **Biocompatibility**: high cell survival; ECs attach, extend, and migrate on the matrix; vascular perfusion and vascular anastomosis are achieved in the CAM.	[87]
0.18 % (v/v) collagen + 2.5 %, 1.25 %, 0.625 % (w/v) fibrin; thrombin as cross-linker Drop-on-demand bioprinting	HUVECs; SMCs	**Printability**: good gel stability, gelation time, swelling ratio; low compaction; high linear modulus and ultimate tensile stress. **Biocompatibility**: promoting endothelial cell adhesion and forming confluent endothelium.	Fibrin: increasing stiffness and rigidity of cross-linked hydrogels. Collagen: reducing water loss. Thrombin: enabling rapid cross-linking of proteins to fibrin to form a matrix.	**Size**: wall thickness up to 425 μm, diameter about 1 mm. **Layers**: three layers of blood vessels showing endothelial, mesothelial and epithelial membranes. **Biocompatibility**: high cell viability (>83 %); specific markers; forming a cell layer; morphology resembles that of small arteries and veins in the body. **Mechanical properties**: perfusable.	[91]
1.33 mg/ml collagen (C) + 5 mg/ml fibrin (F) + 4 wt% gelatin (G) Core-shell bioprinting	HUVEC; HDFs	**Printability**: shear-thinning; structural instability after crosslinking. **Biocompatibility**: supporting fibroblasts to form fibroblast networks; supporting the formation of vascularization and lumenized tubes.	Fibrin and collagen: interpenetrating polymer networks to enhance mechanical properties. Fibrin: preventing contraction and disintegration of the nucleus; facilitating intracellular interactions. Gelatin: ensuring the production of gels with sufficient viscosity and without interfering with the polymerization of collagen and fibronectin networks.	**Size**: microvessels. **Shape**: pre-vascular network. **Biocompatibility**: formed a pre-vascular network.	[32]
7.5 % (w/v) OA + 5 % (w/v) gelatine, 3 % oxidized Dual-nozzle extrusion	ADMSCs	**Printability**: good physicochemical and mechanical properties. **Biocompatibility**: high cell survival; supporting cell proliferation.	OA: increasing the viscosity of the bioink, degradation and swelling rates. Alginate: supporting mechanical properties and increasing Young's modulus. Gelatin: providing cell adhesion substrates.	**Size**: microvessels (400 μm in diameter). **Biocompatibility**: high cell viability and doubling of cell number at 14 days. **Mechanical properties**: high mechanical strength (Young's modulus 56.67 ± 15 kPa).	[89]
GelMA + MeTro FRESH followed by visible light cross-linking	HUVECs	**Printability**: high viscosity; high tensile modulus; smooth flow from nozzle without clogging; mechanically stable and robust after cross-linking, allowing bioprinting of multilayer structures; high fidelity. **Biocompatibility**: fast degradation and bio-integration, for repair of diseased soft tissues; moderate tensile modulus.	MeTro: enhancing the elasticity and mechanical stability of the printed structure. Gelatin: increasing the viscosity of bioink by a factor of 20 and increasing the tensile modulus. GelMA: supporting a tunable cell culture environment.	**Size**: microvessels (200 μm–400 μm in diameter). **Biocompatibility**: cell survival (>85 %); specific markers; good binding to host tissue; low inflammatory response *in vivo*. **Mechanical properties**: low diffusion permeability; barrier function. **Physical properties**: 67.4 ± 11.9 % biodegradation at day 21.	[36]
7.5 % (w/v) 1h heat-treated gelatin +10 mg/ml fibrinogen Rotary bioprinting	HDFs	**Printability**: good rheological properties; shear thinning; adjustable printability of hybrid bioinks through preheat-treated gelatin.	Fibrin: enabling cross-linking with thrombin, and low concentrations of thrombin allowing for the formation of a more homogeneous vascular structure. Gelatin: affecting the shear-thinning properties and the rheological properties of composite biomaterial; to promote the porous structure formation, facilitating cell growth and organization, contributing to rapid and massive coalescence of vascular structures.	**Size**: small diameter (<6 mm), and large diameter (20 mm (L) 4.9 mm (ID) 10.9 mm (OD)). **Layers**: triple **Biocompatibility**: specific markers; cellular deformation. **Mechanical properties**: rupture pressures up to 1110 mmHg, approximately 52 % of saphenous vein rupture pressure and 35 % of ITA rupture pressure. **Processability**: low cost; rapid preparation.	[84]
5 % (w/v) alginate + 5 % (w/v) SF. 13 % (w/v) F127 as sacrificial material Coaxial extrusion	C3A cells (liver cancer cells)	**Printability**: good shear thinning properties; flowability. **Biocompatibility**: favorable for cell proliferation.	Poloxomer: accelerating the transformation of SF from a disordered coil structure to a β-sheet structure. SF: improving the mechanical	**Size**: approximately 500 μm in diameter. **Biocompatibility**: high cell survival (around 99.5 % on day 14). **Mechanical properties**: structural	[103]

(*continued on next page*)

Table 5 (*continued*)

Composite biomaterials and printing methods	Cells	Properties of composite biomaterials	Role of each biomaterials	Printed structures and their evaluation	Ref.
			properties and enabling higher cell viability and proliferation rates.	stability; smooth, regular channels, large surface area.	
3 % (w/v) VdECM + 2 % (w/v) alginate; CPF127: 40 % w/v PF127 containing $CaCl_2$ as the core sacrificial material Coaxial extrusion	Endothelial progenitor cells (EPCs)	**Printability**: Shear thinning properties; storage modulus greater than loss modulus; interconnected pore structure with tens to hundreds of microns. **Biocompatibility**: promoting cell survival, adhesion, spreading and differentiation.	dECM: increasing matrix stiffness; promoting cell survival, maturation, differentiation and migration; enhancing tissue function; accelerating therapeutic effects. CPF127: releasing calcium ions to promote alginate cross-linking; preventing vascular degeneration prior to sacrifice.	**Size**: ID (500 μm–1500 μm), wall thickness in the range of 50 μm–200 μm. **Layers**: with endothelial layer. **Biocompatibility**: high cell survival; specific markers; with intercellular adhesion and interactions; monolayer endothelial formation; perfusion in nude mice hindlimb ischemia models. **Mechanical properties**: weak mechanical strength, difficult to surgically anastomose. **Processability**: controlled vessel diameter and wall thickness.	[35]
1 % alginate + 15 % gelatin Microfluidic coaxial extrusion (bio)printing	Veins: HUVECs, HUVSMCs Arteries: HUASMC; HUAECs	**Printability**: high tensile strength (197.7 kPa) and tensile strain (207.3 %); high strength and tensile, mechanical properties; low energy dissipation; high strain recovery and high toughness. **Biocompatibility**: promoting vascular cell adhesion and proliferation.	Gelatin: maintaining material integrity by forming gelatin networks with low irreversible strain; promoting cell adhesion and proliferation. Alginate: providing physical anchoring, promoting stress transfer and additional energy dissipation.	**Size**: arteries-1mm in diameter, veins-5mm in diameter. **Layers**: bilayer structure (inner endothelial layer and outer smooth muscle layer). **Biocompatibility**: viability above 90 %; specific markers; vascular anastomosis in mouse. **Mechanical properties**: ability to withstand pressure exerted by blood flow, perfusion and barrier function; mechanical strength; insufficient suturing ability; SMCs arrangement different with native vessels. **Processability**: adjustable diameter, wall thickness, and length.	[82]
0.5 % (w/v) alginate + 2.5 mg/ml collagen; 1 % (w/v) alginate + 25 mg/ml fibrinogen A new microfluidic nozzle for multi-axial extrusion	HUVEC; Mouse 3T3 fibroblasts	**Printability**: structurally stable. **Biocompatibility**: excellent cell adhesion.	Fibronectin: allowing ECs to adhere and proliferate, thus resembling the endothelial wall of blood vessels. Crosslinked Alginate-fibrinogen: promoting cell proliferation and the formation of the morphology necessary to form a true lumen.	**Size**: hollow channel sizes from 0.69 ± 0.01 mm to 1.18 ± 0.04 mm, inner gel layer sizes from 1.05 ± 0.02 mm to 1.47 ± 0.05 mm, outer gel layer sizes from 1.85 ± 0.06 mm to 2.31 ± 0.05 mm. **Layers**: multilayer. **Biocompatibility**: cells maintain long-term viability,; cell adhesion. **Mechanical properties**: structural integrity, enabling multilayer. **Processability**: enables multi-diameter size, multi-layer vessel scaffold construction; fast, simple, and low-cost manufacturing.	[15]
2 wt% alginate + 3 wt% PEO Cell electrospinning/3D printing process.	HUVECs; Myoblasts	**Printability**: high elastic modulus. **Biocompatibility**: high cell survival; facilitates cell growth, angiogenesis extension and diffusion.	PEO: as a supporting material, reducing conductivity reduction and surface tension, increasing viscosity and forming beadless fibers. Alginate fiber: providing wettability and protein absorption.	**Size**: microvessels. **Biocompatibility**: high cell viability; HUVEC elongation.	[14]
PEG star polymer + 2,2,6, 6-tetramethyl-1-piperidiny-loxy (TEMPO)-oxidized CNFs Extrusion. Chemical crosslinking under visible light after extrusion	L929 fibroblast cells	**Printability**: versatile and easy to prepare; highly tailored viscoelastic and mechanical properties; shear-thinning; adjustable compressive Young's modulus and shear storage modulus. **Biocompatibility**: good cell viability and proliferation.	CNFs: modulating bioink stiffness and optimizing bioink viscosity through electrostatic interactions with Ca^{2+}. Four-armed PEG-NB: chemical cross-linking of bioinks achieved.	**Biocompatibility**: high cell viability; high cell proliferation rate; uniform cell distribution with elongated structures. **Processability**: controlled pore size of the scaffold.	[62]
7 % (w/v) GelMA + 3 % (w/v) sodium alginate + 2 % (w/v) 4-arm PEGTA Multilayer coaxial extrusion system	HUVECs; Mesenchymal stem cells(MSCs)	**Printability**: shear-thinning behavior; ideal rheological properties and printability, easy extrusion, no nozzle clogging; high print resolution; adjustable mechanical properties. **Biocompatibility**: good biological properties to support the spreading and proliferation of encapsulated endothelial and stem cells, providing	Alginate: improving the printability of bioink; to promote the porous structure formation; facilitating cell migration and diffusion. PEGTA: reducing the degradation rate of hybrid protein-based hydrogels; improving the mechanical properties and stabilizing the cross-linked matrix;	**Size**: average OD: 500 μm–1500 μm, ID: 400 μm–1000 μm, wall thickness: 60 μm–280 μm. **Biocompatibility**: cell survival over 80 %; specific markers; increased cell proliferation and metabolic activity; formation of complete vessel-like structures. **Mechanical properties**: perfusability; fully interconnected	[81]

(*continued on next page*)

Table 5 (*continued*)

Composite biomaterials and printing methods	Cells	Properties of composite biomaterials	Role of each biomaterials	Printed structures and their evaluation	Ref.
		a favorable biochemical and physical microenvironment for the cells.	promoting cellular reactions and new tissue formation; supporting cell growth. GelMA: causing cells to adhere.	luminal structure formed. **Processability**: controlled vessel diameter.	
Sodium alginate + gelatin solution + 0.5 % (w/v) carbon nanotubes Rotary bioprinting	Mouse epidermal fibroblasts	**Printability**: high Young's modulus and critical breaking stress. **Biocompatibility**: low cytotoxicity; high adhesion rate; good cell proliferation.	Alginate: improving the hardness; improving hydrogel printing properties. Carbon nanotubes: improving surface finish, mechanical properties, and deformation recovery of the scaffolds; reducing gelatin degradation rate; promoting cell proliferation and nerve regeneration. Gelatin: guiding cell culture, cell transplantation, drug delivery and tissue regeneration.	**Size**: ID: 3 mm, average wall thickness: 0.5 mm, length: 7 cm–10 cm. **Biocompatibility**: cell adhesion rate of 77.55 ± 4.00 %; cell survival rate of 80.58 ± 6.70 % on day 7; cells evenly distributed in vessel walls. **Processability**: controlled vessel wall thickness.	[33]
35 mg/ml gelatin +7 mg/ml fibrinogen + 3 mg/ml HA + 10 % (v/v) glycerol; PCL as support Extrusion	HUVEC; HDFs	**Printability**: high viscosity. **Biocompatibility**: reduce cell damage due to physical stress.	Fibrinogen: giving the bioprinted gel a high enough viscosity to prevent collapse of the printed structure; providing the permissive ECM necessary to activate ECs for angiogenesis.	**Size**: diameter about 280 μm. **Shape**: branching vessels. **Biocompatibility**: high cell survival; specific markers; formation of actin networks and vascular lumen. **Processability**: controlled vessel shape.	[85, 164]
6 % (w/v) sodium alginate and 13 % (w/v) pluronic — Rotary printing; gelatin and PCL Electrostatic spinning	SMCs; Pericytes	**NA**	PCL: offering mechanical strength and durability; with nanofibers facilitating nutrient exchange and EC adhesion; enhancing resistance to *in vivo* blood pressure. Gelatin: enhancing ECs adhesion and survival; contributing to the formation of a stable endothelial layer. Alginate/pluronic: cross-linkable with calcium ions; ensuring high reproducibility and structural integrity.	**Size**: ID 5 mm. **Layers**: 3. **Biocompatibility**: capable of withstanding blood flow post-implantation; leak-proof; anti-thrombogenic; undergoing remodeling with cellularization and elastin deposition; abundant microvasculature on the surface. **Mechanical properties**: suture retention strength of 2.67 ± 1.11 N; Young's modulus (1.09 ± 0.12 MPa) similar to human coronary artery; estimated burst pressure (1708 ± 167 mmHg) akin to human saphenous vein; good suturability and hemostatic performance. **Processability**: rapid fabrication speed.	[173]
15 mg/mL collagen Bioprint; PCL as support.	ADMSCs	**NA**	Collagen: endothelial and smooth muscle layer formation support. PCL: mechanical support for vascular regeneration; improved suturability and anti-hemorrhage capability; slow degradation for vascular healing and integrity restoration.	**Size**: 1.0 cm in length, ID 5 mm, **Layers**: 2 **Biocompatibility**: endothelial and smooth muscle regeneration; minimal inflammatory response; low biodegradation rate **Mechanical properties**: high Young's modulus and tensile stress; secure anastomotic connections; ensured blood flow patency	[174]

*"Printed structures and their evaluation" include Size, Shape, Layers, Biocompatibility and biological activity, Mechanical properties, Physical properties and Processability. NA if not mentioned.

to natural blood vessels) and branching structures by extrusion printing using mesodermal progenitor cells. This structure could be transplanted into the chicken embryo CAM and found it connected to the blood vessel in the chicken embryo and participated in the blood circulation.

Fibrin, known for its strong adhesion, has also been used in combination with collagen. Schöneberg et al. [91] used collagen-fibrin (CF) complex biomaterials as cell substrates, gelatin as a sacrificial material, and thrombin and transglutaminase as crosslinkers. They used drop-on-demand bioprinting technique to manufacture a blood vessel model containing HUVECs and SMCs with layered structure, whose wall thickness was similar to that of small arteries and veins in human body, which could be cultured for 3 weeks under physiological flow conditions.

4.3.2. *Gelatin-containing biomaterials*

Gelatin is heat-sensitive. It also contains adhesive peptide ligands that contribute to cell adhesion, but it has poor printability and stability. The combination of gelatin, collagen fibers and OA can improve the mechanical properties of the printed structures, and it is expected to better print implantable vessel scaffolds.

Taymour et al. [32] developed a composite biomaterial composed of collagen, fibrin, and gelatin, called collagen-fibrin-gelatin (CFG). This material exhibits shear-thinning properties, making it an ideal candidate for extrusion bioprinting. The fibrin and collagen within CFG form an interpenetrating polymer network, enhancing the overall mechanical performance of the material beyond the limitations of a single material. Furthermore, the collagen and fibrin contained in CFG has the capacity to support angiogenesis, and the gelatin component facilitates the

construction of vascularized structures. These features not only enable CFG to facilitate vascularization but also to support the formation of lumenized tubular structures.

Khalighi et al. [89] printed a soft tissue scaffold with high Young's modulus and perfusive abilities by a dual-nozzle extrusion bioprinter using a hybrid biomaterial of gelatin and OA encapsulated with adipose-derived mesenchymal stem cells (ADMSCs) (Fig. 7A–B). OA and gelatin crosslinked by Schiff base reaction to form biomaterials with high viscosity. OA could improve the degradation rate of biomaterials and enhance cell adhesion, survival, and proliferation. It has the potential to be made into perfusable vessel scaffolds in the future.

Elastic MeTro with intrinsic elasticity and resilience is also a potential agent to improve the viscosity of the mixed biomaterials. The GelMA and MeTro polymers can covalently crosslink to form hybrid biomaterials with high viscosity and high tensile modulus. Lee et al. [36] enhanced the structural elasticity and mechanical stability of the hybrid biomaterials by adding MeTro to GelMA, printing a vascularized heart structure with endothelial barrier function and spontaneous beating of cardiomyocytes by FRESH method (Fig. 7C). About 67.4 % degradation and integration into host tissue were observed on day 21 after implantation of the structure in rats (Fig. 7D), with minimal inflammatory response.

In addition, it is a good option to print blood vessel scaffolds by combining enzyme-crosslinked fibrinogen with gelatin as a composite biomaterial. Freeman et al. [84] prepared a composite biomaterial of gelatin and fibrinogen, which had good elasticity and shear-thinning properties. The vascular structure containing HDFs printed by rotary bioprinting had good elastic modulus, tensile strength and rupture pressure (Fig. 7E), and the rupture pressure could reach 52 % of the human saphenous vein rupture pressure within two months' culture.

4.3.3. Alginate-containing biomaterials

Alginate has reversible crosslinking and good biocompatibility. But it also has some shortcomings, such as long chain flexibility, difficulty in cell adhesion, and slow degradation in human body. Therefore, improvements can be made by combining alginate with the substances possessing good abilities for both printing and cell adhesion.

Zou et al. [42] developed a polysaccharide complex hydrogel for extrusion bioprinting, composed of agarose, sodium alginate and nanocellulose, where agarose could make the biomaterial network solidified and stabilized quickly; nanocellulose improved the cell adhesion of the composite biomaterial. The bioink caused fibroblasts and ECs to aggregate and grow, forming continuous, vaso-like tissue after four weeks.

Elastic SF is also a good choice for preparing the composite biomaterial with alginate. SF can form a double cross-linked network with alginate. Li et al. [103] developed a composite biomaterial composed of alginate and SF with shear-thinning properties. They printed

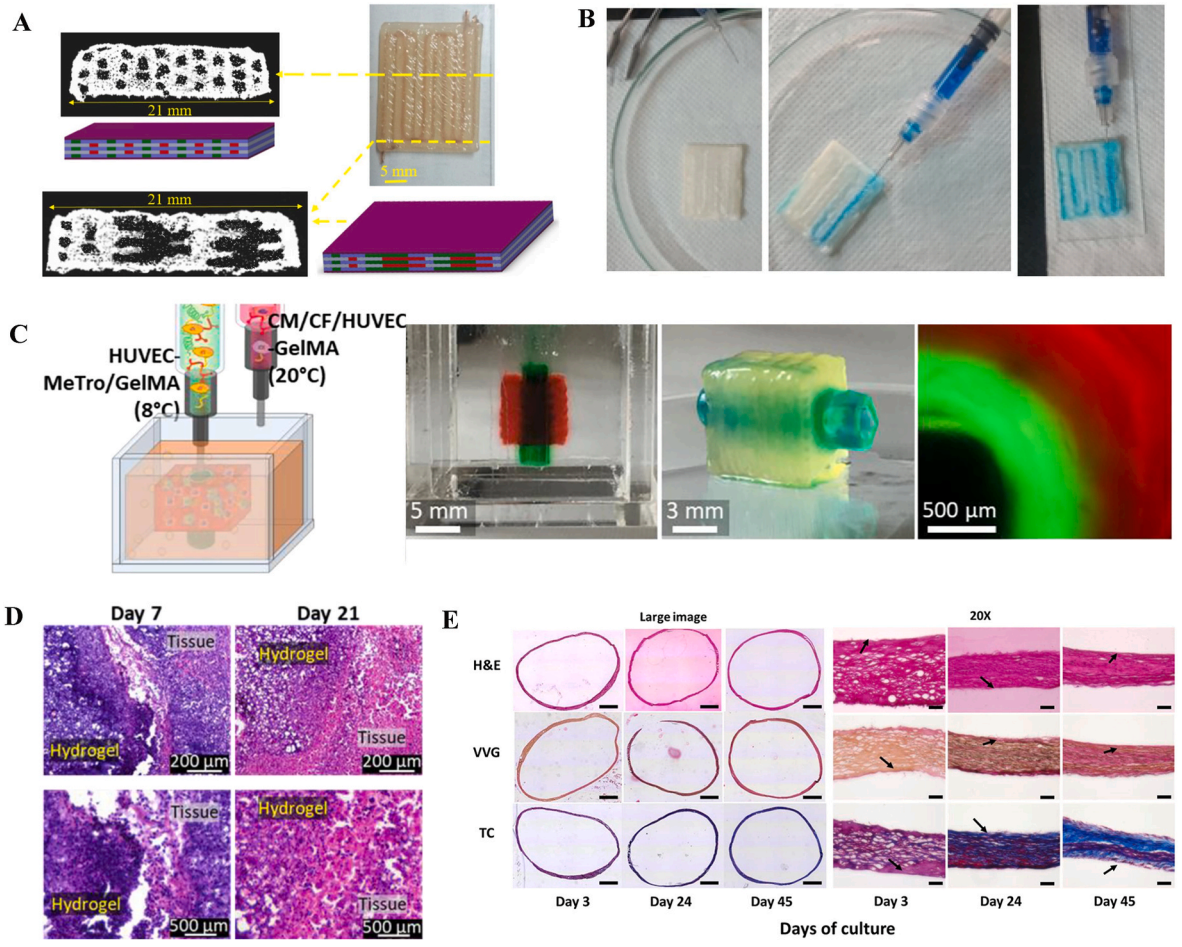

Fig. 7. Composite and hybrid polymers containing gelatin in vessel scaffold printing. A) Micro-CT photographs of the cross section of the bioprinted channel and the cross section of the end point of the attached scaffold. Reproduced and adapted with permission [89]. Copyright 2021, Elsevier. B) Perfusion images of the channel. Reproduced and adapted with permission [89]. Copyright 2021, Elsevier. C) Schematic and cross-sectional fluorescence images of the bioprinted vascularized heart construct. Reproduced and adapted with permission [36]. Copyright 2020, John Wiley and Sons. D) H&E stained images of the vascularized heart constructs on day 7 and day 21 after implantation in rats. Reproduced and adapted with permission [36]. Copyright 2020, John Wiley and Sons. E) Histological sections and cross-sectional images of the vascular constructs at days 3, 24 and 45. Reproduced and adapted with permission [84]. Copyright 2019, Elsevier.

microchannel scaffolds by coaxial extrusion with greater strength, higher compression modulus, more efficient perfusion, and faster cell proliferation similar to blood vessels.

dECM contains key regulators of cell survival, maturation, differentiation, and migration, and can ameliorate the defect of alginate that lacks binding sites for cell attachment and migration. Gao et al. [35] composited vascular-tissue-derived decellularised extracellular matrix (VdECM) with alginate to form a bioink. It could directly print tubes and also improved cellular functions. The composite biomaterial was created using coaxial printing to make blood vessels lined with ECs. These vessels were able to successfully carry out vascular perfusion in a nude mouse model of hindlimb ischemia, resulting in significantly decreased limb loss, foot necrosis, and toe loss.

A hybrid biomaterial that mixed the two has a good ability to print implantable blood vessels. Wang et al. [82] used gelatin and alginate hybrid biomaterial to generate the double-network (DN) hydrogels to produce venous catheters (containing HUVECs and human umbilical vein smooth muscle cells (HUVSMCs)) and arterial catheters (containing HUASMCs and Human umbilical artery ECs (HUAECs)) with high abilities in stretching, perfusions, and barrier properties by microfluidic coaxial extrusion bioprinting (Fig. 8A–B). The excellent mechanical properties of the hybrid biomaterial came from the double cross-linked network with a strong electrostatic interaction. The blood vessel made of the hybrid biomaterial could be used for the test of antiviral drugs and

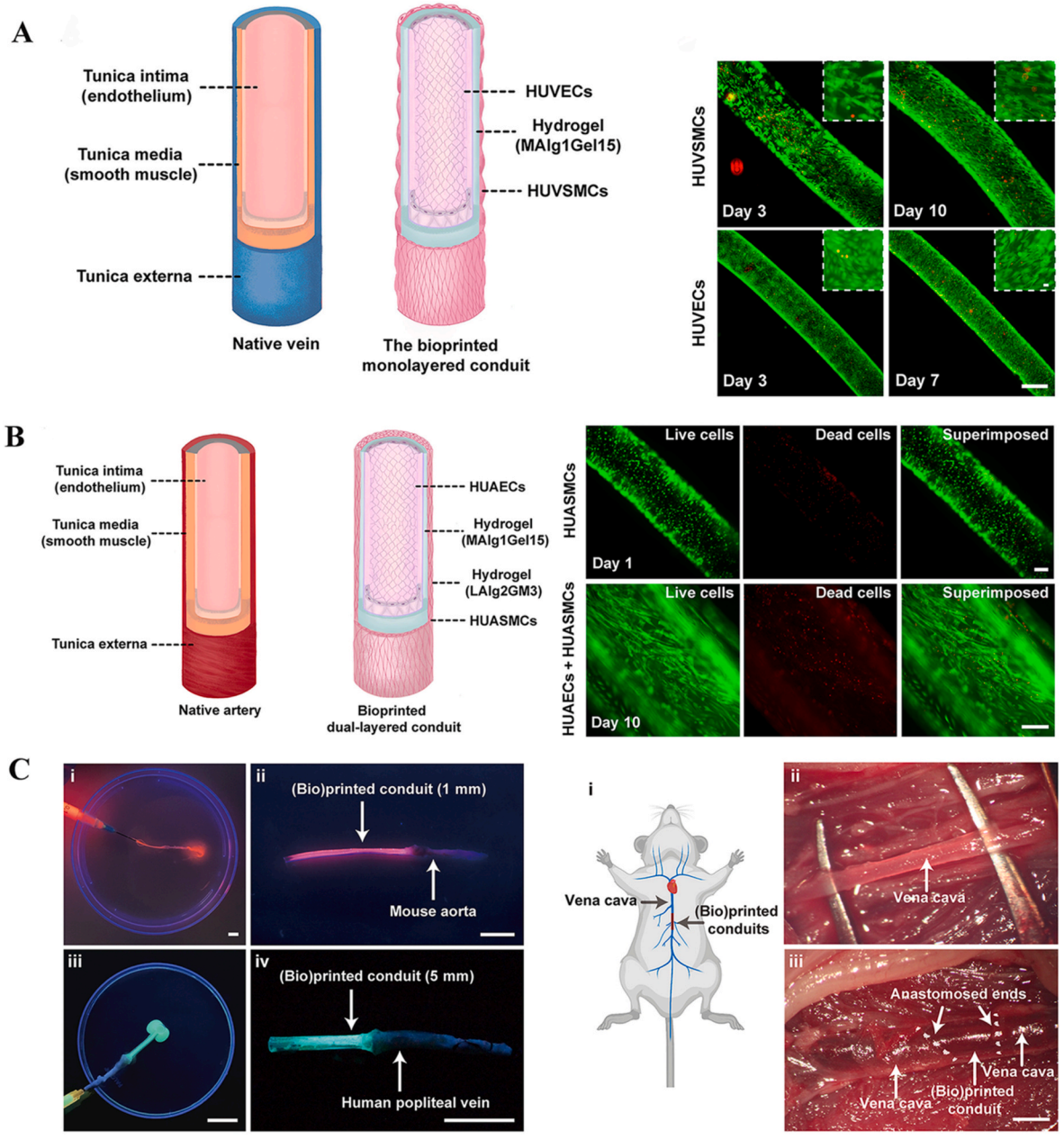

Fig. 8. Arterial and venous catheters printed using alginate and gelatin and their application *in vivo* and *in vitro*. A) Schematic of the structure of the native vein and bioprinted venous conduit, and fluorescence microscopy images of HUVSMCs and HUVECs in the printed vein. Reproduced and adapted with permission [82]. Copyright 2022, American Association for the Advancement of Science. B) Schematic diagram of the structure of native artery and bioprinted arterial conduit, and fluorescence microscopy images of HUASMCs in pairs of printed arteries. Reproduced and adapted with permission [82]. Copyright 2022, American Association for the Advancement of Science. C) *In vitro* attachment and perfusion of bioprinted vascular conduit connected to native vessels via bioglue, and *in vivo* implantation and perfusion of mouse vena cava with printed vascular conduit. Reproduced and adapted with permission [82]. Copyright 2022, American Association for the Advancement of Science.

had the excellent abilities to anastomosis with the natural blood vessels (Fig. 8C).

Attalla et al. [15] mixed alginate with collagen or fibrin to produce a composite biomaterial that could be printed by multi-axial extrusion to create heterogeneously layered, complex structures encasing HUVECs and mouse 3T3 fibroblasts. Collagen and fibrin promoted cell adhesion. Furthermore, cell viability was higher in this composite biomaterial than in alginate alone. In addition, ECs form the vascular like endothelial walls.

4.3.4. *Synthetic polymer-containing biomaterials*

The biocompatibilities and bioactivities of synthetic biomaterials are relatively low. Therefore, it is a common strategy to combine them with natural biomaterials (such as proteins, polysaccharides, cellulose, etc.) to form composite biomaterials with better biocompatibility, biodegradability and bioactivities.

PCL is originally not suitable to encapsulate cells for printing, so Yeo et al. [14] added collagen to PCL promote cell adhesion. They fabricated vessel scaffolds with high elastic modulus and stable mechanical properties by pneumatic extrusion printing using PCL/collagen struts as mechanical supports. When HUVEC was coated on PCL/collagen pillars by electrospinning, slender microvascular structures could be formed. This composite biomaterial was expected to be used in the manufacture of vascularized tissues and vessel scaffolds.

Implantable vessel scaffolds might possess mechanical properties suitable for clinical implantation, as well as structural and physiological functions that mimic the natural vascular endothelium. PCL offers mechanical properties to vessel scaffolds that enhance their structural integrity and functionality. By integrating PCL scaffolds, it is possible to create transplantable vessel scaffolds that combine mechanical performance with biocompatibility and biological activity. Jeong et al. [175] have utilized a dragging 3D printing technique to fabricate multi-layered, small diameter vessel with controllable pore sizes, exhibiting sufficient mechanical properties such as burst pressure, suture retention, and leak resistance, laying a foundation for subsequent vessel scaffold transplantation.

Carrabba et al. [173] have employed co-axial electrospinning technology to fabricate a high-tensile gelatin/PCL inner layer and an elastic PCL layer, with mechanical properties, including Young's modulus and estimated burst pressure, closely resembling those of human blood vessels. Subsequently, they utilized rotational printing techniques on the PCL scaffold, incorporating alginate and pluronic to construct a tunica media enriched with vascular SMCs and an adventitia containing pericytes. In animal studies, the vessel scaffold demonstrated exceptional suture retention, hemostasis, endothelialization, and antithrombogenic properties, along with vascular remodeling characterized by elastin deposition and the emergence of a rich microvasculature.

Recently, a study has utilized PCL to create a bilayer, transplantable vessel scaffold, which has notably demonstrated promising graft outcomes in animal experiments [174]. Upon implantation into the abdominal aorta of rhesus monkeys, the vessel scaffold exhibited a low inflammatory response and facilitated the regeneration of the endothelial and smooth muscle layers, with the vascular morphology closely resembling that of a normal abdominal aorta after 640 days. Although the scaffold maintained robust mechanical properties, with a Young's modulus of 79.55 MPa and a tensile stress of 5.91 MPa at 170 days post-implantation, its low *in vivo* degradation rate suggests the need for further research to enhance and regulate the degradation rate of PCL, thereby optimizing its application as a vessel scaffold material.

PEG is also a synthetic biomaterial that is not easy for cell encapsulation. Monfared et al. [62] mixed PEG with oxidized CNFs to form PEG-CNF composite biomaterial for extrusion printing, which could form a covalent interpenetrating network through the double cross-linking method, to produce scaffolds with adjustable mechanical properties. The composite biomaterial could support the fibroblasts seeded on the surface to maintain good cell viability and proliferation ability, showing its potential for the vascular implant fabrications.

PEGTA can be combined with natural biomaterials to further improve its capability in vessel scaffold printing. Jia et al. [81] mixed PEGTA with GelMA and alginate to form a bioink that can support the nutrients diffusion and the proliferation of ECs with stem cells in the channel. The electrostatic interaction of positively charged gelatin with negatively charged alginate and the covalent cross-linking of PEGTA with GelMA results in the formation of hybrid biomaterials with ideal rheological properties and high mechanical properties. This hybrid biomaterial could be printed with multiple layers of coaxial printing to produce vessel scaffolds with complex layers, decent perfusiability and good biological characteristics, showing a good potential for implantation (Fig. 9A).

Finally, an example of carbon nanotubes in vessel scaffold printing is introduced into the composite biomaterial system. Carbon nanotubes are a nanomaterial with exceptional mechanical properties, enhancing the strength of natural materials [176]. Their biocompatibility and ability to promote cell growth offer the potential for developing durable vessel scaffolds, designed for both longevity and tissue repair in biomedical applications [33]. Li et al. [33] added carbon nanotubes into gelatin and alginate to print a multi-layer bionic blood vessel with physiological activities and metabolic functions with the rotary axis scheme (Fig. 9B–C). A small amount of carbon nanotubes exhibited low toxicity to cells. It could support the adhesion and growth of mouse epidermal fibroblasts on their surface, thereby significantly improving the mechanical properties and the recovery ability after deformation. However, the addition of carbon nanotubes reduced the roughness of the scaffold wall. It also reduced the adhesion and migration of cells. Therefore, further research is needed to provide more vascular cell adhesion sites for the construction of bioactive vessel scaffolds with carbon nanotubes.

5. Demand on biomaterials for bioprinting implantable vessel scaffolds

When assessing the suitability of implantable vessel scaffolds based on biocompatibility and biological activity, mechanical properties, physical properties and processability, Tables 4 and 5 indicate that currently bioprinted vessel scaffolds have not fully met the criteria for implantation. Although these vascular structures exhibit excellent biocompatibility, such as high cellular activity, proper expressions of vascular markers, and the formation of functional endothelium, they lack research in aspects of nonimmunogenicity, nonthrombogenicity, infection resistance, and growth capacity in pediatric patients, which may be due to a lack of in-depth *in vivo* studies and human trials. In terms of mechanical properties, most research has focused on the tensile and compressive strength of vessel scaffolds, with little study on functional aspects such as suture retention.

In the manufacturing process of bioprinted vessel scaffolds, there are three main challenges: (1) the creation of complex multi-layered structures that mimic the morphology of natural blood vessels; (2) achieving mechanical properties that match human blood vessels [177], such as burst pressure [84]; (3) ensuring that the vessel scaffolds can perform their intended physiological functions in the body, such as the transport of oxygen and nutrients [16,136]. Despite progress in the manufacture of vessel scaffolds using natural, synthetic, and composite hybrid biomaterials, there are still challenges in leveraging the biological and physical properties of biomaterials. This requires us to find a balance between the printability and biocompatibility of biomaterials to achieve vascular structures with high shape fidelity and mechanical stability.

This section proposes design schemes to improve the performance of biomaterials, aiming to enhance the biological and mechanical properties of vessel scaffolds. To efficiently select and develop biomaterials, it is necessary to study mathematical models that can predict the performance of biomaterials, considering parameters such as composition and concentration. At the same time, the physical properties of biomaterials

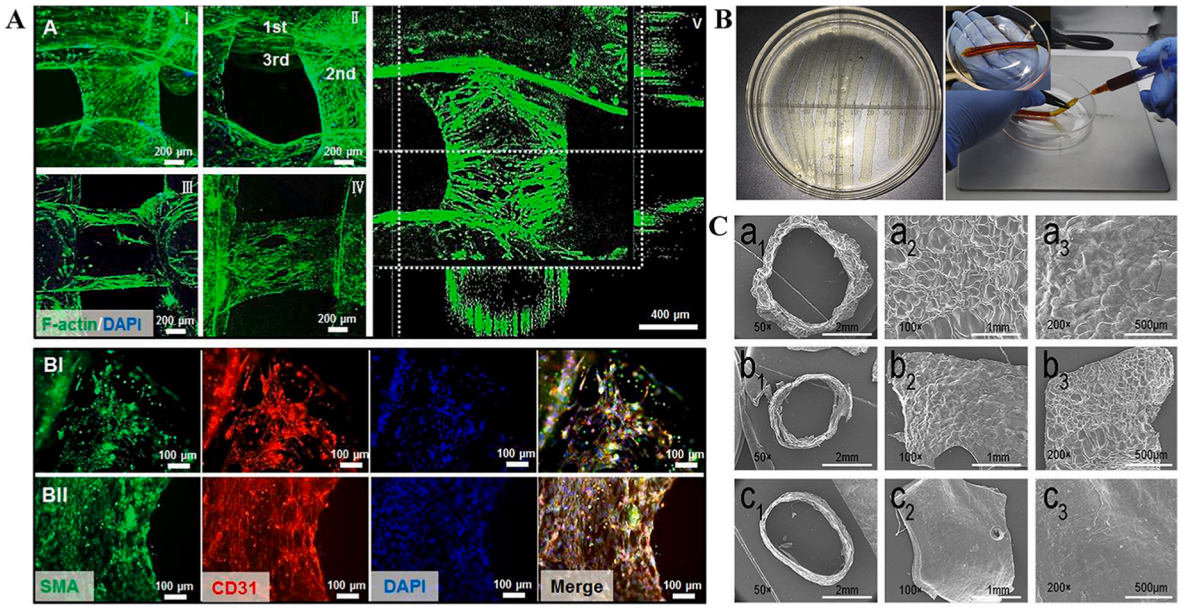

Fig. 9. Composite and hybrid polymers containing synthetic polymer in vessel scaffold printing. A) Representative confocal micrographs of F-actin/nuclear staining after 21 days of culture after bioprinting and confocal images of vascular structures after 14 (I) and 21 (II) days of culture. Reproduced and adapted with permission [81]. Copyright 2016, Elsevier. B) Bulk print products of vessel scaffolds and red dye perfusion assays of scaffolds. Reproduced and adapted with permission [33]. Copyright 2020, Elsevier. C) SEM images of vessel scaffolds with different carbon nanotube concentrations (0 %, 0.5 % and 1 %). Reproduced and adapted with permission [33]. Copyright 2020, Elsevier.

have a significant impact on printability and printing fidelity. In addition, some vessel scaffolds have shown potentials for transplantation in animal experiments [82,173,174,178,179]. When considering the replication of the vessel scaffold's function *in vivo*, the metabolic control and dynamic characteristics of biomaterials should not be overlooked [99,180]. With the advancement of bioprinting technology and the innovation of biomaterials science, it is anticipated that safer, more effective, and more personalized vessel scaffold products will be developed in the future to meet the stringent requirements of clinical applications.

5.1. Printability and biocompatibility of biomaterials for fabricating implantable vessel scaffolds

For implantable vessel scaffolds, it is recommended to evaluate them based on biocompatibility and biological activity, mechanical properties, physical properties and processability, as shown in Table 2. For the biomaterials therein, it is necessary to evaluate them in terms of both printability and biocompatibility.

Printability is the basis and premise to ensure the printing of implantable vessel scaffold structure, majorly influenced by rheological properties, crosslinking mechanisms, and printing conditions [99]. Rheological properties refer to the resistance of the material to flow, typically measured by viscosity, elasticity, and yield stress [63,181]. Crosslinking is the process where polymer chains are connected through physical or chemical means to form a stable hydrogel network, with mechanisms including ionic, thermal, photo, and enzymatic crosslinking [181]. Printing conditions, such as nozzle size, affect the shear stress experienced by the material, thereby influencing its printability [99]. Different printing techniques have specific requirements for the rheological characteristics of materials [99]. In extrusion printing, high viscosity materials are needed to maintain the shape of the printed structure, but excessively high viscosity may be harmful to cells [181]. An ideal biomaterial should exhibit shear-thinning properties, reduced viscosity for extrusion and quick-recovering properties to protect cells post-printing. For instance, alginate, which is commonly used in vessel scaffold printing, exhibits shear thinning properties [16]. Inkjet printing requires biomaterials with lower viscosity to facilitate smooth ejection of ink from the nozzle. The Ohnesorge number, which considers viscosity, density, surface tension, and nozzle radius, is an indicator of printability for inkjet printing, with values between 0.1 and 1 being suitable [99]. For projection photopolymerization (e.g., DLP), biomaterials need rapid photo-crosslinking capability, high crosslinking density, and good flowability [78]. Rapid photo-crosslinking aids in solidification, high crosslinking density provides rigidity, and good flowability facilitates precise shaping and separation during printing [78]. Therefore, biomaterials that are difficult to quickly photo-cure or have excessively high viscosity are generally not suitable for DLP-based printing techniques. To overcome these limitations, material modification can be used to optimize their applicability. For example, by modifying gelatin into GelMA, the photo-curing ability of gelatin can be enhanced, thereby making the material meet the requirements of DLP printing [47].

Biocompatibility is the guarantee to make the printed vessel scaffold with good biological functions, even for the sufficient potential of clinical applications, including cytotoxicity, immune rejection, cell adhesion, biodegradable, etc [99,181]. In Section 5.2, we will focus on the specific requirements of these properties along with the correspondent strategies to improve the printing qualities. Balancing printability and biocompatibility of biomaterials is one of the focuses of the researches today (Fig. 10).

The balance between printability and biocompatibility of biomaterials is important, but can be majorly affected by these three factors: (1) the types and formulations of the biomaterial; (2) the printing methods; (3) the cells contained within the scaffold.

Firstly, the types of biomaterials determine the properties of bioinks for printing, and modified or composite biomaterials can be prepared by optimizing system design to make up for the defects of a single biomaterial. The concentration of the biomaterial determines its viscosity, cytotoxicity, and other properties. For example, in CFG composite biomaterials, the addition of gelatin improved the viscosity of the composite biomaterials, but too much gelatin interfered with the polymerization of collagen and fibronectin networks [32]. Only at the appropriate concentration the biomaterials can perform required

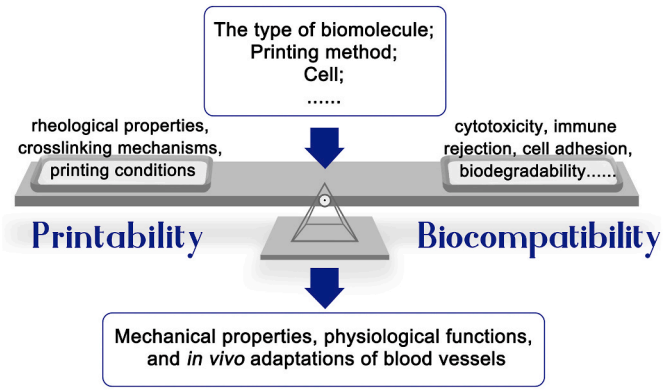

Fig. 10. Printability and biocompatibility of biomaterials need to be balanced.

functions.

Secondly, suitable printing methods can effectively utilize bioinks with versatile properties (e.g., FRESH [37,182], indirect bioprinting [86,183–185], coaxial bioprinting [186], rotary 3D printing [84]). The effective integration of bioprinting method with other advanced biofabrication techniques can also improve the quality of printing vessel scaffolds for possible transplantations (e.g., electrospinning [14], interstitial electrophoresis [138], microfluidics [187], voxelated modalities [188] etc).

Thirdly, cells are one of the most fundamental building blocks in living organisms as well as bioprinting (in some cases). The survivals, differentiations, functions, and interactions of cells can affect the structures and functions of implantable vessel scaffolds. Increased cell concentrations can accelerate the processes of angiogenesis and tissue maturation [90], while certain cell types (i.e. MSCs) may have anti-inflammatory and immunomodulatory capabilities [89]. Cells also affect the physical properties of biomaterials (e.g., in SLA, the existence of cells prevents the penetration of ultraviolet light, reducing the depth of cure of biomaterials) [96].

Although achieving the ideal printability and biocompatibility of biomaterials is crucial, current research may focus on the optimization of single factors, overlooking the interplay and balance between them. For instance, increasing the concentration of biomaterials to enhance viscosity might affect the survival and function of cells [167]. Moreover, printing methods that do not consider the interaction between cells and materials may fail to achieve optimal cell distribution and scaffold functionality, impacting the performance of the final product. Faced with these challenges, future research needs to consider all relevant factors holistically, deeply analysing how they work together to affect the performance of the final structure. Adopting a comprehensive approach is essential for optimizing the printing process. This ensures the effective distribution of cells and enhances the functionality of the scaffold, ultimately improving the overall performance of vessel scaffolds.

5.2. Designing biomaterials for better performance

When fabricating vessel scaffolds for implantation, it is crucial to precisely balance the printability and biocompatibility of the biomaterials used. To enhance the safety and functionality of vessel scaffolds, it is imperative to select biomaterials that are non-cytotoxic or have low cytotoxicity and that promote cell adhesion [29]. These characteristics are essential for promoting the growth, adhesion, and migration of vascular cells, contributing to the formation of a functional endothelial layer [29]. Concurrently, choosing materials that can minimize the risks of thrombosis and inflammation is equally important to prevent scaffold damage and rejection [29,189]. Moreover, to prevent infections during vascular transplantation, the antimicrobial properties of biomaterials should be considered [190]. Biodegradability is a crucial attribute that not only influences cell and tissue growth but also significantly impacts biocompatibility [191]. Therefore, in terms of biocompatibility, the design of biomaterials must meet conditions including, but not limited to, non-cytotoxicity or low cytotoxicity, enhanced cell adhesion capabilities, anti-inflammatory properties, antimicrobial performance, and biodegradability.

Regarding printability, the physicochemical properties of biomaterials are vital for ensuring their mechanical performance and stability [167], which ensures that the printed vessel scaffolds possess the required geometric accuracy and structural integrity. Additionally, the design of biomaterials should also consider their rheological properties during the bioprinting process to ensure that the printed scaffolds can maintain their shape and meet the requirements of bioprinting technology [63]. By meticulously designing biomaterials, we can manufacture vessel scaffolds that are both safe and effective, meeting the demands of clinical applications.

5.2.1. Biomaterials for non-/low cytotoxicity

Cytotoxicity can cause organ dysfunction and health issues, so vessel scaffold biomaterials must be non-cytotoxic. High levels of nitric oxide (NO), reactive oxygen species (ROS), and the subsequent oxidative stress are key mechanisms of severe cellular toxicity and organ dysfunction [190]. Therefore, it's crucial to assess biomaterials' cytotoxicity first. For instance, using stem cell models to test NO and ROS production and screen for non-toxic low-toxicity materials [192]. Moreover, designing ROS-responsive biomaterials can reduce cytotoxicity, thereby improving the tissue microenvironment and regeneration [193].

5.2.2. Biomaterials for enhancing cell adhesion

Improperly integrated biomaterials can compromise the longevity and functionality of artificial implants [194]. For vessel scaffolds to integrate with tissues, the biomaterials must interact with nearby cells and tissues [195], primarily through cellular adhesion forces. Therefore, designing biomaterials with cell integrins to enhance cell adhesion is crucial for promoting tissue regeneration and integration [196]. There are mainly two possible approaches: (1) Blend or couple ECM proteins like collagen and fibronectin into biomaterials to interact with integrins (2) Design biomaterials with recombinant proteins (e.g., Scl-2). and synthetic peptides as integrin receptors to enhance cell adhesion [197], using ECM motifs and RGD sequences. Design ligands targeting integrins related to angiogenesis for graft-host vessel integration. Please refer to the literature [197] for details on specific integrins.

5.2.3. Biomaterials for anti-inflammation

Vessel scaffolds risk damage or rejection from thrombosis or inflammation, harming patient health. To mitigate this, they should utilize autologous cells and biomaterials that prevent thrombogenic and inflammatory responses [189]. Protein adsorption on non-biological materials upon blood contact can trigger the complement system, platelet responses, and coagulation, causing thrombosis and inflammation [189]. Therefore, biomaterial design should prioritize strategies to prevent or modulate these reactions to minimize adverse post-implantation effects. Improving biomaterial surface biocompatibility involves: (1) Encapsulating synthetic polymers like PEG to prevent non-specific protein adsorption [189]. (2) Immobilizing heparan sulfate on surfaces to mimic ECs [189]. (3) Coupling peptides to recruit complement regulators like RCAs Factor H and C4BP to avoid complement attack. (4) Immobilizing apyrase to inhibit platelet activation and coagulation [189]. Additionally, adding anti-inflammatory biomaterials helps eliminate early inflammation signals, complementing strategies targeting blood components [198].

5.2.4. Biomaterials for antimicrobial resistance

Infections are major health complications, and infected vessel scaffolds can be very harmful [199]. Thus, biomaterials for vessel scaffolds need antimicrobial properties. Microorganisms have diverse cell walls

and resistance mechanisms, affecting their sensitivity to antimicrobials [199]. Antimicrobial biomaterial design addresses both "non-specific" and "specific" antimicrobial strategies. (1) Non-specific antimicrobial materials "repel" bacterial adhesion or "kill" bacteria by incorporating superhydrophobic structures or antimicrobial agents, which can affect all cells and microorganisms. (2) Targeted antimicrobials require the development of selective antimicrobial peptides or polymers against specific bacteria to be used as ligands for surface functionalization of biomaterials in order to develop smart antimicrobial materials [200]. Additionally, by tweaking biomaterial molecular structures and adding specific chemical bonds, stimulus-responsive materials that react to physical or bacterial stimuli can be designed [199].

5.2.5. Biomaterials for biodegradability

The biodegradability of vessel scaffold biomaterials is crucial for their biocompatibility. Rapid cell proliferation and neovascularization, as well as host-tissue integration, necessitate materials with a quick degradation rate in microscale; while tissue durability and resistance in mechanics rely on materials with a slower degradation profile in macroscale [61]. Biodegradable vessel scaffolds can be replaced by autologous tissue, thereby avoiding secondary surgeries and reducing the long-term complications caused by permanent foreign bodies [201].

To achieve a balance between the biodegradability and biocompatibility of biomaterials, it is essential to understand the conditions that influence the degradation of materials. The degradation of materials is jointly affected by internal and external factors [202]. Internal factors encompass the chemical composition, such as molecular weight, chemical structure, additives, or modifiers. External factors include abiotic and biotic elements (such as the action of enzymes) [202]. Abiotic factors include mechanical degradation (such as mechanical injuries to vessel scaffolds caused by blood or external forces), light degradation, thermal degradation, and chemical degradation [203]. Considering the factors previously discussed, it seems that the delicate adjustment of materials' chemical characteristics and the careful management of physiological conditions could potentially be pivotal in striking a harmonious balance between biodegradability and biocompatibility.

To optimize the chemical properties of materials and regulate the physiological environment, the following two design approaches can be considered: (1) design materials that contain hydrolysable covalent bonds, such as ester, ether, anhydride, amide, urea, ester-amide (polyurethane), and other groups [203]. For instance, by adjusting the ratio of ester bonds to amide bonds in the synthesis of hydrogels, it is possible to design synthetic hydrogels with tunable *in vivo* degradation kinetics [204]. (2) controlled release of enzymes that promote material degradation: the gradual release of immobilized enzymes in the physiological environment can be used to regulate the degradation rate of biomaterials. For example, a novel structure that combines immobilized cellulase and controlled release has achieved controllable degradation of bacterial cellulose [205].

For precisely designing materials that achieve a balance between degradability and biocompatibility, machine learning can predict the relationship between the degradation rates of polymers and their potential chemical structures. This capability allows for the swift identification of polymer structures with the desired biocompatibility and degradation profiles [206]. Detailed discussion on the use of machine learning to optimize biomaterials is presented in section "5.3.3 Using machine learning to optimize biomaterials".

However, the application of machine learning in predicting material degradation still faces challenges due to the scarcity of degradation time datasets and the lack of standardized data characterization methods [206]. In order to obtain a substantial and effective dataset, we should also update the techniques for studying the relationship between biocompatibility and degradation. Traditional *in vitro* degradation and animal experiments, though useful for investigating the degradation properties of materials, cannot precisely predict the *in vivo* environment [201]. Non-invasive imaging techniques represent an effective approach for tracking the *in vivo* degradation of biomaterials labeled with fluorescent tags, such as quantum dots (QDs), thereby facilitating the assessment of tissue healing in conjunction with material breakdown [201,207]. Additionally, proteomic studies based on mass spectrometry imaging technology can investigate the spatial and temporal interactions between biomaterials and biological systems by assessing the adsorption of proteins on the material surfaces [208].

In summary of this section, by comprehensively considering the chemical properties of materials, modulation of the physiological environment, and advanced imaging techniques, it is possible to design biomaterials that possess good biocompatibility and meet specific degradation requirements.

5.2.6. Biomaterials for enhanced physicochemical properties

The suitability of biomaterials in the fabrication process of vascular structures primarily hinges on their physicochemical properties, which needs to align with the operational conditions of specific bioprinters, including the printing environment and parameters [99]. To ensure the printed vessel scaffolds can effectively function within the body, it is necessary to possess good shape fidelity and mechanical properties that meet physiological requirements. In order for vessel scaffolds to meet mechanical requirements such as burst pressure, biomaterials need to be modified or blended to enhance physicochemical properties. For example, the addition of diacrylate groups to PEG chains to make fast crosslinked PEGDA [155], mixed PEG with oxidized CNFs to form an interpenetrating network [62], and electrostatic interactions between sodium alginate and gelatin to promote crosslinking [82]. Molecular sliding also contributes to the synthesis of tough and stretchable materials [209]. These all require an in-depth study of the reactive bonds and groups in the molecular structure of the materials to predict their cross-linking.

Studying the molecular structures and biological interactions of biomaterials is crucial for ensuring the biocompatibility and biological activity, mechanical properties and physical properties of vessel scaffolds. Additionally, cost reduction is also a significant research focus. Biomaterial design should balance functionality, economy, and feasibility to enhance cost-effectiveness and advance vessel scaffold technology.

5.3. The selection and optimization of biomaterials for implantable vessel scaffolds

5.3.1. Current use of biomaterials

In general, it is challenging to use one single biomaterial for the construction of multilayer vessel scaffolds, and even more difficult to meet the requirements for biocompatibility and biological activity, mechanical properties and physical properties of the printed structures. Therefore, composite biomaterials or combinations of multiple biomaterials are usually utilized for bioprinting. From Tables 4 and 5, the composite of biomaterials consisting of alginate, collagen, fibronectin, and gelatin are more promising for achieving the ideal bioprinting of vessel scaffolds.

By counting and comparing the number of biomaterials used in bioprinted vessel scaffolds and the earliest use of the biomaterials discussed in this review (Fig. 11), it has been noticed that gelatin, alginate, and collagen are the three most used biomaterials, with fibrin ranking sixth. All of these above materials (gelatin, alginate, collagen and fibrin) belong to the natural biomaterials, with good biocompatibility. While single-component of these biomaterials have poor printability, composite biomaterials have significantly improved printability due to the ability to form interpenetrating cross-linked networks [47]. In addition, there are biocompatible cross-linking agents (e.g. Ca^{2+}, thrombin, mTG) to promote cross-linking [38,84,112]. Therefore, these four materials have good potential as the basic elements of composite biomaterials for bioprinting vessel scaffolds.

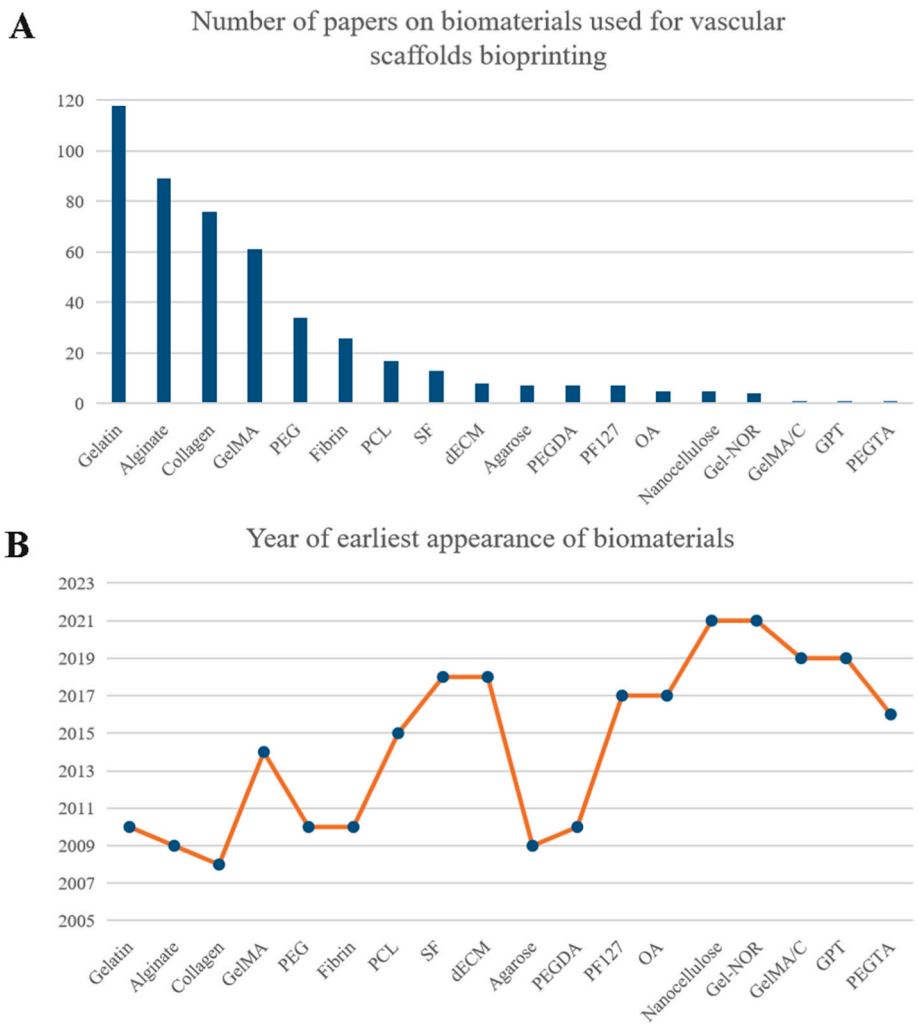

Fig. 11. A) Number of papers on biomaterials used for vessel scaffolds bioprinting, and B) year of earliest appearance of biomaterials. (These data were taken from the pubmed platform and the keywords entered were: bioprint/bio-print + blood vessel/vascular scaffold/graft + name of each biomaterial).

In contrast, the use of synthetic biomaterials is relatively limited. On the one hand, the potential threat to organisms from synthetic or modified biomaterials is difficult to ignore [18]. On the other hand, this limitation may be due to the fact that these synthetic and modified biomaterials are relatively new and initiated later. Despite the limited use of synthetic and modified biomaterials, there are potential application prospects and opportunities for development.

5.3.2. *Biomaterials for vessel scaffolds of different sizes*

Based on the previously discussed biomaterial properties and the size of the vessel scaffolds they fabricate, we have summarized the preferred types of biomaterials for various sizes of vessel scaffolds in detail in Table 6.

Table 6
Biomaterials used in vessel scaffolds of different sizes.

Types of vessel scaffolds	Diameter	Commonly used biomaterials	Ref.
Microvessels	<1 mm	Alginate, OA, Agarose, Collagen, Gelatin, GelMA, Gel-NOR, GelMA/C, GPT, SF, PEG, PEGTA, PCL, PF127	[14,32,36,81,85,87,89,103,164]
Small vessels	1 ~ 6 mm	Alginate, Collagen, Gelatin, GelMA, Fibrin, dECM, PEG-co-PDP/RGDS, PEGTA, PCL, PF127	[15,33,35,38,81,82,84,91,173,174]
Large vessels	>6 mm	PEG-co-PDP/RGDS, PCL	[94,178]

Table 6 reveals a trend: biomaterials for microvessels are typically characterized by lower viscosities, with the viscosity of these materials increasing in correlation with larger vessel diameters. In addition, natural-origin biomaterials are widely used for printing microvessels and small-vessel scaffolds, while synthetic ones are versatile for all vessel sizes.

Light-based printing methods are particularly suitable for the fabrication of microvessels, as they offer high precision and are compatible with biomaterials that have a lower viscosity [8,210]. For larger vessels, higher viscosity biomaterials are essential to preserve structural integrity due to their increased diameter and need for robust mechanical properties [167]. When it comes to large diameter vessel scaffolds, synthetic biomaterials are typically employed. This is because synthetic materials generally exhibit good mechanical properties, which are essential for creating larger vessel scaffolds [211]. In contrast, natural biomaterials tend to have inferior mechanical properties, longer gelation times, faster degradation rate, and result in vessel scaffolds with weaker mechanical performance [28,133]. These factors make it challenging to manufacture large vessels using natural biomaterials.

However, natural biomaterials are well-suited for the fabrication of both microvessels and small vessels. On the other hand, synthetic biomaterials are applicable for bioprinting of vessels across all scales, due to their advantages such as rapid gelation and tunable mechanical properties [90]. The selection of natural versus synthetic biomaterials hinges on the unique requirements of each printed vascular structure, as each

provides distinct advantages throughout the biofabrication process.

5.3.3. Using machine learning to optimize biomaterials

Artificial Intelligence (AI) has made substantial progress in medical imaging over the past two decades, notably in analyzing images and signals for cardiovascular diagnostics [212]. Machine learning, a core AI technique, has refined its capabilities by learning from historical data, enabling accurate and robust vessel segmentation that improves the accuracy of diagnosing vascular conditions [213]. Additionally, machine learning models now predict post-surgery outcomes for transcatheter aortic valve implantation (TAVI) using pre-procedural computed tomography (CT), highlighting AI's growing role in advancing medical imaging [214].

Machine learning methods have demonstrated considerable potential in predicting the overall mechanical properties of composites with tubular structures, as evidenced by recent studies [215]. Furthermore, these techniques accurately predict material damage response, rivaling precision even in the presence of minor geometric discrepancies [216]. Integrating machine learning into biomaterials research, especially for optimizing bioprinted vascular graft formulations and parameters, marks an exciting frontier with the potential for significant field advancements.

There are many factors that affect bioprinting, such as ink reservoir temperature, print pressure, nozzle diameter, nozzle type, print head speed and platform temperature, cross-linking method, amount of cross-linking agent, and cross-linking time [217]. Traditional trial-and-error optimization methods encounter challenges in efficiently and effectively adjusting the numerous printing variables to determine the optimal printing conditions. Therefore, it is required that machine learning rapidly assimilates vast and intricate data to determine the optimal conditions [217,218].

Machine learning is an automated, highly flexible and computationally intensive method that learns from data to recognize the trends in complex data, saving time and materials compared to traditional methods [219]. Here, we have summarized two potential usages of machine learning in bioprinting: (i) exploring the importance of each parameter in the printing process and the potential relationship between the parameters [220]; (ii) predicting the effects of different parameters on the bioprinting results and deriving the optimal parameter combinations. Between them, the parameters can be the types or the ratios of materials in bioink/biomaterial ink [221,222] and the parameters of printing conditions during the bioprinting process [217,223]. The goals for optimizations may involve the rheological behaviors and extrudability of the substrate [224] or parameters related to cells [218,220,225].

To refine bioprinting parameters for implantable vessel scaffolds with machine learning, it is critical to set up a comprehensive database encompassing biomaterial property, printing parameters, and outcomes. It can be built through extensive experimentation, leveraging public datasets, and forging collaborative partnerships. Such a data-rich repository is vital, offering a key asset for machine learning applications and driving biomaterial innovation in vessel scaffold biofabrication.

5.4. Bioprinted vessel scaffolds in animal experiments

Animal and clinical studies are crucial to confirming the viability of bioprinted vessel scaffolds [226]. Currently, most clinical vessel scaffolds are crafted from rigid polyethylene terephthalate (PET) and ePTFE [227].The stiffness of these materials can lead to a discrepancy in viscoelastic properties between the synthetic grafts and human vasculature, potentially causing complications such as intimal hyperplasia (IH) [227]. However, vessel scaffolds produced through bioprinting exhibit favorable viscoelasticity, and numerous animal model studies have demonstrated their potential in clinical applications of vessel transplantation.

Animal models facilitate a more in-depth investigation of the critical properties of vessel scaffolds, such as anastomosis, endothelialization, and degradation [226]. Therefore, the selection of appropriate animal models is crucial for advancing clinical research. Animal models include small animal models (e.g., CAM [87], rodents [35,45,211,228,229], and rabbits [230]) and large animal models (e.g., dogs [231], sheep [227,232–235], pigs [173,178,236], and primates [174,226]). While small animal models are relatively common, they exhibit significant differences from humans in terms of cell size, genetics, and *in vivo* environment [236]. In contrast, large animal models can more accurately simulate the human blood environment [226], providing more compelling research outcomes. Examples of such large animal models include sheep, pigs, and non-human primates, which are physiologically similar to humans.

Sheep, whose anatomical and hemodynamic conditions are similar to humans, are the preferred animal models for studying cardiovascular implants *in vivo* [234]. For instance, as referenced by Hoerstrup et al. [234], a study that spanned 100 weeks utilized a growing lamb model to investigated a pulmonary artery vessel scaffold created using the heat application welding technique. The study evaluated the mechanical performance, tissue characteristics, and biocompatibility of the blood vessels through methods such as angiography and histology. Similarly, Koobatian et al. [233] used the carotid artery of an ovine model to study the implantation of acellular tissue engineered vessels, achieved endothelialization and remodeling of the implanted vessels.

Pigs are anatomically, physiologically, immunologically, and lifespan-wisely similar to humans, making them suitable models for studying graft endothelialization [236]. But the porcine model has the drawback of high maintenance costs [237]. However, the model is continuously being refined; for instance, Itoh et al. [236] improved the original operational immunodeficient pig (OIDP) model, which demonstrating better long-term accommodation of vascular grafts compared to the conventional immunosuppressive pig (CISP) model.

Non-human primates are ideal candidates for vascular transplant research due to their genetic, hemostatic, and mechanical similarities to humans [226]. Anderson et al. [226] improved vascular graft surgery techniques by performing abdominal aortic bypass in baboon models. While this model has been successful in research, its industrial application remains limited and costly [226].

Compared to traditional manufacturing methods, bioprinted vessel scaffolds have been often utilized in small animal models such as rodents and rabbits. Melchiorri et al. [211] investigated the endothelialization of vessel scaffolds six months post-implantation in the mouse venous system, creating scaffolds that prevent thrombosis and facilitate vascular tissue repair and remodeling. Sohn et al. [45] used a rat model to investigate the endothelialization and thrombogenicity of vessel scaffold after 30 days of implantation. Although small animal models took a significant portion of the research in the field of vascular bioprinting, an increasing number of studies have begun to employ large animal models to delve into the mechanical properties and biocompatibility of vessel scaffolds after *in vivo* transplantation. These studies aid in more accurately assessing the clinical application potential of vessel scaffolds. Yeung et al. [178] used a porcine pulmonary artery (PA) reconstruction model to examine the circumferential tensile strength, compliance, patency, degradability, neo-tissue, and vascular system formation of PCL vessel scaffolds created by a combination of bioprinting and electrospinning. Notably, the wall shear stress and pressure drop of these scaffolds were comparable to those of natural blood vessels, and they demonstrated potential for tissue remodeling. Fukunishi et al. [179] studied acellular venous scaffolds made from polyglycolic acid (PGA) and poly-L-lactic acid-co-ε-caprolactone (PLCL) in the inferior vena cava of sheep, focusing on the patency, cellular infiltration, and mechanical properties of the scaffolds post-implantation. Jiang et al. [174] employed rhesus monkeys to study a PCL-based bilayer vessel scaffold, as previously mentioned in section 4.3.4.

Bioprinted vessel scaffolds still face several challenges in animal experiments: (1) limited application in large animal models, possibly

due to insufficient mechanical properties [211] and size limitations of the scaffolds [238]; (2) differences between animal models and human physiology; (3) high surgical skill requirements for implantation [226]; (4) a lack of standardized protocols for model selection, condition setting, research orientation, and methodological standardization.

To enhance the study of bioprinted vessel scaffolds using animal models, the following improvements can be made: (1) prioritize the use of large animal models (such as sheep and primates) for long-term experiments to better mimic human conditions [226,234]. (2) employ bioinformatics to analyze the similarities and differences in vascular signaling pathways between animals and humans, predicting the adaptability of vessel scaffolds in humans through animal models [235]. (3) establish experimental standards and risk assessment strategies for animal vascular transplant models [228]. (4) develop hemodynamic models that simulate the human vascular environment through computer-aided modeling and simulation [178,211]. (5) utilize advanced imaging technologies like MRI, CT, and optical coherence tomography for the visualization and quantification of the *in vivo* response of transplanted vessels [226].

5.5. Controlled catabolism and dynamics of biomaterials for the fabrication of implantable vessel scaffolds

Biomaterials not only play an important role in the process of bioprinting vessel scaffolds, but also influence the function of vessel scaffolds after implantation. Therefore, the state of the biomaterials after transplantation in the printed vessel scaffolds into body should also be considered. This mainly includes the catabolism and dynamics of biomaterials *in vivo*.

On the one hand, the degradation of different types of biomaterials varies after the printed scaffold is implanted into the body. For instance, biomaterials such as gelatin and PCL can be degraded in living organisms, further breaking down into nutrients that can be absorbed by the body or excreted through metabolism [158,239]. However, biomaterials such as agarose and PEG are difficult to biodegrade *in vivo* [152,240]. Therefore, further researches and improvements are still needed to discover the degradation ability of these biomaterials. On the other hand, blood vessels undergo dynamic renewal in the tissue to adapt to the dynamic environment within the body. 4D bioprinting is an advanced technology that enables the printed structure to function by adjusting its shape under external stimulations [16]. This technique requires the use of biomaterials capable of responding to stimuli from the external environment [180], such as adding variable groups or dynamic molecules to existing biomaterials. It is believed that a large number of such biomaterials will emerge in the printing of vessel scaffolds in near future, which will produce vessel scaffolds that can be adapted to changes in the internal environment and respond effectively.

In summary, biomaterials for vessel scaffolds should possess controllable metabolic capabilities and the ability to adapt to the dynamic internal environment of the human body. This necessitates the biodegradability of vessel scaffolds, ensuring that they gradually integrate with surrounding tissues post-implantation, promoting tissue growth and vascular regeneration. The deposition and remodeling of the extracellular matrix are crucial for the formation of functional vascular structures. Biodegradable materials are typically designed to lose their structural integrity over time, providing a temporal window for the formation of new vessels. Moreover, as the biomechanical environment changes with patient growth or tissue healing, degradable vessels can adjust progressively to accommodate these shifts. This adaptability is vital for the long-term therapeutic repair following the transplantation of bioprinted vessel scaffolds.

From the foregoing, to achieve bioprinted vessel scaffolds capable of human implantation, these biomaterials need to leveraging printability and biocompatibility. In addition, it is also necessary to possess the capacity for controlled catabolism as well as adaptability to dynamic changes within the human body for these printed vessel scaffolds.

6. Conclusions and future perspectives

With the rapid progress in the fields of tissue engineering and regenerative medicine, the demand for high-quality vessel scaffolds is continuously increasing. Although large-diameter vessel scaffolds have seen successful clinical applications [178,236], the ongoing challenge of low patency rates post-transplantation underscores the imperative for ongoing innovation in this field. Bioprinting offers a novel strategy for fabricating scaffolds tailored to specific patient needs. To ensure compliance with the stringent requirements of clinical trials, meticulous selection and engineering of biomaterials are essential to tackle pivotal challenges, including low patency rates and the risk of thrombosis.

This article examines the role of biomaterials in vessel scaffold bioprinting, highlighting the inherent bioactivity of natural materials like alginate, collagen, and SF. It also introduces the untapped potential for enhancing the biocompatibility of synthetic materials, such as PEG and PCL. In our view, future research will focus on optimizing the physicochemical and biological properties of these materials, particularly leveraging the characteristics of printability, biocompatibility, controllable metabolism, and adaptability to dynamic *in vivo* changes.

Continuous efforts in research will certainly prioritize the identification of optimal methods for blending synthetic and natural materials. Meanwhile, novel engineering approaches, such as machine learning, will also be employed to refine the selection of the biomaterials and the parameters for the printing process. The bioreactor technology which can replicate the *in vivo* conditions, provides the environment for the maturation of printed vessel scaffolds, facilitating cellular activities, ECM deposition, and tissue remodeling [241,242]. Additionally, the development of simulation technologies that models vascular structures fabricated with mechanically enforced biomaterials is also critical for adapting the scaffolds to the dynamic *in vivo* environment [243]. Lastly, it is necessary to further select or develop more appropriate animal models for obtaining reliable pre-transplant assessments of vessel scaffolds and to explore alternatives to animal models, such as organ-on-chips [244], which may offer new avenues for reducing costs and time. The broader application of implantable vessel scaffolds in the future is poised to revolutionize the field of regenerative medicine and vascular surgery.

Abbreviations

Full name	Abbreviation
Cardiovascular diseases	CVDs
Three-dimensional	3D
Bioresorbable vascular scaffolds	BVS
Natural vascular scaffolding	NVS
Endothelial cells	ECs
Human umbilical vein endothelial cells	HUVECs
Smooth muscle cells	SMCs
Human umbilical artery smooth muscle cells	HUASMCs
Human umbilical vein smooth muscle cells	HUVSMCs
Endothelial progenitor cells	EPCs
Human umbilical artery ECs	HUAECs
Mesenchymal stem cells	MSCs
Adipose-derived mesenchymal stem cells	ADMSCs
Human induced mesodermal progenitor cells	hiMPCs
α-Smooth muscle actin	α-SMA
Extracellular matrix	ECM
Decellularized extracellular matrix	dECM
Vascular-tissue-derived decellularised extracellular matrix	VdECM
Freeform reversible embedding of suspended hydrogels	FRESH
Polyethylene glycol	PEG
Poly(ethylene glycol) diacrylate	PEGDA
Poly(-ethylene glycol) -tetra -acrylate	PEGTA
Poly(ethylene glycol) methacrylate	PEGMA
Vascular endothelial growth factor	VEGF
Polycaprolactone	PCL
Polyethylene oxide	PEO
Pluronic F127	PF127
Oxidized alginate	OA

(*continued on next page*)

(*continued*)

Matrix metalloproteinase-cleavable linker	MMPQK
Methacrylated gelatin	GelMA
Gelatin-norbornene	Gel-NOR
Catecholin-functionalized methacrylate gelatin	GelMA/C
Gelatin-PEG-tyramine	GPT
Dielectrophoresis	DEP
Human dermal fibroblasts	HDFs
Matrix metalloproteinases	MMP
Hyaluronic acid	HA
Chorioallantoic membrane	CAM
Collagen-fibrin-gelatin	CFG
Collagen-fibrin	CF
Methacryloyl-substituted recombinant human tropoelastin	MeTro
Double-network	DN
Microbial transglutaminase	mTG
Cellulose nanofibril	CNF
Cellulose nanocrystal	CNC
Bacterial nanocellulose	BNC
Tissue engineered vascular grafts	TEVGs
Silk fibroin	SF
Poly(dl-lactide)–poly(ethylene glycol)	PELA
Decellularized aortic matrix	DAM
Poly-L-lactide acid	PLLA
Laser-induced forward transfer	LIFT
Digital micromirror device	DMD
Stereolithography	SLA
Pulmonary artery	PA
Inner diameter	ID
Outer diameter	OD
Polyethylene terephthalate	PET
Expanded polytetrafluoroethylene	ePTFE
Digital light processing	DLP
Artificial intelligence	AI
Transcatheter aortic valve implantation	TAVI
Computed tomography	CT
Intimal hyperplasia	IH
Quantum dots	QDs

CRediT authorship contribution statement

Tianhong Chen: Writing – original draft. **Haihong Jiang:** Writing – review & editing. **Ruoxuan Zhang:** Writing – review & editing. **Fan He:** Writing – review & editing. **Ning Han:** Funding acquisition. **Zhimin Wang:** Funding acquisition. **Jia Jia:** Writing – review & editing, Funding acquisition, Conceptualization.

Declaration of Competing interest

We declare that we have no financial and personal relationships with other people or organizations that can inappropriately influence our work, there is no professional or other personal interest of any nature or kind in any product, service and/or company that could be construed as influencing the position presented in, or the review of, the manuscript entitled, “Leveraging Printability and Biocompatibility in Materials for Printing Implantable Vessel Scaffolds”.

Acknowledgements

T.H.C. and H.H.J. contributed equally to this work. R.X.Z. and F.H. engaged in a thorough review of the manuscripts, focusing on improving the clarity, coherence, and accuracy of the content. This work was financially supported by Zhimin Wang reports financial support that was provided by National Natural Science Foundation of China (No.51833006), China and Innovation Promotion Program of NHC and Shanghai Key Labs, SIBPT, China (No. CX2023-03). Jia Jia reports financial support was provided by Shanghai University (No. N-58-D305-22-204), China.

Data availability

No data was used for the research described in the article.

References

[1] D. Mozaffarian, E.J. Benjamin, A.S. Go, D.K. Arnett, M.J. Blaha, M. Cushman, S. de Ferranti, J.P. Despres, H.J. Fullerton, V.J. Howard, M.D. Huffman, S. E. Judd, B.M. Kissela, D.T. Lackland, J.H. Lichtman, L.D. Lisabeth, S. Liu, R. H. Mackey, D.B. Matchar, D.K. McGuire, E.R. Mohler 3rd, C.S. Moy, P. Muntner, M.E. Mussolino, K. Nasir, R.W. Neumar, G. Nichol, L. Palaniappan, D.K. Pandey, M.J. Reeves, C.J. Rodriguez, P.D. Sorlie, J. Stein, A. Towfighi, T.N. Turan, S. S. Virani, J.Z. Willey, D. Woo, R.W. Yeh, M.B. Turner, C. American Heart Association Statistics, S. Stroke Statistics, Heart disease and stroke statistics–2015 update: a report from the American Heart Association, Circulation 131 (4) (2015) e29–e322.

[2] C.D. Mathers, D. Loncar, Projections of global mortality and burden of disease from 2002 to 2030, PLoS Med. 3 (11) (2006) e442.

[3] Z. Zhang, B. Wang, D. Hui, J. Qiu, S. Wang, 3D bioprinting of soft materials-based regenerative vascular structures and tissues, Compos. B Eng. 123 (2017) 279–291.

[4] D.P. Leong, P.G. Joseph, M. McKee, S.S. Anand, K.K. Teo, J.D. Schwalm, S. Yusuf, Reducing the global burden of cardiovascular disease, Part 2: prevention and treatment of cardiovascular disease, Circ. Res. 121 (6) (2017) 695–710.

[5] S. Abdollahi, J. Boktor, N. Hibino, Bioprinting of freestanding vascular grafts and the regulatory considerations for additively manufactured vascular prostheses, Transl. Res. 211 (2019) 123–138.

[6] T. Pennel, G. Fercana, D. Bezuidenhout, A. Simionescu, T.-H. Chuang, P. Zilla, D. Simionescu, The performance of cross-linked acellular arterial scaffolds as vascular grafts; pre-clinical testing in direct and isolation loop circulatory models, Biomaterials 35 (24) (2014) 6311–6322.

[7] C.C. Jadlowiec, M. Lavallee, E.M. Mannion, M.G. Brown, An outcomes comparison of native arteriovenous fistulae, polytetrafluorethylene grafts, and cryopreserved vein allografts, Ann. Vasc. Surg. 29 (8) (2015) 1642–1647.

[8] X. Cao, S. Maharjan, R. Ashfaq, J. Shin, Y.S. Zhang, Bioprinting of small-diameter blood vessels, Engineering 7 (6) (2021) 832–844.

[9] J.M. Scott, S. Armenian, S. Giralt, J. Moslehi, T. Wang, L.W. Jones, Cardiovascular disease following hematopoietic stem cell transplantation: pathogenesis, detection, and the cardioprotective role of aerobic training, Crit. Rev. Oncol. Hematol. 98 (2016) 222–234.

[10] A. Weekes, N. Bartnikowski, N. Pinto, J. Jenkins, C. Meinert, T.J. Klein, Biofabrication of small diameter tissue-engineered vascular grafts, Acta Biomater. 138 (2022) 92–111.

[11] S. Liu, C. Dong, G. Lu, Q. Lu, Z. Li, D.L. Kaplan, H. Zhu, Bilayered vascular grafts based on silk proteins, Acta Biomater. 9 (11) (2013) 8991–9003.

[12] S. Oliveira, T. Felizardo, S. Amorim, S.M. Mithieux, R.A. Pires, R.L. Reis, A. Martins, A.S. Weiss, N.M. Neves, Tubular fibrous scaffolds functionalized with tropoelastin as a small-diameter vascular graft, Biomacromolecules 21 (9) (2020) 3582–3595.

[13] R. Gauvin, Y.C. Chen, J.W. Lee, P. Soman, P. Zorlutuna, J.W. Nichol, H. Bae, S. Chen, A. Khademhosseini, Microfabrication of complex porous tissue engineering scaffolds using 3D projection stereolithography, Biomaterials 33 (15) (2012) 3824–3834.

[14] M. Yeo, G. Kim, Micro/nano-hierarchical scaffold fabricated using a cell electrospinning/3D printing process for co-culturing myoblasts and HUVECs to induce myoblast alignment and differentiation, Acta Biomater. 107 (2020) 102–114.

[15] R. Attalla, E. Puersten, N. Jain, P.R. Selvaganapathy, 3D bioprinting of heterogeneous bi- and tri-layered hollow channels within gel scaffolds using scalable multi-axial microfluidic extrusion nozzle, Biofabrication 11 (1) (2018) 015012.

[16] P. Rastogi, B. Kandasubramanian, Review of alginate-based hydrogel bioprinting for application in tissue engineering, Biofabrication 11 (4) (2019) 042001.

[17] J. Bansal, K. Neuman, V.K. Greene Jr., D.A. Rubenstein, Development of 3D printed electrospun scaffolds for the fabrication of porous scaffolds for vascular applications, 3D Print. Addit. Manuf. 9 (5) (2022) 380–388.

[18] S. Reakasame, A.R. Boccaccini, Oxidized alginate-based hydrogels for tissue engineering applications: a review, Biomacromolecules 19 (1) (2018) 3–21.

[19] J. Huling, S.I. Min, D.S. Kim, I.K. Ko, A. Atala, J.J. Yoo, Kidney regeneration with biomimetic vascular scaffolds based on vascular corrosion casts, Acta Biomater. 95 (2019) 328–336.

[20] K. Kauser, K.S. Warner, B. Anderson, E.D. Keyes, R.B. Hayes, E. Kawamoto, D. H. Perkins, R. Scott, J. Isaacson, B. Haberer, A. Spaans, R. Utecht, H. Hauser, A. G. Roberts, M. Greenberg, Creating a natural vascular scaffold by photochemical treatment of the extracellular matrix for vascular applications, Int. J. Mol. Sci. 23 (2) (2022).

[21] E. Mahmud, R.R. Reeves, Bioresorbable vascular scaffolds: back to the drawing board, JACC Cardiovasc. Interv. 11 (7) (2018) 645–647.

[22] D.J. Kereiakes, Y. Onuma, P.W. Serruys, G.W. Stone, Bioresorbable vascular scaffolds for coronary revascularization, Circulation 134 (2) (2016) 168–182.

[23] S. Liu, L. Yao, Y. Wang, Y. Li, Y. Jia, Y. Yang, N. Li, Y. Hu, D. Kong, X. Dong, K. Wang, M. Zhu, Immunomodulatory hybrid micro-nanofiber scaffolds enhance vascular regeneration, Bioact. Mater. 21 (2023) 464–482.

[24] A. Chaus, B.F. Uretsky, Bioresorbable vascular scaffolds: a dissolving dream? Cardiovasc. Drugs Ther. 37 (1) (2023) 1–3.
[25] J.D. Abbott, C. Bavishi, Next-generation bioresorbable vascular scaffolds: when to get our hopes up? JACC Cardiovasc. Interv. 12 (3) (2019) 256–258.
[26] S. Bangalore, E.R. Edelman, D.L. Bhatt, First-generation bioresorbable vascular scaffolds: disappearing stents or disappearing evidence? J. Am. Coll. Cardiol. 69 (25) (2017) 3067–3069.
[27] P. Datta, B. Ayan, I.T. Ozbolat, Bioprinting for vascular and vascularized tissue biofabrication, Acta Biomater. 51 (2017) 1–20.
[28] M.L. Bedell, A.M. Navara, Y. Du, S. Zhang, A.G. Mikos, Polymeric systems for bioprinting, Chem Rev 120 (19) (2020) 10744–10792.
[29] F. Fazal, S. Raghav, A. Callanan, V. Koutsos, N. Radacsi, Recent advancements in the bioprinting of vascular grafts, Biofabrication 13 (3) (2021).
[30] K. Sung, N.R. Patel, N. Ashammakhi, K.L. Nguyen, 3-Dimensional bioprinting of cardiovascular tissues: emerging technology, JACC Basic Transl Sci 6 (5) (2021) 467–482.
[31] H. Xu, Y. Su, Z. Liao, Z. Liu, X. Huang, L. Zhao, R. Duan, Y. Hu, Y. Wei, X. Lian, D. Huang, Coaxial bioprinting vascular constructs: a review, Eur. Polym. J. 179 (2022).
[32] R. Taymour, N.A. Chicaiza-Cabezas, M. Gelinsky, A. Lode, Core-shell bioprinting of vascularizedin vitroliver sinusoid models, Biofabrication 14 (4) (2022).
[33] L. Li, S. Qin, J. Peng, A. Chen, Y. Nie, T. Liu, K. Song, Engineering gelatin-based alginate/carbon nanotubes blend bioink for direct 3D printing of vessel constructs, Int. J. Biol. Macromol. 145 (2020) 262–271.
[34] A.N. Leberfinger, S. Dinda, Y. Wu, S.V. Koduru, V. Ozbolat, D.J. Ravnic, I. T. Ozbolat, Bioprinting functional tissues, Acta Biomater. 95 (2019) 32–49.
[35] G. Gao, J.H. Lee, J. Jang, D.H. Lee, J.S. Kong, B.S. Kim, Y.J. Choi, W.B. Jang, Y. J. Hong, S.M. Kwon, D.W. Cho, Tissue engineered bio-blood-vessels constructed using a tissue-specific bioink and 3D coaxial cell printing technique: a novel therapy for ischemic disease, Adv. Funct. Mater. 27 (33) (2017).
[36] S. Lee, E.S. Sani, A.R. Spencer, Y. Guan, A.S. Weiss, N. Annabi, Human-recombinant-elastin-based bioinks for 3D bioprinting of vascularized soft tissues, Adv Mater 32 (45) (2020) e2003915.
[37] H. Cui, W. Zhu, Y. Huang, C. Liu, Z.X. Yu, M. Nowicki, S. Miao, Y. Cheng, X. Zhou, S.J. Lee, Y. Zhou, S. Wang, M. Mohiuddin, K. Horvath, L.G. Zhang, In vitro and in vivo evaluation of 3D bioprinted small-diameter vasculature with smooth muscle and endothelium, Biofabrication 12 (1) (2019) 015004.
[38] Q. Jin, Y. Fu, G. Zhang, L. Xu, G. Jin, L. Tang, J. Ju, W. Zhao, R. Hou, Nanofiber electrospinning combined with rotary bioprinting for fabricating small-diameter vessels with endothelium and smooth muscle, Compos. B Eng. 234 (2022).
[39] J. Groll, J.A. Burdick, D.W. Cho, B. Derby, M. Gelinsky, S.C. Heilshorn, T. Jüngst, J. Malda, V.A. Mironov, K. Nakayama, A. Ovsianikov, W. Sun, S. Takeuchi, J. J. Yoo, T.B.F. Woodfield, A definition of bioinks and their distinction from biomaterial inks, Biofabrication 11 (1) (2018) 013001.
[40] L. Bova, F. Billi, E. Cimetta, Mini-review: advances in 3D bioprinting of vascularized constructs, Biol. Direct 15 (1) (2020) 22.
[41] G.A. Salg, A. Blaeser, J.S. Gerhardus, T. Hackert, H.G. Kenngott, Vascularization in bioartificial parenchymal tissue: bioink and bioprinting strategies, Int. J. Mol. Sci. 23 (15) (2022).
[42] Q. Zou, X. Tian, S. Luo, D. Yuan, S. Xu, L. Yang, M. Ma, C. Ye, Agarose composite hydrogel and PVA sacrificial materials for bioprinting large-scale, personalized face-like with nutrient networks, Carbohydr. Polym. 269 (2021) 118222.
[43] X. Cui, J. Li, Y. Hartanto, M. Durham, J. Tang, H. Zhang, G. Hooper, K. Lim, T. Woodfield, Advances in extrusion 3D bioprinting: a focus on multicomponent hydrogel-based bioinks, Adv Healthc Mater 9 (15) (2020) e1901648.
[44] D.F. Williams, Biocompatibility pathways and mechanisms for bioactive materials: the bioactivity zone, Bioact. Mater. 10 (2022) 306–322.
[45] S.H. Sohn, T.H. Kim, T.S. Kim, T.J. Min, J.H. Lee, S.M. Yoo, J.W. Kim, J.E. Lee, C. H. Kim, S.H. Park, W.M. Jo, Evaluation of 3D templated synthetic vascular graft compared with standard graft in a rat model: potential use as an artificial vascular graft in cardiovascular disease, Materials 14 (5) (2021).
[46] V. Catto, S. Farè, G. Freddi, M.C. Tanzi, Vascular Tissue Engineering: Recent Advances in Small Diameter Blood Vessel Regeneration, vol. 2014, ISRN Vascular Medicine, 2014, pp. 1–27.
[47] Y. Zhang, P. Kumar, S. Lv, D. Xiong, H. Zhao, Z. Cai, X. Zhao, Recent advances in 3D bioprinting of vascularized tissues, Mater. Des. 199 (2021).
[48] D. Richards, J. Jia, M. Yost, R. Markwald, Y. Mei, 3D bioprinting for vascularized tissue fabrication, Ann. Biomed. Eng. 45 (1) (2017) 132–147.
[49] P. Wang, Y. Sun, X. Shi, H. Shen, H. Ning, H. Liu, 3D printing of tissue engineering scaffolds: a focus on vascular regeneration, Biodes Manuf 4 (2) (2021) 344–378.
[50] T. Zhang, W. Zhao, X.H. Zijie, X.W. Wang, K.X. Zhang, J.B. Yin, Bioink design for extrusion-based bioprinting, Appl. Mater. Today 25 (2021).
[51] W. Holnthoner, A. Banfi, J. Kirkpatrick, H. Redl, Vascularization for Tissue Engineering and Regenerative Medicine, Springer Cham, 2021. https://doi.org/10.1007/978-3-319-54586-8.
[52] A. Kruger-Genge, A. Blocki, R.P. Franke, F. Jung, Vascular endothelial cell biology: an update, Int. J. Mol. Sci. 20 (18) (2019).
[53] S.I. Murtada, Y. Kawamura, D. Weiss, J.D. Humphrey, Differential biomechanical responses of elastic and muscular arteries to angiotensin II-induced hypertension, J. Biomech. 119 (2021) 110297.
[54] B.A. Perler, Rutherford's Vascular Surgery and Endovascular Therapy, 2-Volume Set, 2018.
[55] H. Jiang, X. Li, T. Chen, Y. Liu, Q. Wang, Z. Wang, J. Jia, Bioprinted vascular tissue: assessing functions from cellular, tissue to organ levels, Mater Today Bio 23 (2023) 100846.
[56] E.S. Ng, G. Sarila, J.Y. Li, H.S. Edirisinghe, R. Saxena, S. Sun, F.F. Bruveris, T. Labonne, N. Sleebs, A. Maytum, R.Y. Yow, C. Inguanti, A. Motazedian, V. Calvanese, S. Capellera-Garcia, F. Ma, H.T. Nim, M. Ramialison, C. Bonifer, H. K.A. Mikkola, E.G. Stanley, A.G. Elefanty, Long-term engrafting multilineage hematopoietic cells differentiated from human induced pluripotent stem cells, Nat. Biotechnol. (2024). https://doi.org/10.1038/s41587-024-02360-7.
[57] D.Y. Fozdar, P. Soman, J.W. Lee, L.H. Han, S. Chen, Three-dimensional polymer constructs exhibiting a tunable negative Poisson's ratio, Adv. Funct. Mater. 21 (14) (2011) 2712–2720.
[58] C.B. Ahn, J.H. Kim, J.-H. Lee, K.Y. Park, K.H. Son, J.W. Lee, Development of multi-layer tubular vascular scaffold to enhance compliance by exhibiting a negative Poisson's ratio, International Journal of Precision Engineering and Manufacturing-Green Technology 8 (3) (2021) 841–853.
[59] V.A. Kumar, J.M. Caves, C.A. Haller, E.B. Dai, L.Y. Liu, S. Grainger, E.L. Chaikof, Acellular vascular grafts generated from collagen and elastin analogs, Acta Biomater. 9 (9) (2013) 8067–8074.
[60] C. Brandt-Wunderlich, C. Schwerdt, P. Behrens, N. Grabow, K.-P. Schmitz, W. Schmidt, A method to determine the kink resistance of stents and stent delivery systems according to international standards, Current Directions in Biomedical Engineering 2 (1) (2016) 289–292.
[61] M. Jurak, A.E. Wiacek, A. Ladniak, K. Przykaza, K. Szafran, What affects the biocompatibility of polymers? Adv. Colloid Interface Sci. 294 (2021) 102451.
[62] M. Monfared, D. Mawad, J. Rnjak-Kovacina, M.H. Stenzel, 3D bioprinting of dual-crosslinked nanocellulose hydrogels for tissue engineering applications, J. Mater. Chem. B 9 (31) (2021) 6163–6175.
[63] A. Schwab, R. Levato, M. D'Este, S. Piluso, D. Eglin, J. Malda, Printability and shape fidelity of bioinks in 3D bioprinting, Chem Rev 120 (19) (2020) 11028–11055.
[64] Y. Liu, J. Lu, H. Li, J. Wei, X. Li, Engineering blood vessels through micropatterned co-culture of vascular endothelial and smooth muscle cells on bilayered electrospun fibrous mats with pDNA inoculation, Acta Biomater. 11 (2015) 114–125.
[65] C. Grandi, F. Martorina, S. Lora, D. Dalzoppo, P. Amista, L. Sartore, R. Di Liddo, M.T. Conconi, P.P. Parnigotto, ECM-based triple layered scaffolds for vascular tissue engineering, Int. J. Mol. Med. 28 (6) (2011) 947–952.
[66] Z.H. Syedain, L.A. Meier, M.T. Lahti, S.L. Johnson, R.T. Tranquillo, Implantation of completely biological engineered grafts following decellularization into the sheep femoral artery, Tissue Eng Pt A 20 (11–12) (2014) 1726–1734.
[67] A. Hasan, A. Paul, A. Memic, A. Khademhosseini, A multilayered microfluidic blood vessel-like structure, Biomed. Microdevices 17 (5) (2015).
[68] J.M. Bourget, R. Gauvin, D. Larouche, A. Lavoie, R. Labbé, F.A. Auger, L. Germain, Human fibroblast-derived ECM as a scaffold for vascular tissue engineering, Biomaterials 33 (36) (2012) 9205–9213.
[69] N. L'Heureux, N. Dusserre, G. Konig, B. Victor, P. Keire, T.N. Wight, N.A. F. Chronos, A.E. Kyles, C.R. Gregory, G. Hoyt, R.C. Robbins, T.N. McAllister, Human tissue-engineered blood vessels for adult arterial revascularization, Nat Med 12 (3) (2006) 361–365.
[70] J. Zhou, C. Cao, X. Ma, A novel three-dimensional tubular scaffold prepared from silk fibroin by electrospinning, Int. J. Biol. Macromol. 45 (5) (2009) 504–510.
[71] S.S. Liu, C.F. Dong, G.Z. Lu, Q. Lu, Z.X. Li, D.L. Kaplan, H.S. Zhu, Bilayered vascular grafts based on silk proteins, Acta Biomater. 9 (11) (2013) 8991–9003.
[72] H. Ravanbakhsh, V. Karamzadeh, G. Bao, L. Mongeau, D. Juncker, Y.S. Zhang, Emerging technologies in multi-material bioprinting, Adv Mater 33 (49) (2021) e2104730.
[73] W.L. Ng, X. Huang, V. Shkolnikov, R. Suntornnond, W.Y. Yeong, Polyvinylpyrrolidone-based bioink: influence of bioink properties on printing performance and cell proliferation during inkjet-based bioprinting, Bio-Des Manuf 6 (6) (2023) 676–690.
[74] W.L. Ng, J.M. Lee, M. Zhou, Y.W. Chen, K.A. Lee, W.Y. Yeong, Y.F. Shen, Vat polymerization-based bioprinting-process, materials, applications and regulatory challenges, Biofabrication 12 (2) (2020) 022001.
[75] W. Li, L.S. Mille, J.A. Robledo, T. Uribe, V. Huerta, Y.S. Zhang, Recent advances in formulating and processing biomaterial inks for vat polymerization-based 3D printing, Adv Healthc Mater 9 (15) (2020) e2000156.
[76] S. Boularaoui, G. Al Hussein, K.A. Khan, N. Christoforou, C. Stefanini, An overview of extrusion-based bioprinting with a focus on induced shear stress and its effect on cell viability, Bioprinting 20 (2020).
[77] W.L. Ng, X. Huang, V. Shkolnikov, G.L. Goh, R. Suntornnond, W.Y. Yeong, Controlling droplet impact velocity and droplet volume: key factors to achieving high cell viability in sub-nanoliter droplet-based bioprinting, Int J Bioprinting 8 (1) (2022).
[78] K. Yu, X. Zhang, Y. Sun, Q. Gao, J. Fu, X. Cai, Y. He, Printability during projection-based 3D bioprinting, Bioact. Mater. 11 (2022) 254–267.
[79] J. Jia, D.J. Richards, S. Pollard, Y. Tan, J. Rodriguez, R.P. Visconti, T.C. Trusk, M. J. Yost, H. Yao, R.R. Markwald, Y. Mei, Engineering alginate as bioink for bioprinting, Acta Biomater. 10 (10) (2014) 4323–4331.
[80] K. Peng, X. Liu, H. Zhao, H. Lu, F. Lv, L. Liu, Y. Huang, S. Wang, Q. Gu, 3D bioprinting of reinforced vessels by dual-cross-linked biocompatible hydrogels, ACS Appl. Bio Mater. 4 (5) (2021) 4549–4556.
[81] W. Jia, P.S. Gungor-Ozkerim, Y.S. Zhang, K. Yue, K. Zhu, W. Liu, Q. Pi, B. Byambaa, M.R. Dokmeci, S.R. Shin, A. Khademhosseini, Direct 3D bioprinting of perfusable vascular constructs using a blend bioink, Biomaterials 106 (2016) 58–68.
[82] D. Wang, S. Maharjan, X. Kuang, Z. Wang, L.S. Mille, M. Tao, P. Yu, X. Cao, L. Lian, L. Lv, J.J. He, G. Tang, H. Yuk, C.K. Ozaki, X. Zhao, Y.S. Zhang,

Microfluidic bioprinting of tough hydrogel-based vascular conduits for functional blood vessels, Sci. Adv. 8 (43) (2022) eabq6900.
[83] Y. Fang, Y. Guo, B. Wu, Z. Liu, M. Ye, Y. Xu, M. Ji, L. Chen, B. Lu, K. Nie, Z. Wang, J. Luo, T. Zhang, W. Sun, Z. Xiong, Expanding embedded 3D bioprinting capability for engineering complex organs with freeform vascular networks, Adv Mater 35 (22) (2023) e2205082.
[84] S. Freeman, R. Ramos, P. Alexis Chando, L. Zhou, K. Reeser, S. Jin, P. Soman, K. Ye, A bioink blend for rotary 3D bioprinting tissue engineered small-diameter vascular constructs, Acta Biomater. 95 (2019) 152–164.
[85] G. Zhang, M. Varkey, Z. Wang, B. Xie, R. Hou, A. Atala, ECM concentration and cell-mediated traction forces play a role in vascular network assembly in 3D bioprinted tissue, Biotechnol. Bioeng. 117 (4) (2020) 1148–1158.
[86] Y. Xu, Y. Hu, C. Liu, H. Yao, B. Liu, S. Mi, A novel strategy for creating tissue-engineered biomimetic blood vessels using 3D bioprinting technology, Materials 11 (9) (2018).
[87] L. Dogan, R. Scheuring, N. Wagner, Y. Ueda, S. Schmidt, P. Worsdorfer, J. Groll, S. Ergun, Human iPSC-derived mesodermal progenitor cells preserve their vasculogenesis potential after extrusion and form hierarchically organized blood vessels, Biofabrication 13 (4) (2021).
[88] S. Hong, J.S. Kim, B. Jung, C. Won, C. Hwang, Coaxial bioprinting of cell-laden vascular constructs using a gelatin-tyramine bioink, Biomater. Sci. 7 (11) (2019) 4578–4587.
[89] S. Khalighi, M. Saadatmand, Bioprinting a thick and cell-laden partially oxidized alginate-gelatin scaffold with embedded micro-channels as future soft tissue platform, Int. J. Biol. Macromol. 193 (Pt B) (2021) 2153–2164.
[90] M. Kopf, D.F. Campos, A. Blaeser, K.S. Sen, H. Fischer, A tailored three-dimensionally printable agarose-collagen blend allows encapsulation, spreading, and attachment of human umbilical artery smooth muscle cells, Biofabrication 8 (2) (2016) 025011.
[91] J. Schoneberg, F. De Lorenzi, B. Theek, A. Blaeser, D. Rommel, A.J.C. Kuehne, F. Kiessling, H. Fischer, Engineering biofunctional in vitro vessel models using a multilayer bioprinting technique, Sci. Rep. 8 (1) (2018) 10430.
[92] P.K. Wu, B.R. Ringeisen, Development of human umbilical vein endothelial cell (HUVEC) and human umbilical vein smooth muscle cell (HUVSMC) branch/stem structures on hydrogel layers via biological laser printing (BioLP), Biofabrication 2 (1) (2010) 014111.
[93] R. Xiong, Z. Zhang, W. Chai, Y. Huang, D.B. Chrisey, Freeform drop-on-demand laser printing of 3D alginate and cellular constructs, Biofabrication 7 (4) (2015) 045011.
[94] L. Elomaa, C.C. Pan, Y. Shanjani, A. Malkovskiy, J.V. Seppala, Y. Yang, Three-dimensional fabrication of cell-laden biodegradable poly(ethylene glycol-co-depsipeptide) hydrogels by visible light stereolithography, J. Mater. Chem. B 3 (42) (2015) 8348–8358.
[95] S. Schuller-Ravoo, E. Zant, J. Feijen, D.W. Grijpma, Preparation of a designed poly(trimethylene carbonate) microvascular network by stereolithography, Adv Healthc Mater 3 (12) (2014) 2004–2011.
[96] S. Wadnap, S. Krishnamoorthy, Z. Zhang, C. Xu, Biofabrication of 3D cell-encapsulated tubular constructs using dynamic optical projection stereolithography, J. Mater. Sci. Mater. Med. 30 (3) (2019) 36.
[97] S. Krishnamoorthy, S. Wadnap, B. Noorani, H. Xu, C. Xu, Investigation of gelatin methacrylate working curves in dynamic optical projection stereolithography of vascular-like constructs, Eur. Polym. J. 124 (2020).
[98] B.G. Soliman, G.S. Major, P. Atienza-Roca, C.A. Murphy, A. Longoni, C.R. Alcala-Orozco, J. Rnjak-Kovacina, D. Gawlitta, T.B.F. Woodfield, K.S. Lim, Development and characterization of gelatin-norbornene bioink to understand the interplay between physical architecture and micro-capillary formation in biofabricated vascularized constructs, Adv Healthc Mater 11 (2) (2022) e2101873.
[99] Z. Zhang, Y. Jin, J. Yin, C.X. Xu, R.T. Xiong, K. Christensen, B.R. Ringeisen, D. B. Chrisey, Y. Huang, Evaluation of bioink printability for bioprinting applications, Appl. Phys. Rev. 5 (4) (2018).
[100] K.S. Lim, J.H. Galarraga, X. Cui, G.C.J. Lindberg, J.A. Burdick, T.B.F. Woodfield, Fundamentals and applications of photo-cross-linking in bioprinting, Chem Rev 120 (19) (2020) 10662–10694.
[101] K. Elkhoury, J. Zuazola, S. Vijayavenkataraman, Bioprinting the future using light: a review on photocrosslinking reactions, photoreactive groups, and photoinitiators, SLAS Technol 28 (3) (2023) 142–151.
[102] W. Aljohani, M.W. Ullah, X. Zhang, G. Yang, Bioprinting and its applications in tissue engineering and regenerative medicine, Int. J. Biol. Macromol. 107 (Pt A) (2018) 261–275.
[103] H. Li, N. Li, H. Zhang, Y. Zhang, H. Suo, L. Wang, M. Xu, Three-dimensional bioprinting of perfusable hierarchical microchannels with alginate and silk fibroin double cross-linked network, 3D Print. Addit. Manuf. 7 (2) (2020) 78–84.
[104] R.W. Barrs, J. Jia, M. Ward, D.J. Richards, H. Yao, M.J. Yost, Y. Mei, Engineering a chemically defined hydrogel bioink for direct bioprinting of microvasculature, Biomacromolecules 22 (2) (2021) 275–288.
[105] S. Sakai, S. Yamaguchi, T. Takei, K. Kawakami, Oxidized alginate-cross-linked alginate/gelatin hydrogel fibers for fabricating tubular constructs with layered smooth muscle cells and endothelial cells in collagen gels, Biomacromolecules 9 (7) (2008) 2036–2041.
[106] L. De Moor, I. Merovci, S. Baetens, J. Verstraeten, P. Kowalska, D.V. Krysko, W. H. De Vos, H. Declercq, High-throughput fabrication of vascularized spheroids for bioprinting, Biofabrication 10 (3) (2018) 035009.
[107] Y.C. Chen, R.Z. Lin, H. Qi, Y. Yang, H. Bae, J.M. Melero-Martin, A. Khademhosseini, Functional human vascular network generated in photocrosslinkable gelatin methacrylate hydrogels, Adv. Funct. Mater. 22 (10) (2012) 2027–2039.
[108] J. Radhakrishnan, A. Subramanian, U.M. Krishnan, S. Sethuraman, Injectable and 3D bioprinted polysaccharide hydrogels: from cartilage to osteochondral tissue engineering, Biomacromolecules 18 (1) (2017) 1–26.
[109] Q. Zou, X. Tian, S. Luo, D. Yuan, S. Xu, L. Yang, M. Ma, C. Ye, Agarose composite hydrogel and PVA sacrificial materials for bioprinting large-scale, personalized face-like with nutrient networks, Carbohydrate Polymers 269 (2021) 118222.
[110] A.G. Tabriz, M.A. Hermida, N.R. Leslie, W. Shu, Three-dimensional bioprinting of complex cell laden alginate hydrogel structures, Biofabrication 7 (4) (2015) 045012.
[111] I. Gorronogoitia, U. Urtaza, A. Zubiarrain-Laserna, A. Alonso-Varona, A. M. Zaldua, A study of the printability of alginate-based bioinks by 3D bioprinting for articular cartilage tissue engineering, Polymers 14 (2) (2022).
[112] Y. Yu, R. Xie, Y. He, F. Zhao, Q. Zhang, W. Wang, Y. Zhang, J. Hu, D. Luo, W. Peng, Dual-core coaxial bioprinting of double-channel constructs with a potential for perfusion and interaction of cells, Biofabrication 14 (3) (2022).
[113] J. Sun, Y. Gong, M. Xu, H. Chen, H. Shao, R. Zhou, Coaxial 3D bioprinting process research and performance tests on vascular scaffolds, Micromachines 15 (4) (2024).
[114] R. Yao, A.Y.F. Alkhawtani, R. Chen, J. Luan, M. Xu, Rapid and efficient in vivo angiogenesis directed by electro-assisted bioprinting of alginate/collagen microspheres with human umbilical vein endothelial cell coating layer, Int J Bioprint 5 (2.1) (2019) 194.
[115] C.G. Gomez, M. Rinaudo, M.A. Villar, Oxidation of sodium alginate and characterization of the oxidized derivatives, Carbohydrate Polymers 67 (3) (2007) 296–304.
[116] T.A. Ulrich, A. Jain, K. Tanner, J.L. MacKay, S. Kumar, Probing cellular mechanobiology in three-dimensional culture with collagen-agarose matrices, Biomaterials 31 (7) (2010) 1875–1884.
[117] P. Zarrintaj, S. Manouchehri, Z. Ahmadi, M.R. Saeb, A.M. Urbanska, D.L. Kaplan, M. Mozafari, Agarose-based biomaterials for tissue engineering, Carbohydr. Polym. 187 (2018) 66–84.
[118] C. Norotte, F.S. Marga, L.E. Niklason, G. Forgacs, Scaffold-free vascular tissue engineering using bioprinting, Biomaterials 30 (30) (2009) 5910–5917.
[119] R. Curvello, V.S. Raghuwanshi, G. Garnier, Engineering nanocellulose hydrogels for biomedical applications, Adv. Colloid Interface Sci. 267 (2019) 47–61.
[120] Y. Shi, H. Jiao, J. Sun, X. Lu, S. Yu, L. Cheng, Q. Wang, H. Liu, S. Biranje, J. Wang, J. Liu, Functionalization of nanocellulose applied with biological molecules for biomedical application: a review, Carbohydr. Polym. 285 (2022) 119208.
[121] Q. Zou, X.B. Tian, S.W. Luo, D.Z. Yuan, S.N. Xu, L. Yang, M.X. Ma, C. Ye, Agarose composite hydrogel and PVA sacrificial materials for bioprinting large-scale, personalized face-like with nutrient networks, Carbohydr. Polym. 269 (2021).
[122] E. Cambria, S. Brunner, S. Heusser, P. Fisch, W. Hitzl, S.J. Ferguson, K. Wuertz-Kozak, Cell-Laden agarose-collagen composite hydrogels for mechanotransduction studies, Front Bioeng Biotech 8 (2020).
[123] L. Su, Y. Feng, K. Wei, X. Xu, R. Liu, G. Chen, Carbohydrate-based macromolecular biomaterials, Chem Rev 121 (18) (2021) 10950–11029.
[124] L. Benning, L. Gutzweiler, K. Trondle, J. Riba, R. Zengerle, P. Koltay, S. Zimmermann, G.B. Stark, G. Finkenzeller, Assessment of hydrogels for bioprinting of endothelial cells, J. Biomed. Mater. Res. 106 (4) (2018) 935–947.
[125] B. An, D.L. Kaplan, B. Brodsky, Engineered recombinant bacterial collagen as an alternative collagen-based biomaterial for tissue engineering, Front. Chem. 2 (2014) 40.
[126] Y.L. Yang, L.J. Kaufman, Rheology and confocal reflectance microscopy as probes of mechanical properties and structure during collagen and collagen/hyaluronan self-assembly, Biophys. J. 96 (4) (2009) 1566–1585.
[127] O. Kerouredan, J.M. Bourget, M. Remy, S. Crauste-Manciet, J. Kalisky, S. Catros, N.B. Thebaud, R. Devillard, Micropatterning of endothelial cells to create a capillary-like network with defined architecture by laser-assisted bioprinting, J. Mater. Sci. Mater. Med. 30 (2) (2019) 28.
[128] E. Ruoslahti, M.D. Pierschbacher, New perspectives in cell adhesion: RGD and integrins, Science 238 (4826) (1987) 491–497.
[129] G.E. Davis, D.R. Senger, Endothelial extracellular matrix: biosynthesis, remodeling, and functions during vascular morphogenesis and neovessel stabilization, Circ. Res. 97 (11) (2005) 1093–1107.
[130] R.W. Barrs, J. Jia, S.E. Silver, M. Yost, Y. Mei, Biomaterials for bioprinting microvasculature, Chem Rev 120 (19) (2020) 10887–10949.
[131] M.G. McCoy, B.R. Seo, S. Choi, C. Fischbach, Collagen I hydrogel microstructure and composition conjointly regulate vascular network formation, Acta Biomater. 44 (2016) 200–208.
[132] M.G. McCoy, J.M. Wei, S. Choi, J.P. Goerger, W. Zipfel, C. Fischbach, Collagen fiber orientation regulates 3D vascular network formation and alignment, ACS Biomater. Sci. Eng. 4 (8) (2018) 2967–2976.
[133] M. Hospodiuk, M. Dey, D. Sosnoski, I.T. Ozbolat, The bioink: a comprehensive review on bioprintable materials, Biotechnol. Adv. 35 (2) (2017) 217–239.
[134] A. Panwar, L.P. Tan, Current status of bioinks for micro-extrusion-based 3D bioprinting, Molecules 21 (6) (2016).
[135] V.G. Muir, J.A. Burdick, Chemically modified biopolymers for the formation of biomedical hydrogels, Chem Rev 121 (18) (2021) 10908–10949.
[136] L. Shao, Q. Gao, C. Xie, J. Fu, M. Xiang, Y. He, Directly coaxial 3D bioprinting of large-scale vascularized tissue constructs, Biofabrication 12 (3) (2020) 035014.
[137] M. Abudupataer, N. Chen, S. Yan, F. Alam, Y. Shi, L. Wang, H. Lai, J. Li, K. Zhu, C. Wang, Bioprinting a 3D vascular construct for engineering a vessel-on-a-chip, Biomed. Microdevices 22 (1) (2019) 10.
[138] J. Ramon-Azcon, S. Ahadian, R. Obregon, G. Camci-Unal, S. Ostrovidov, V. Hosseini, H. Kaji, K. Ino, H. Shiku, A. Khademhosseini, T. Matsue, Gelatin methacrylate as a promising hydrogel for 3D microscale organization and

proliferation of dielectrophoretically patterned cells, Lab Chip 12 (16) (2012) 2959–2969.
[139] I. Noshadi, S. Hong, K.E. Sullivan, E. Shirzaei Sani, R. Portillo-Lara, A. Tamayol, S. R. Shin, A.E. Gao, W.L. Stoppel, L.D. Black III, A. Khademhosseini, N. Annabi, In vitro and in vivo analysis of visible light crosslinkable gelatin methacryloyl (GelMA) hydrogels, Biomater. Sci. 5 (10) (2017) 2093–2105.
[140] H. Kumar, P. Ambhorkar, I. Foulds, K. Golovin, K. Kim, A kinetic model for predicting imperfections in bioink photopolymerization during visible-light stereolithography printing, Addit. Manuf. 55 (2022).
[141] M. Dey, B. Ayan, M. Yurieva, D. Unutmaz, I.T. Ozbolat, Studying tumor angiogenesis and cancer invasion in a three-dimensional vascularized breast cancer micro-environment, Adv Biol (Weinh) 5 (7) (2021) e2100090.
[142] D.F. Duarte Campos, S. Zhang, F. Kreimendahl, M. Kopf, H. Fischer, M. Vogt, A. Blaeser, C. Apel, M. Esteves-Oliveira, Hand-held bioprinting for de novo vascular formation applicable to dental pulp regeneration, Connect. Tissue Res. 61 (2) (2020) 205–215.
[143] K. Trondle, F. Koch, G. Finkenzeller, G.B. Stark, R. Zengerle, P. Koltay, S. Zimmermann, Bioprinting of high cell-density constructs leads to controlled lumen formation with self-assembly of endothelial cells, J Tissue Eng Regen Med 13 (10) (2019) 1883–1895.
[144] Z. Chen, Q. Zhang, H. Li, Q. Wei, X. Zhao, F. Chen, Elastin-like polypeptide modified silk fibroin porous scaffold promotes osteochondral repair, Bioact. Mater. 6 (3) (2021) 589–601.
[145] Y. Yan, B. Cheng, K. Chen, W. Cui, J. Qi, X. Li, L. Deng, Enhanced osteogenesis of bone marrow-derived mesenchymal stem cells by a functionalized silk fibroin hydrogel for bone defect repair, Adv Healthc Mater 8 (3) (2019) e1801043.
[146] Y. Wang, H.J. Kim, G. Vunjak-Novakovic, D.L. Kaplan, Stem cell-based tissue engineering with silk biomaterials, Biomaterials 27 (36) (2006) 6064–6082.
[147] G.H. Altman, F. Diaz, C. Jakuba, T. Calabro, R.L. Horan, J. Chen, H. Lu, J. Richmond, D.L. Kaplan, Silk-based biomaterials, Biomaterials 24 (3) (2003) 401–416.
[148] S. Gomes, I.B. Leonor, J.F. Mano, R.L. Reis, D.L. Kaplan, Natural and genetically engineered proteins for tissue engineering, Prog. Polym. Sci. 37 (1) (2012) 1–17.
[149] A.A. Szklanny, M. Machour, I. Redenski, V. Chochola, I. Goldfracht, B. Kaplan, M. Epshtein, H. Simaan Yameen, U. Merdler, A. Feinberg, D. Seliktar, N. Korin, J. Jaros, S. Levenberg, 3D bioprinting of engineered tissue flaps with hierarchical vessel networks (VesselNet) for direct host-to-implant perfusion, Adv Mater 33 (42) (2021) e2102661.
[150] G. Decante, J.B. Costa, J. Silva-Correia, M.N. Collins, R.L. Reis, J.M. Oliveira, Engineering bioinks for 3D bioprinting, Biofabrication 13 (3) (2021).
[151] W. Han, N.K. Singh, J.J. Kim, H. Kim, B.S. Kim, J.Y. Park, J. Jang, D.W. Cho, Directed differential behaviors of multipotent adult stem cells from decellularized tissue/organ extracellular matrix bioinks, Biomaterials 224 (2019) 119496.
[152] S. Lee, X. Tong, F. Yang, Effects of the poly(ethylene glycol) hydrogel crosslinking mechanism on protein release, Biomater. Sci. 4 (3) (2016) 405–411.
[153] J.S. Lee, J.M. Hong, J.W. Jung, J.H. Shim, J.H. Oh, D.W. Cho, 3D printing of composite tissue with complex shape applied to ear regeneration, Biofabrication 6 (2) (2014) 024103.
[154] N.A. Alcantar, E.S. Aydil, J.N. Israelachvili, Polyethylene glycol-coated biocompatible surfaces, J. Biomed. Mater. Res. 51 (3) (2000) 343–351.
[155] R. Xie, W. Zheng, L. Guan, Y. Ai, Q. Liang, Engineering of hydrogel materials with perfusable microchannels for building vascularized tissues, Small 16 (15) (2020) e1902838.
[156] A. Skardal, J. Zhang, G.D. Prestwich, Bioprinting vessel-like constructs using hyaluronan hydrogels crosslinked with tetrahedral polyethylene glycol tetracrylates, Biomaterials 31 (24) (2010) 6173–6181.
[157] L. Schukur, P. Zorlutuna, J.M. Cha, H. Bae, A. Khademhosseini, Directed differentiation of size-controlled embryoid bodies towards endothelial and cardiac lineages in RGD-modified poly(ethylene glycol) hydrogels, Adv Healthc Mater 2 (1) (2013) 195–205.
[158] M.A. Woodruff, D.W. Hutmacher, The return of a forgotten polymer—polycaprolactone in the 21st century, Prog. Polym. Sci. 35 (10) (2010) 1217–1256.
[159] S.A.V. Dananjaya, V.S. Chevali, J.P. Dear, P. Potluri, C. Abeykoon, 3D printing of biodegradable polymers and their composites – current state-of-the-art, properties, applications, and machine learning for potential future applications, Prog. Mater. Sci. 146 (2024).
[160] Y. Yoon, H. Park, S. An, J.H. Ahn, B. Kim, J. Shin, Y.E. Kim, J. Yeon, J.H. Chung, D. Kim, M. Cho, Bacterial degradation kinetics of poly(E-caprolactone) (PCL) film by Aquabacterium sp. CY2-9 isolated from plastic-contaminated landfill, J Environ Manage 335 (2023) 117493.
[161] Z. Donik, B. Necemer, M. Vesenjak, S. Glodez, J. Kramberger, Computational analysis of mechanical performance for composite polymer biodegradable stents, Materials 14 (20) (2021).
[162] C. Piard, H. Baker, T. Kamalitdinov, J. Fisher, Bioprinted osteon-like scaffolds enhance in vivo neovascularization, Biofabrication 11 (2) (2019) 025013.
[163] Y.W. Chen, Y.F. Shen, C.C. Ho, J. Yu, Y.A. Wu, K. Wang, C.T. Shih, M.Y. Shie, Osteogenic and angiogenic potentials of the cell-laden hydrogel/mussel-inspired calcium silicate complex hierarchical porous scaffold fabricated by 3D bioprinting, Mater Sci Eng C Mater Biol Appl 91 (2018) 679–687.
[164] G. Zhang, G. Cao, C. Gu, Y. Fu, G. Jin, L. Tang, H. Wang, J. Li, Y. Le, S. Cao, F. Han, J. Ju, B. Li, R. Hou, Regulation of vascular branch formation in 3D bioprinted tissues using confining force, Appl. Mater. Today 26 (2022).
[165] S. Ji, M. Guvendiren, Recent advances in bioink design for 3D bioprinting of tissues and organs, Front. Bioeng. Biotechnol. 5 (2017) 23.
[166] R.E.B. Fitzsimmons, M.S. Aquilino, J. Quigley, O. Chebotarev, F. Tarlan, C. A. Simmons, Generating vascular channels within hydrogel constructs using an economical open-source 3D bioprinter and thermoreversible gels, Bioprinting 9 (2018) 7–18.
[167] J. Malda, J. Visser, F.P. Melchels, T. Jungst, W.E. Hennink, W.J. Dhert, J. Groll, D. W. Hutmacher, 25th anniversary article: engineering hydrogels for biofabrication, Adv Mater 25 (36) (2013) 5011–5028.
[168] R.N. Shamma, R.H. Sayed, H. Madry, N.S. El Sayed, M. Cucchiarini, Triblock copolymer bioinks in hydrogel three-dimensional printing for regenerative medicine: a focus on pluronic F127, Tissue Eng Part B Rev 28 (2) (2022) 451–463.
[169] S. Li, J. Jin, C. Zhang, X. Yang, Y. Liu, P. Lei, Y. Hu, 3D bioprinting vascular networks in suspension baths, Appl. Mater. Today 30 (2023).
[170] Y. Zhang, P. Kumar, S.W. Lv, D. Xiong, H.B. Zhao, Z.Q. Cai, X.B. Zhao, Recent advances in 3D bioprinting of vascularized tissues, Mater Design 199 (2021).
[171] M.A. Woodruff, D.W. Hutmacher, The return of a forgotten polymer-Polycaprolactone in the 21st century, Prog. Polym. Sci. 35 (10) (2010) 1217–1256.
[172] S. Lee, X.M. Tong, F. Yang, Effects of the poly(ethylene glycol) hydrogel crosslinking mechanism on protein release, Biomater Sci-Uk 4 (3) (2016) 405–411.
[173] M. Carrabba, M. Fagnano, M.T. Ghorbel, F. Rapetto, B. Su, C. De Maria, G. Vozzi, G. Biglino, A.W. Perriman, M. Caputo, P. Madeddu, Development of a novel hierarchically biofabricated blood vessel mimic decorated with three vascular cell populations for the reconstruction of small-diameter arteries, Adv. Funct. Mater. 34 (7) (2024).
[174] X. Jiang, X. Zuo, H. Wang, P. Zhu, Y.J. Kang, Fabrication of vascular grafts using poly(epsilon-caprolactone) and collagen-encapsuled ADSCs for interposition implantation of abdominal aorta in rhesus monkeys, ACS Biomater. Sci. Eng. 10 (5) (2024) 3120–3135.
[175] H.J. Jeong, H. Nam, J.S. Kim, S. Cho, H.H. Park, Y.S. Cho, H. Jeon, J. Jang, S. J. Lee, Dragging 3D printing technique controls pore sizes of tissue engineered blood vessels to induce spontaneous cellular assembly, Bioact. Mater. 31 (2024) 590–602.
[176] B. Gorain, H. Choudhury, M. Pandey, P. Kesharwani, M.M. Abeer, R.K. Tekade, Z. Hussain, Carbon nanotube scaffolds as emerging nanoplatform for myocardial tissue regeneration: a review of recent developments and therapeutic implications, Biomed. Pharmacother. 104 (2018) 496–508.
[177] W.L. Ng, C.K. Chua, Y.F. Shen, Print me an organ! Why we are not there yet, Prog. Polym. Sci. 97 (2019).
[178] E. Yeung, T. Inoue, H. Matsushita, J. Opfermann, P. Mass, S. Aslan, J. Johnson, K. Nelson, B. Kim, L. Olivieri, A. Krieger, N. Hibino, In vivo implantation of 3-dimensional printed customized branched tissue engineered vascular graft in a porcine model, J. Thorac. Cardiovasc. Surg. 159 (5) (2020) 1971–1981, e1.
[179] T. Fukunishi, C.A. Best, T. Sugiura, J. Opfermann, C.S. Ong, T. Shinoka, C. K. Breuer, A. Krieger, J. Johnson, N. Hibino, Preclinical study of patient-specific cell-free nanofiber tissue-engineered vascular grafts using 3-dimensional printing in a sheep model, J Thorac Cardiov Sur 153 (4) (2017) 924–932.
[180] A.K. Miri, A. Khalilpour, B. Cecen, S. Maharjan, S.R. Shin, A. Khademhosseini, Multiscale bioprinting of vascularized models, Biomaterials 198 (2019) 204–216.
[181] X.B. Chen, A. Fazel Anvari-Yazdi, X. Duan, A. Zimmerling, R. Gharraei, N. K. Sharma, S. Sweilem, L. Ning, Biomaterials/bioinks and extrusion bioprinting, Bioact. Mater. 28 (2023) 511–536.
[182] F. Kreimendahl, C. Kniebs, A.M. Tavares Sobreiro, T. Schmitz-Rode, S. Jockenhoevel, A.L. Thiebes, FRESH bioprinting technology for tissue engineering - the influence of printing process and bioink composition on cell behavior and vascularization, J. Appl. Biomater. Funct. Mater. 19 (2021) 22808000211028808.
[183] J. Schöneberg, F. De Lorenzi, B. Theek, A. Blaeser, D. Rommel, A.J.C. Kuehne, F. Kießling, H. Fischer, Engineering biofunctional in vitro vessel models using a multilayer bioprinting technique, Sci. Rep. 8 (1) (2018) 10430.
[184] K. Peng, X. Liu, H. Zhao, H. Lu, F. Lv, L. Liu, Y. Huang, S. Wang, Q. Gu, 3D bioprinting of reinforced vessels by dual-cross-linked biocompatible hydrogels, ACS Appl. Bio Mater. 4 (5) (2021) 4549–4556.
[185] Y. Ze, Y. Li, L. Huang, Y. Shi, P. Li, P. Gong, J. Lin, Y. Yao, Biodegradable inks in indirect three-dimensional bioprinting for tissue vascularization, Front. Bioeng. Biotechnol. 10 (2022) 856398.
[186] C. Dikyol, P. Bartolo, B. Koc, Multimaterial bioprinting approaches and their implementations for vascular and vascularized tissues, Bioprinting 24 (2021) e00159.
[187] L. Serex, A. Bertsch, P. Renaud, Microfluidics: a new layer of control for extrusion-based 3D printing, Micromachines 9 (2) (2018).
[188] M.A. Skylar-Scott, J. Mueller, C.W. Visser, J.A. Lewis, Voxelated soft matter via multimaterial multinozzle 3D printing, Nature 575 (7782) (2019) 330–335.
[189] Z.X. Tu, Y.L. Zhong, H.Z. Hu, D. Shao, R.N. Haag, M. Schirner, J. Lee, B. Sullenger, K.W. Leong, Design of therapeutic biomaterials to control inflammation, Nat. Rev. Mater. 7 (7) (2022) 557–574.
[190] Y. Zhang, Cell toxicity mechanism and biomarker, Clin. Transl. Med. 7 (1) (2018) 34.
[191] M. Jurak, A.E. Wiacek, A. Ladniak, K. Przykaza, K. Szafran, What affects the biocompatibility of polymers? Adv Colloid Interfac 294 (2021).
[192] U. Ahmed, R. Ahmed, M.S. Masoud, M. Tariq, U.A. Ashfaq, R. Augustine, A. Hasan, Stem cells based in vitro models: trends and prospects in biomaterials cytotoxicity studies, Biomed Mater 16 (4) (2021) 042003.
[193] Y. Yao, H. Zhang, Z. Wang, J. Ding, S. Wang, B. Huang, S. Ke, C. Gao, Reactive oxygen species (ROS)-responsive biomaterials mediate tissue microenvironments and tissue regeneration, J. Mater. Chem. B 7 (33) (2019) 5019–5037.

[194] D.A. Wang, C.G. Williams, F. Yang, J.H. Elisseeff, Enhancing the tissue-biomaterial interface: tissue-initiated integration of biomaterials, Adv. Funct. Mater. 14 (12) (2004) 1152–1159.
[195] N. Wiesmann, S. Mendler, C.R. Buhr, U. Ritz, P.W. Kämmerer, J. Brieger, Zinc oxide nanoparticles exhibit favorable properties to promote tissue integration of biomaterials, Biomedicines 9 (10) (2021).
[196] J.X. Ma, Z.Y. Zhou, M.M. Gao, B.S. Yu, D.M. Xiao, X.N. Zou, C. Bünger, Biosynthesis of bioadaptive materials: a review on developing materials available for tissue adaptation, J. Mater. Sci. Technol. 32 (9) (2016) 810–814.
[197] P. Dhavalikar, A. Robinson, Z.Y. Lan, D. Jenkins, M. Chwatko, K. Salhadar, A. Jose, R. Kar, E. Shoga, A. Kannapiran, E. Cosgriff-Hernandez, Review of integrin-targeting biomaterials in tissue engineering, Adv. Healthcare Mater. 9 (23) (2020).
[198] K.N. Ekdahl, S. Huang, B. Nilsson, Y. Teramura, Complement inhibition in biomaterial- and biosurface-induced thromboinflammation, Semin. Immunol. 28 (3) (2016) 268–277.
[199] X.H. Wang, M.Y. Shan, S.K. Zhang, X. Chen, W.T. Liu, J.Z. Chen, X.Y. Liu, Stimuli-responsive antibacterial materials: molecular structures, design principles, and biomedical applications, Adv. Sci. 9 (13) (2022).
[200] P. Makvandi, H. Song, C.K.Y. Yiu, R. Sartorius, E.N. Zare, N. Rabiee, W.X. Wu, A. C. Paiva-Santos, X.D. Wang, C.Z. Yu, F.R. Tay, Bioengineered materials with selective antimicrobial toxicity in biomedicine (vol 10, 8, 2023), Military Med Res 10 (1) (2023).
[201] N. Artzi, N. Oliva, C. Puron, S. Shitreet, S. Artzi, A. bon Ramos, A. Groothuis, G. Sahagian, E.R. Edelman, In vivo and in vitro tracking of erosion in biodegradable materials using non-invasive fluorescence imaging, Nat. Mater. 10 (9) (2011) 704–709.
[202] S.A.V. Dananjaya, V.S. Chevali, J.P. Dear, P. Potluri, C. Abeykoon, 3D printing of biodegradable polymers and their composites - current state-of-the-art, properties, applications, and machine learning for potential future applications, Prog. Mater. Sci. 146 (2024).
[203] N. Lucas, C. Bienaime, C. Belloy, M. Queneudec, F. Silvestre, J.E. Nava-Saucedo, Polymer biodegradation: mechanisms and estimation techniques, Chemosphere 73 (4) (2008) 429–442.
[204] K.E. Martin, M.D. Hunckler, E. Chee, J.D. Caplin, G.F. Barber, P.P. Kalelkar, R. S. Schneider, A.J. Garcia, Hydrolytic hydrogels tune mesenchymal stem cell persistence and immunomodulation for enhanced diabetic cutaneous wound healing, Biomaterials 301 (2023) 122256.
[205] G.D. Liu, F.X. Zou, W. He, J.F. Li, Y.J. Xie, M.J. Ma, Y.D. Zheng, The controlled degradation of bacterial cellulose in simulated physiological environment by immobilization and release of cellulase, Carbohydr. Polym. 314 (2023).
[206] S.M. McDonald, E.K. Augustine, Q. Lanners, C. Rudin, L.C. Brinson, M.L. Becker, Applied machine learning as a driver for polymeric biomaterials design, Nat. Commun. 14 (1) (2023).
[207] K.H. Sim, M. Mir, S. Jelke, S. Tarafder, J. Kim, C.H. Lee, Quantum dots-labeled polymeric scaffolds for in vivo tracking of degradation and tissue formation, Bioact. Mater. 16 (2022) 285–292.
[208] Z. Othman, B.C. Pastor, S. van Rijt, P. Habibovic, Understanding interactions between biomaterials and biological systems using proteomics, Biomaterials 167 (2018) 191–204.
[209] Y.S. Zhang, A. Khademhosseini, Advances in engineering hydrogels, Science 356 (6337) (2017).
[210] W.L. Ng, A. Chan, Y.S. Ong, C.K. Chua, Deep learning for fabrication and maturation of 3D bioprinted tissues and organs, Virtual Phys Prototy 15 (3) (2020) 340–358.
[211] A.J. Melchiorri, N. Hibino, C.A. Best, T. Yi, Y.U. Lee, C.A. Kraynak, L.K. Kimerer, A. Krieger, P. Kim, C.K. Breuer, J.P. Fisher, 3D-Printed biodegradable polymeric vascular grafts, Adv Healthc Mater 5 (3) (2016) 319–325.
[212] M. Sermesant, H. Delingette, H. Cochet, P. Jais, N. Ayache, Applications of artificial intelligence in cardiovascular imaging, Nat. Rev. Cardiol. 18 (8) (2021) 600–609.
[213] F.J. Zhao, Y.R. Chen, Y.Q. Hou, X.W. He, Segmentation of blood vessels using rule-based and machine-learning-based methods: a review, Multimedia Syst 25 (2) (2019) 109–118.
[214] J. Kwiecinski, K. Grodecki, K. Pieszko, M. Dabrowski, Z. Chmielak, P. Slomka, W. Wojakowski, A. Witkowski, D. Dey, Preprocedural computed tomography angiography for prediction of transcatheter aortic valve implantation outcomes. A machine learning study, Eur. Heart J. 44 (2023).
[215] W.H. Wang, H. Wang, J.N. Zhou, H.L. Fan, X. Liu, Machine learning prediction of mechanical properties of braided-textile reinforced tubular structures, Mater. Des. 212 (2021).
[216] E. Sakaridis, N. Karathanasopoulos, D. Mohr, Machine-learning based prediction of crash response of tubular structures, Int. J. Impact Eng. 166 (2022).
[217] K. Ruberu, M. Senadeera, S. Rana, S. Gupta, J. Chung, Z.L. Yue, S. Venkatesh, G. Wallace, Coupling machine learning with 3D bioprinting to fast track optimisation of extrusion printing, Appl. Mater. Today 22 (2021).
[218] J.A. Guan, S.T. You, Y. Xiang, J. Schimelman, J. Alido, X.Y. Ma, M. Tang, S. C. Chen, Compensating the cell-induced light scattering effect in light-based bioprinting using deep learning, Biofabrication 14 (1) (2022).
[219] T. Jiang, J.L. Gradus, A.J. Rosellini, Supervised machine learning: a brief primer, Behav. Ther. 51 (5) (2020) 675–687.
[220] H.Q. Xu, Q.Y. Liu, J. Casillas, M. Mcanally, N. Mubtasim, L.S. Gollahon, D.Z. Wu, C.X. Xu, Prediction of cell viability in dynamic optical projection stereolithography-based bioprinting using machine learning, J. Intell. Manuf. 33 (4) (2022) 995–1005.
[221] J. Lee, S.J. Oh, S.H. An, W.D. Kim, S.H. Kim, Machine learning-based design strategy for 3D printable bioink: elastic modulus and yield stress determine printability, Biofabrication 12 (3) (2020).
[222] Q. Qiao, X. Zhang, Z.H. Yan, C.Y. Hou, J.L. Zhang, Y. He, N. Zhao, S.J. Yan, Y. P. Gong, Q. Li, The use of machine learning to predict the effects of cryoprotective agents on the GelMA-based bioinks used in extrusion cryobioprinting, Bio-Des Manuf 6 (4) (2023) 464–477.
[223] J. Shi, J.C. Song, B. Song, W.F. Lu, Multi-objective optimization design through machine learning for drop-on-demand bioprinting, Engineering 5 (3) (2019) 586–593.
[224] C.A. Verheyen, S.G.M. Uzel, A. Kurum, E.T. Roche, J.A. Lewis, Integrated data-driven modeling and experimental optimization of granular hydrogel matrices, Matter-Us 6 (3) (2023) 1015–1036.
[225] X. Huang, W.L. Ng, W.Y. Yeong, Predicting the number of printed cells during inkjet-based bioprinting process based on droplet velocity profile using machine learning approaches, J. Intell. Manuf. 35 (5) (2024) 2349–2364.
[226] D.E.J. Anderson, G. Pohan, J. Raman, F. Konecny, E.K.F. Yim, M.T. Hinds, Improving surgical methods for studying vascular grafts in animal models, Tissue Eng Part C Methods 24 (8) (2018) 457–464.
[227] M. Ahmed, G. Hamilton, A.M. Seifalian, The performance of a small-calibre graft for vascular reconstructions in a senescent sheep model, Biomaterials 35 (33) (2014) 9033–9040.
[228] A. Assmann, K. Zwirnmann, F. Heidelberg, F. Schiffer, K. Horstkotter, H. Munakata, F. Gremse, M. Barth, A. Lichtenberg, P. Akhyari, The degeneration of biological cardiovascular prostheses under pro-calcific metabolic conditions in a small animal model, Biomaterials 35 (26) (2014) 7416–7428.
[229] C. Gangloff, O. Grimault, M. Theron, K. Pichavant, H. Galinat, F. Mingant, Y. Ozier, A clinically relevant and bias-controlled murine model to study acute traumatic coagulopathy, Sci. Rep. 8 (1) (2018) 5783.
[230] D.W. Jin, S.T. Wu, H.Z. Kuang, P. Zhang, M. Yin, Preliminary application of a cell-free mono-layered vascular scaffold in a rabbit model, Mater. Des. 198 (2021).
[231] E.H. Jang, J.H. Kim, J.Y. Ryu, J. Lee, H.H. Kim, Y.N. Youn, Time-dependent pathobiological and physiological changes of implanted vein grafts in a canine model, J Cardiovasc Transl Res 15 (5) (2022) 1108–1118.
[232] S. Row, H. Peng, E.M. Schlaich, C. Koenigsknecht, S.T. Andreadis, D.D. Swartz, Arterial grafts exhibiting unprecedented cellular infiltration and remodeling in vivo: the role of cells in the vascular wall, Biomaterials 50 (2015) 115–126.
[233] M.T. Koobatian, S. Row, R.J. Smith Jr., C. Koenigsknecht, S.T. Andreadis, D. D. Swartz, Successful endothelialization and remodeling of a cell-free small-diameter arterial graft in a large animal model, Biomaterials 76 (2016) 344–358.
[234] S.P. Hoerstrup, I. Cummings Mrcs, M. Lachat, F.J. Schoen, R. Jenni, S. Leschka, S. Neuenschwander, D. Schmidt, A. Mol, C. Gunter, M. Gossi, M. Genoni, G. Zund, Functional growth in tissue-engineered living, vascular grafts: follow-up at 100 weeks in a large animal model, Circulation 114 (1 Suppl) (2006) I159–I166.
[235] T. Fukunishi, C.S. Ong, P. Yesantharao, C.A. Best, T. Yi, H. Zhang, G. Mattson, J. Boktor, K. Nelson, T. Shinoka, C.K. Breuer, J. Johnson, N. Hibino, Different degradation rates of nanofiber vascular grafts in small and large animal models, J Tissue Eng Regen Med 14 (2) (2020) 203–214.
[236] M. Itoh, Y. Mukae, T. Kitsuka, K. Arai, A. Nakamura, K. Uchihashi, S. Toda, K. Matsubayashi, J.I. Oyama, K. Node, D. Kami, S. Gojo, S. Morita, T. Nishida, K. Nakayama, E. Kobayashi, Development of an immunodeficient pig model allowing long-term accommodation of artificial human vascular tubes, Nat. Commun. 10 (1) (2019) 2244.
[237] R.H. Liu, C.S. Ong, T. Fukunishi, K. Ong, N. Hibino, Review of vascular graft studies in large animal models, Tissue Eng Part B Rev 24 (2) (2018) 133–143.
[238] Y. Matsuzaki, A. Ulziibayar, T. Shoji, T. Shinoka, Heparin-eluting tissue-engineered bioabsorbable vascular grafts, Appl Sci-Basel 11 (10) (2021).
[239] Y. Zhang, P. Kumar, S. Lv, D. Xiong, H. Zhao, Z. Cai, X. Zhao, Recent advances in 3D bioprinting of vascularized tissues, Mater. Des. 199 (2021) 109398.
[240] P. Zarrintaj, S. Manouchehri, Z. Ahmadi, M.R. Saeb, A.M. Urbanska, D.L. Kaplan, M. Mozafari, Agarose-based biomaterials for tissue engineering, Carbohydrate Polymers 187 (2018) 66–84.
[241] O.O. Akintewe, E.G. Roberts, N.-G. Rim, M.A.H. Ferguson, J.Y. Wong, Design Approaches to Myocardial and Vascular Tissue Engineering, vol. 19, 2017, pp. 389–414, vols. 19, 2017.
[242] J.M. Tarbell, S.I. Simon, F.-R.E. Curry, Mechanosensing at the Vascular Interface, vol. 16, 2014, pp. 505–532, vols. 16, 2014.
[243] L. West-Livingston, J.W. Lim, S.J. Lee, Translational tissue-engineered vascular grafts: from bench to bedside, Biomaterials 302 (2023) 122322.
[244] B. Zhang, M. Montgomery, M.D. Chamberlain, S. Ogawa, A. Korolj, A. Pahnke, L. A. Wells, S. Masse, J. Kim, L. Reis, A. Momen, S.S. Nunes, A.R. Wheeler, K. Nanthakumar, G. Keller, M.V. Sefton, M. Radisic, Biodegradable scaffold with built-in vasculature for organ-on-a-chip engineering and direct surgical anastomosis, Nat. Mater. 15 (6) (2016) 669–678.